INFORMATION TO USERS

This manuscript has been reproduced from the microfilm master. UMI films the text directly from the original or copy submitted. Thus, some thesis and dissertation copies are in typewriter face, while others may be from any type of computer printer.

The quality of this reproduction is dependent upon the quality of the copy submitted. Broken or indistinct print, colored or poor quality illustrations and photographs, print bleedthrough, substandard margins, and improper alignment can adversely affect reproduction.

In the unlikely event that the author did not send UMI a complete manuscript and there are missing pages, these will be noted. Also, if unauthorized copyright material had to be removed, a note will indicate the deletion.

Oversize materials (e.g., maps, drawings, charts) are reproduced by sectioning the original, beginning at the upper left-hand corner and continuing from left to right in equal sections with small overlaps.

Photographs included in the original manuscript have been reproduced xerographically in this copy. Higher quality 6" x 9" black and white photographic prints are available for any photographs or illustrations appearing in this copy for an additional charge. Contact UMI directly to order.

Bell & Howell Information and Learning
300 North Zeeb Road, Ann Arbor, MI 48106-1346 USA

UMI®
800-521-0600

TORSIONAL-AXIAL COUPLING
IN THE LINE SHAFTING VIBRATIONS
IN MERCHANT OCEAN GOING SHIPS

Davor Šverko

A Thesis

in

The Department

of

Mechanical Engineering

Presented in Partial Fulfillment of the Requirements
for the Degree of Master of Applied Science at
Concordia University
Montreal, Quebec, Canada

October 1997

ABSTRACT

Torsional-Axial Coupling

in the Line Shafting Vibration in Merchant Ocean Going Ships

Davor Šverko

Mutual interaction of the two major vibration modes, i.e. torsional and axial, resulting from propeller action in the solid elastic shaft of the merchant ocean going ships is analyzed in this thesis. This type of vibration interaction can be described as torsionally-induced propeller thrust fluctuation. Generated longitudinal vibrations due to the thrust variation, can be the cause of excessive ship hull vibrations in modern merchant ocean going ships. The aim of this study is twofold; i.e. to show how the design of the propulsion line shafting affects the coupling phenomenon between torsional and axial vibrations, and to correlate line shafting design with potential structural problems of the hull.

The line shafting design is first addressed using conventional approach which yields information about torsional and axial eigenvalues and stresses. It provides no details regarding propeller coupling. The method used in the analysis is transfer matrix method, which suits well the rotor systems on modern ocean going ships. Vibration coupling computation is then performed using finite element method to demonstrate the

importance of obtaining torsionally induced axial force. It is shown that dynamic response of the ship hull will be greatly affected by longitudinal force generated by propeller coupling of torsional and axial vibrations.

ACKNOWLEDGMENTS

I would like to thank my thesis supervisor Dr. Rama Bhat for valuable comments and input in this thesis, as well as for his support throughout my studies. I am also indebted to Uljanik Shipyard - Diesel Engine Factory Project Department, for their contribution of necessary data.

TABLE OF CONTENTS

CHAPTER III

LIST OF FIGURES

LIST OF TABLES

LIST OF SYMBOLS

A - area of the cross section [m^2]

[B] - matrix of the shape function derivatives

c - damping coefficient (in [Nms/rad] for torsion, or [Nm/s] for axial)

[c] - element's damping matrix

[C] - system's damping matrix

d - differentiation operator

d - diameter [m]

[d] - derivative operators matrix

D - dissipative forces [N]

[D^*] - Choleski decomposition matrix

E - elastic modulus [N/m^2]

[E] - elasticity matrix

f - body force [N]

{f} - body forces vector

F - force [N]

F_n - normal force [N]

F_t - tangential force [N]

F_r - radial force [N]

F_k - connecting-rod force [N]

{F} - solution force vector

[F] - field matrix

G - shear modulus [N/m^2]

{h} - normalized eigenvector

[h] - normalized eigenvector-spectrum

H - Hamiltonian

I - mass moment of inertia [kgm^2], also used for areal moment of inertia [m^4]

I_p - polar moment of inertia [kgm^2], also used for polar areal moment of inertia [m^4]

J - Jacobian, also used mass moment of inertia [kgm^2]

k_t - torsional stiffness [Nm/rad]

k_a - axial stiffness [N/m]

k_b - bending stiffness [N/m]

[k] - element's stiffness matrix

[K] - system's stiffness matrix

L - Lagrangean

m - mass [kg]

[m] - element's mass-inertia matrix

M - moment [Nm]

[M] - system's mass-inertia matrix

n - rotational speed [rpm]

N - longitudinal force [N]

N - shape function

[N] - shape function matrix

p - pressure [N/m^2]

p_{bme} - brake mean effective pressure [N/m^2]

p_{mep} - mean effective pressure [N/m^2]

P - concentrate force [N]

$\{P\}$ - concentrated forces vector

$[P]$ - point matrix

q - general nodal displacement[mm]

$q_{,t}$ - general nodal-velocity [m/s]

$q_{,tt}$ - general nodal-acceleration [m/s^2]

$\{q\}$ - general nodal displacement vector

$\{q_{,t}\}$ - general nodal-velocity vector

$\{q_{,tt}\}$ - general nodal-acceleration vector

$\{Q\}$ - excitation forces vector

$\{Q_i\}$ - initial strain-stress forces vector

$\{Q_b\}$ - body forces vector

$\{Q_s\}$ - surface traction vector

r - crank radius [m], also used for radial coordinate [m], and absolute damping coefficient (in [Nms/rad] for torsion)

$\{R\}$ - nodal forces vector

S - surface [m^2]

t - time [s], also used for surface traction [N]

$\{t\}$ - vector of the surface traction

T - torque [Nm], also used for kinetic energy [Nm], and time period [s]

u - displacement

{u} - displacement vector

U - strain energy [Nm]

V - potential energy of external forces [Nm]

V - volume [m^3]

V - ship speed [m/sec];[knot]

V_A - ship advanced speed (wake speed) [m/sec];[knot]

w - wake coefficient

W - work done [Nm]

x,y,z - Cartesian coordinates [m]

X - amplitude of longitudinal coordinate [m]

{X} - eingenvector

[X] - eigenvector spectrum

{z} - state vector

α - phase angle

[2Γ] - normalized-damping matrix

δ - variation operator

ζ - nondimensional damping coefficient; also used for natural coordinate

η_m - mechanical efficiency coefficient

η - natural coordinate

ξ - natural coordinate

Θ - torsional angular displacement [rad]

λ - eigenvalue, also used for Lame's constant

μ - Lame's constant (shear modulus)

ν - Poisson's coefficient

Π - total potential energy [Nm]

ρ - material density [kg/m^3]

σ - stress [N/m^2]

σ_o - prescribed stress [N/m^2]

$\{\sigma\}$ - stress vector

$\{\sigma_t\}$ - prescribed stress vector

ε - strain

ε_o - prescribed strain

$\{\varepsilon\}$ - strain vector

$\{\varepsilon_o\}$ - prescribed strain vector

τ - torsional stress [N/m^2]

φ - phase angle [rad]

ϕ - field variable

ω - natural frequency [rad/s]

$[\omega 2]$ - normalized-stiffness matrix

∂ - partial derivative operator

CHAPTER I

INTRODUCTION

Ship propulsion line shafting is designed taking into account dynamic excitations that act on the system, among which dominates the oscillatory torque generated in the main drive. Furthermore, the line shafting design affects dynamic behaviour of the propeller which operates in the nonhomogeneous inflow generated behind the ship. Thus, the torque fluctuation on the propeller will cause variations in the propeller angle of attack which results in fluctuations in the thrust produced by the propeller. This phenomenon is known as torsionally induced axial vibration coupling. Analysis of the coupled torsional and axial vibrations will provide important information about the exciting force that is acting through line shafting on the thrust bearing. This force can reach high intensity and cause large vibration amplitudes in the ship hull structure which surpass the allowable ISO limits, it can be annoying to the crew, and damage the onboard machinery and equipment.

A conventional approach in design of the shafting which considers separate analysis of the torsional and axial vibration modes and disregards the vibration transmission to the ship hull structure. From the design point of view it is not only necessary to satisfy line shafting structural requirements, such as the shafting geometry and material properties, but it is also important to know how a particular line shafting geometry influences vibration of the ship hull structure.

Shafting geometry and material properties include line shafting diameters, length, surface roughness, tensile and yield strength, elasticity and shear modules, notch factors, etc. All these characteristics must satisfy allowable limits proposed by selected Classification Societies, or simply strength requirements for dynamically loaded structures, such as fatigue life, stress concentration, etc.

Lack of information about axial force acting on the thrust bearing at the very early stage in the ship design can have substantial consequences, leading to large expenses for reduction of the vibration level of the ship structure in service.

Axial forces on the thrust bearing are mainly generated by following causes:

- mean propeller thrust,
- oscillation of the propeller thrust,
- torsionally induced axial forces due to propeller coupling,
- torsionally induced axial forces due to coupling that occurs in crankshaft of the main engine.

Modern ships have more efficient propulsion, thanks to new diesel engines which have commercially attractive design with low fuel oil consumption per unit power. These engines on the other hand introduce excitation frequencies close to the ship's hull natural vibration modes. The necessity to calculate torsionally induced axial vibrations is particularly obvious for the modern commercial ocean-going ships (bulk carriers, tankers, container ships, Ro-Ro, etc.), with low speed two stroke diesel engines as a main drive.

Vibration interaction and vibration coupling in the diesel engine driven propulsion systems have been intensified with new engine design and with engine's position

onboard. The engines have lower number of cylinders and lower operating speed. This is the reason why the engine excitation is close to the resonance frequencies of the hull structures, which together with large excitation forces create conditions that can affect the safe operation of the ship. Moreover, low speed engine demands bigger propeller in order to maintain required propulsion. Having larger, and low revolution propeller is better from the point of view of ship's propulsion, but not desirable for line shafting design because of higher torsional amplitudes and therefore higher stresses in the shafting.

Diesel engine makers, who usually bear responsibility for shafting design, mostly focus on the required strength criteria for the shafting and the crankshaft of the engine. Hull designers, on the other hand, will be pushed by often tight time schedule, to minimize their efforts in hull design in order to meet the requirements of Classification Societies. Information exchange between these two parties is seldom sufficient.

In this study torsional-axial coupling in the line shafting vibrations in merchant ocean going ships due to propeller action is studied. Taking into account axial force generated by torsional coupling will allow selection of an optimal engine which will better suit line shafting strength and ship hull dynamic response requirements.

In order to demonstrate the importance of the coupled vibration phenomenon, analysis was carried out using transfer matrix method to calculate separately the two basic vibration forms, and using finite element method to calculate the torsionally induced propeller thrust variations. Computer software programming was conducted on a personal

computer, in 'C' and 'C++'. [1]

In addition to calculations and theoretical analysis, vibration measurements on the line shafting and on the ship hull structure are presented (Appendices D and E) in order to confirm the connection between excessive vibrations on the hull and the propeller-coupled torsionally induced axial excitation.

I.1. LITERATURE REVIEW

Engine and propeller selection in the preliminary stage of ship design is described in MAN B&W Engine Selection Guide (1993), and it is entirely adopted here. Selection process is based on statistical analysis of numerous ships and the data presented in the Guide is a reliable source for conventional ship designs.

Engine excitation is well known and thoroughly defined in the literature (Mikulicic (1976)). For the engine chosen as main drive in this study (MAN B&W), excitation data is used in the form of tabulated harmonic components. Data is presented for the first 16 harmonic orders for tangential and radial harmonic pressures at crank pin of the engine. Mass and elasticity of the crankshaft of the engine, and damping values are adopted from the engine maker for accuracy, rather than calculated from the formulas presented in Homori, et al. (1989), Jeon, et al. (1974) and Johnson, et al. (1963).

A major problem in modelling the crankshaft is the characterization of its

[1] All computer programs used for vibration analysis in this thesis are original design of the author.

stiffness. Mathematical means available for modelling and computation of crankshaft stiffness are still not reliable enough. Finite element modelling has been found as an easier and more effective way to do so. Measurements are another possibility for accurate assessment of the stiffness of the crankshaft. Finite element approach is fully adopted by engine makers, and principles of the analysis are shown in Jakobsen (1991), Jenzer, et al. (1991), Bureau Veritas (1981) and Homori, et al. (1989). The procedure for stiffness calculation is to define detailed 3-D finite element model of the single crank-throw of the crankshaft, from which influence coefficients are calculated. Then by applying static condensation, a super-element is created that has all the properties necessary for simplified vibration analysis in which crankshaft is treated as a linear discrete model.

Propeller coefficients using Lifting Surface Theory are adopted here. Added mass, damping and interaction between different vibration modes are well explained and justified in Hylarides, et al. (1979) and Vassilopoulos, et al. (1981). Mathematical background of the Lifting Surface Theory can be found in Tsakonas, et al. (1973) and Van Gent (1975). In their three dimensional approach, propeller is operating in nonuniform wake field generated by the ship hull. Two dimensional theories can also define propeller forces (see Parson, et al. (1980), Parson and Vorus (1981) and Breslin (1975)), with somewhat lower accuracy than the lifting surface theory. Correction factors must be applied in this case. The wake field generated by the ship is difficult to estimate theoretically, and therefore experimental data are adopted from Hadler and Cheng (1965) and Lewis (1988).

Conventional line shafting design is based on required criteria established by

acting Classification Societies. These requirements are a set of rules that regulate line shafting geometry in accordance with strength and fatigue criteria. If the line shafting satisfies required criteria, it will be approved by Class. However, as rules do not require computation of forces transmitted to the structure, no such calculation is usually performed by shipbuilders, and the shipowner has no firm argument to require it.

There is a long record of publications related to the line shafting design. For example Van Manen and Wereldsma (1960) analyze propeller thrust variation as percentage of the average value of the thrust. However, they do not analyze propeller coupling, and the reason was that on the old designs coupling was almost insignificant. The other analysis by Lewis (1969) similarly did not include propeller coupling effect.

Engines of the older design were of much lower excitation per cylinder. Location of the engine on the ship was not pushed towards the aft of the ship, and therefore line shafting was more flexible. Operational speed of the propulsion installations was much higher, and the propeller was of relatively smaller diameter. All these characteristics have led to low torsionally induced axial thrust.

Numerous studies have been carried out which analyze propulsion system and its interference with surroundings. But, although first considerations and definition of the propeller coupling of different modes of vibration date as far as the late 1950's, this problem was not particularly interesting for the ship propulsion, because the generated forces were low. Lewis and Auslander (1960) have discussed propeller coupling, but due to very low excitation, even in a very detailed analysis such as that of Jonson and McClimont (1963), the propeller coupling was not considered. Analysis was performed

by applying same requirements that most of the Classification Societies require nowadays too; i.e. separate analysis of each vibration form.

It was not until oil crises and the jump in oil prices in 1970's, that engine makers were forced to design more efficient diesel engines, resulting in low speed, long stroke, small number of cylinders with high excitation per cylinder. Shipbuilders increased cargo space and pushed engine as close to the aft as possible, increasing line shafting stiffness at the same time. Propeller diameter increased in order to accommodate propulsion requirements. All these changes resulted in lower excitation frequency which came dangerously close to the resonant frequencies of the hull structure. Moreover, as the engine excitation rose, the torsionally induced axial thrust rose proportionally, creating optimal conditions for excessive ship hull vibrations.

With application of lifting surface theory (Breslin and Andersen (1994), Van Gent (1975); Tsakonas, Jacobs and Ali (1973); Sparenberg (1960)) to the marine screw propeller design and analysis, a method for accurate calculation of propeller generated forces and moments has been developed. Previously used lifting line theory was not as reliable. Moreover, development of computer technology allowed complex and lengthy computations to be performed.

Studies such as those by Breslin (1975), Hylarides and Van Gent (1979), Parsons, Vorus and Richard (1980), Parsons and Vorus (1981), dealt with propeller vibratory forces and propeller hydrodynamic reaction with surrounding media. Parsons and Vorus (1981) calculate added masses and damping for vibrating propeller using lifting line theory, with incorporated lifting surface corrections. Breslin (1975) in his

study uses lifting surface theory in definition of the vibratory forces generated by the propeller. Hylarides and Van Gent (1975) analyze propulsion system transverse vibrations using lifting surface theory. However, no particular discussions were carried out related to propeller coupling and its possible consequences.

One particularly useful analysis which applies lifting surface theory, by Hylarides and Van Gent (1979), provides on hand data about screw propeller hydrodynamic reactions in ship generated nonuniform inflow. Data are presented (tabulated and in graphical form) only for Wageningen B screw series. The fact that this screw series is widely used gives high credibility to Hylarides and Van Gent's study, providing designers with necessary information for initial estimation of the forces generated by the propeller. Lack of similar studies for other propeller series put additional requirements on the designers. It requires either calculation of the propeller's hydrodynamic coefficient using lifting surface theory, or in case accurate propeller data are not available, making a rough estimate about possible excitation.

Studies that considered the problem of propeller vibration coupling were not of interest since forces caused by such an effect on propeller are not at a dangerous level. Jeon and Tsuda (1974) gave theoretical analysis of the coupled torsional and axial forced vibration of the marine diesel engine shafting. They considered only coupling effect that occurs in the crankshaft. The study presented by Parson (1983) examined mode coupling on the propeller in torsional and longitudinal shafting vibrations. More recent studies by two major engine makers, MAN-B&W and Sulzer, analyzed coupling effect in the crankshaft primarily, and discussed application of the axial vibration dampers and

detuners installed on the free crankshaft end. Jenzer and Welte (1991) conducted the analysis for New Sulzer Diesel engine showing the significance of the crankshaft's capability to couple torsional and axial vibrations. Jacobsen (1991) in his paper discusses crankshaft coupling on MAN B&W engines. Although his attention was primarily on the crankshaft coupling, Jacobsen also mentioned problems that can arise from hydrodynamic forces generated due to propeller operation in unsteady wake field behind the ship, and suggested that propeller generated thrust depends on shafting design.

The accent in this study is on torsionally induced axial vibrations due to propeller coupling. The axial vibrations in the line shafting are separated from the axial vibrations in the crankshaft of the main engine by the thrust bearing. Therefore, each coupling effect can be treated separately. In this study particular attention has been drawn to the problems that relate to optimal selection of the line shafting geometry from the point of view of its influence on the intensity of the axial force generation and transmission.

The parameters influencing the line shafting design, the excitation from the engine and the propeller are discussed in Chapter II. Chapter III describes the conventional approach in line shafting design. Chapter IV presents the torsionally induced axial vibrations due to coupling including application of the analysis on an example and discussion of the results. Finally Chapter V provides conclusions.

CHAPTER II

STIPULATIONS OF THE LINE SHAFTING DESIGN

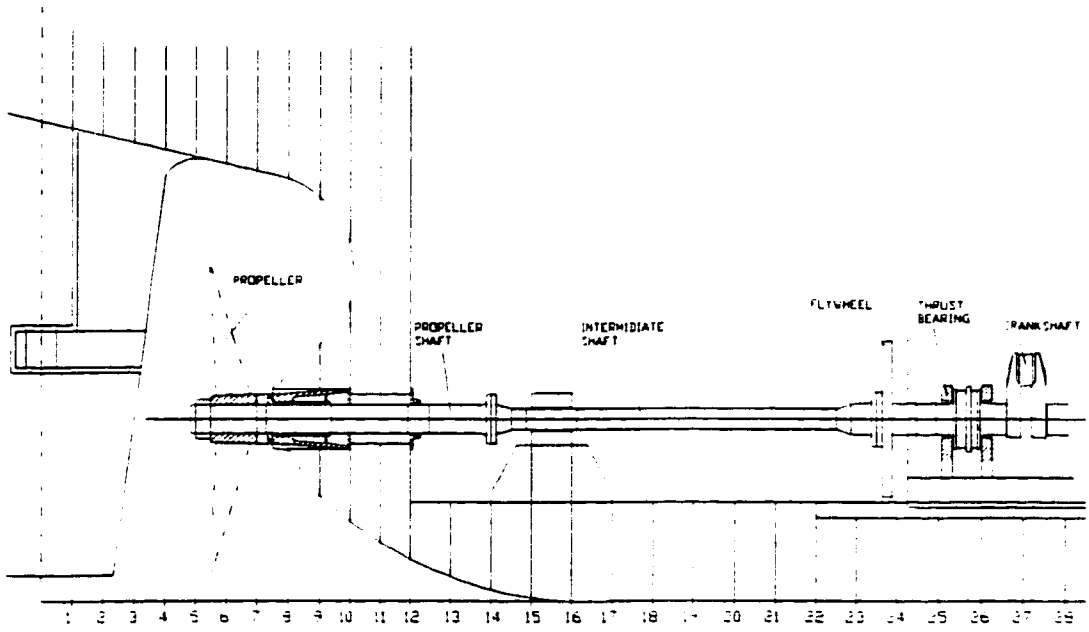

Figure II Line Shafting System

The line shafting design will be characterized by the following parameters:

- structural characteristics of the ship
- selection of diesel engine and propeller
- diesel engine characteristics, and
- propeller characteristics.

All these parameters, coupled with commercial aspects, influence the shafting design. Detailed explanation of each particular parameter and its contribution to shafting design is presented below.

In Figure II a typical propulsion system for a merchant ocean going ship is presented. Such a propulsion installation consists of diesel engine as a main drive and propeller which are directly coupled via line shafting. The line shafting is divided into intermediate and the propeller shaft because of different strength criteria applied to each of them. The thrust bearing located in the main engine provides support for the thrust force generated by the propeller and the main engine.

II.1. STRUCTURAL CHARACTERISTICS OF THE SHIP

In order to be competitive on the market and to reduce (or at least not to increase) the price of the ship, ship makers are searching for different cost-reduction approaches. The approach which results in the highest cost reduction is to reduce the thickness of the hull steel plates. Less material installed will make ship lighter, therefore cheaper, and it will increase ship's capability to carry more cargo. In the long run these benefits can be annihilated because a thinner structure is more susceptible to corrosion and vibration. A lighter ship means that ship structure will be more sensitive to the exciting dynamic

forces, resulting in higher stress levels[2], particularly the deck house which has to accommodate crew and which holds navigation and other sensitive equipment.

Maximization of the cargo area is another reason why the ship's superstructure is almost directly above the engine room at the very rear of the ship, making it very sensitive and directly exposed to the vibration that originates from the engine, from the propeller and their mutual interaction.

All of the above mentioned details show the importance of performing more thorough analysis than the usually performed (and required by Classification Society), in order to secure information about the forces acting on the ship structure. This will allow one to choose the engine with the lowest number of cylinders for the particular ship, which will still maintain ship's safety from the exciting dynamic forces generated by the engine, propeller and sea.

Analysis of the torsionally induced axial vibrations is important in order to provide information about forces acting on the ship structure, which are often neglected. Moreover, these computations are not particularly time consuming, nor expensive, compared to the comprehensive analysis of the whole ship structure. By not performing analysis of this kind, ship owners are forced to accept less competitive solutions such as to increase the number of cylinders in order to reduce excessive structural vibrations.

---

[2] Hull structure exposed to the higher stresses can be designed of high tensile steel, instead to increase the thickness of the plate. However, usage of high tensile steel is very much disregarded by ship owners for the reason of corrosion.

II.2. SELECTION OF THE DIESEL ENGINE AND PROPELLER

Selection of the engine and propeller depends on the demands of the ship owner, i.e. the purpose of the ship and intended operating profile. The power and speed of the engine are selected according to basic ship characteristics: the type of the ship, its deadweight and speed. The type of engine and its cylinder number should be optimized according to the available space for the engine, and according to preliminary propeller diameter and speed, overall operating cost, and vibration and noise in the ship. In order to optimize these parameters some iterative procedure needs to be applied when choosing the engine and defining the propeller. At the beginning of the project stage, with only the ship size and speed stipulated, the other characteristics such as:

- length between perpendiculars (Lpp)
- breadth (B)
- draught (T)
- block coefficient (δ)
- engine power
- propeller size

need to be chosen based on the existing statistics of shapes; as provided in Figures II-1 to II-3.

The ship geometry is defined first from the diagram in Figure II-1. Engine power is estimated from Figure II-2, for given ship speed and deadweight tonnage. And from Figure II-3, the propeller diameter is chosen.

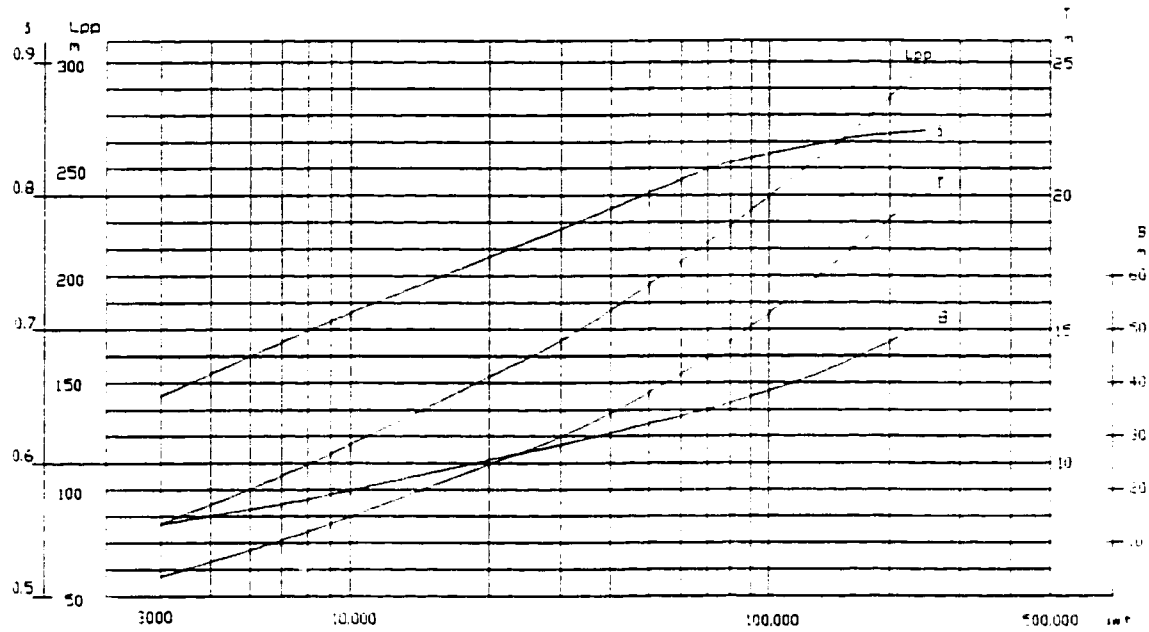

Figure II-1 Main particulars of bulk carriers, tankers and general cargo ships (Source MAN B&W Project Guide 1993)

Having defined the main specifications for the ship, the engine can be selected. Main criteria will be the overall engine cost, which includes the purchase price, and engine exploitation price. The larger the engine cylinder number, the higher the price. Same goes with fuel consumption and maintenance expenses. Moreover, for engines with larger number of cylinders, cargo space will be reduced in proportion to required space for additional cylinders. Smaller number of cylinders will induce proportionally lower fuel consumption. Maintenance cost will be lower for the engines with smaller number of cylinders.

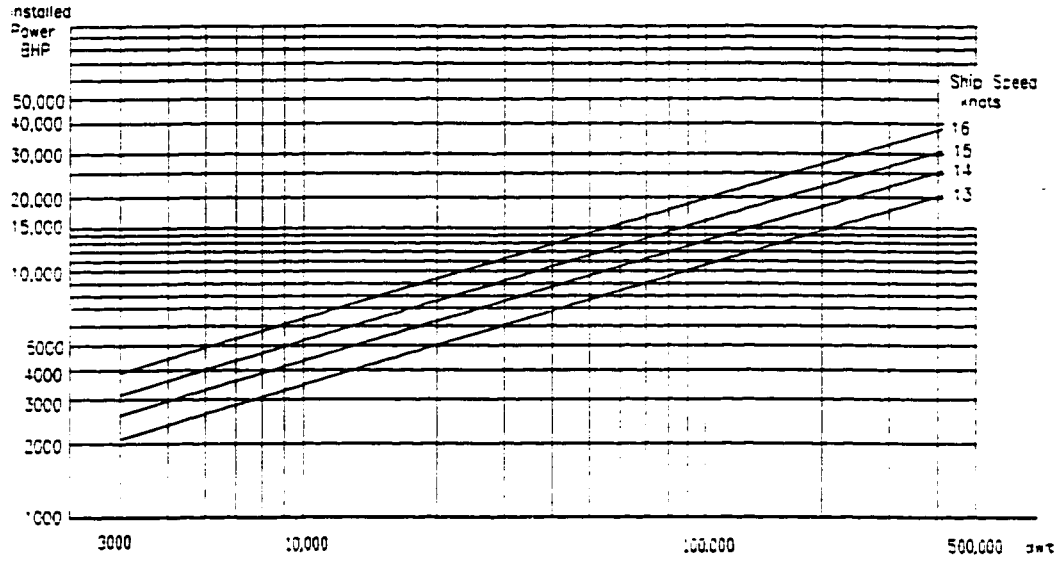

Figure II-2 Installed power for bulk carriers, tankers and general cargo ships (Source MAN B&W Project Guide 1993)

However, there are tradeoffs between the benefits of the modern diesel engines with very low number of cylinders and disadvantages linked to the engine's dynamic nature, such as:

- The lower the number of cylinders of the engine, the lower the operating speeds of the engine, causing engine frequency to get closer to ship hull's natural frequencies
- Irregularity of the engine excitation is higher with smaller cylinder number.

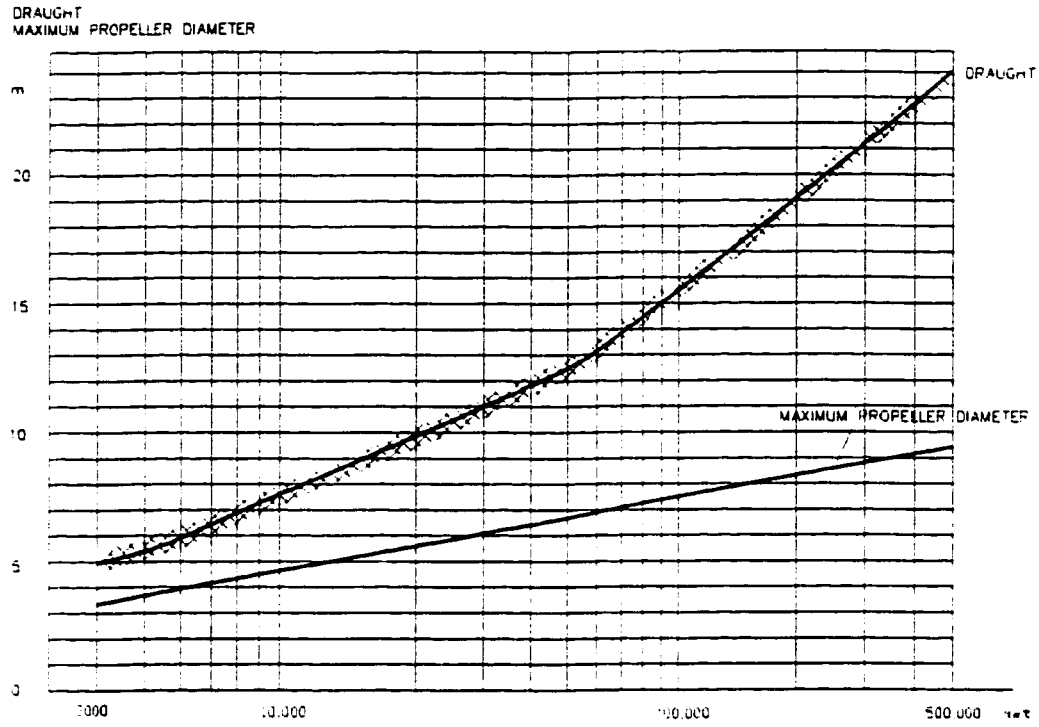

Figure II-3 Propeller Selection, tankers and general cargo ships (Source MAN B&W Project Guide 1993)

II.2.1. **Engine Selection Example 40,000 DWT Tanker**

The chosen example is an oil tanker of 40,000 DWT that must maintain an operational speed of 14 knots. A vessel of this kind is very common, and it is selected as an example of engine selection procedure, as well as a representative for the design of the line shafting.

From Figure II-1 to II-3, ship's main particulars are found to be:

- length between perpendiculars Lpp = 176 m

- breadth B = 30 m

- draught T = 12 m

- block coefficient δ = 0.785

- engine power P = 9,200 BHP

- propeller diameter D = 6.15 m

The four cylinder engine has the lowest number of cylinders in use, and these engines are very rare. The problems with four cylinder engines are their unbalanced inertia forces of the first order, and high irregularity of the excitation torque. The solution with five cylinder engine can maintain much lower torque irregularity than a four cylinder engine. Between the two main world wide engine producers, i.e. MAN B&W, and Sulzer, a five cylinder engine from the MAN B&W is chosen.

To maintain the speed of the ship at 14 knots, engine must have a minimum power of 6,800 kW (9,200 BHP). For a five cylinder engine, required power per cylinder will be 1,360 kW. From the engine producer catalog (in this case MAN B&W Engine Project Guide) engine with maximum continuous rating of 7,200 kW (9,800 BHP) and nominal speed of 123 rpm is chosen. Higher power than actually required is welcome to accommodate the sea margin (heavy sea, wind), deterioration of propeller, and fouling of the ship hull that can be expected during the ship exploitation.

Selected engine has following main particulars:

- cylinder diameter 600 mm

- stroke 1.9 m

- L/R = 2.407

- Maximum combustion pressure 130 bar

- Main indicated pressure 17.2 bar

II.3. **DIESEL ENGINE CHARACTERISTICS**

Modern diesel engines for commercial ocean going ships emerged in the nineteen seventies as the result of the world oil crisis. High prices of the fuel oil required new engines which would have lower oil consumption for the same power developed.

The development was oriented toward increase in efficiency of the engine; i.e. to maximize work done on the crankshaft from the energy accumulated in the fuel. To achieve that result, combustion pressure is increased and stroke of the piston is extended. Engine revolution is lowered, while cylinder diameters are made larger.

All these changes lead to the present engine, which is a two stroke crosshead diesel engine with the following characteristics:

- high efficiency (thermal efficiency is greater than 95%)

- low speed (from 74 to 200 rpm)

- long stroke (stroke to bore ratio is increased to 3.8 : 1)

- high combustion pressure (120 bar and higher)

- low fuel consumption (down to 170 g/kW per hour)

- high power developed per cylinder (up to 4500 kW for 900 mm cylinder diameter).

- small number of cylinders (except container ships)

Engines are not unique products tailor made for the particular installation. Each engine type (from the same maker) is covering a certain range of rated powers and speeds, and therefore in early project stage engine can be optimally chosen to suit power and speed requirements of the ship. However, engine excitation is also well known and available from the engine producer, so that thorough and accurate analysis is possible at early design stage of the ship. As far as of engine excitation and force transmission to the surrounding structure, modern engines have characteristics as described below.

Engines are high and are of relatively flexible structures, that require additional stays (top bracing) to be installed to support the engine top, and minimize engine's movement relative to its bedframe. Such stays solve the problems for the engine, but transfer the forces to the ship structure producing an additional transverse excitation. This excitation can cause significant transverse vibration if hull structure supporting engine's stays is not stiff enough and if it falls in resonance with the exciting force. Solution to this problem is to increase stiffness of the structure in the engine room, or to install hydraulically controlled stays.

Engine is rigidly connected to the foundation. Due to low operational speeds and heavy weight of the engine, it is not possible to mount it resiliently to the ship structure. Therefore, engine will directly excite the surrounding structure through the foundation. Engines have high installed power, and there is no commercially acceptable possibility to detach the engine elastically from the propulsion system; i.e. no elastic coupling is

possible. This results in high sensitivity of the propulsion system to the engine excitation, and intensifies effects of the propeller axial and torsional excitation coupling.

Engines have thrust bearing incorporated in their bedframe. The primary function of the thrust bearing is to provide support for the propeller reaction forces. Thrust forces are dynamic in nature, caused by propeller operation in unsteady wake field, and by induced forces due to coupling effect that occurs on the propeller. Thus the thrust bearing will function as the point at which longitudinal forces, generated by and on propeller, are transmitted to the ship hull structure.

Dynamic characteristics of modern engines are their major disadvantage. Only proper consideration of these forces can ensure good design of the ship. These forces are of high intensity because of the characteristics of the modern diesel engines and propulsion shafting installation, i.e :

- high engine excitation
- relatively rigid engine-propeller connection, and
- rigid mounting of the engine to the structure.

II.4. ENGINE EXCITATION

II.4.1. General

In order to obtain maximum output at the crankshaft from the fuel burned in the engine, modern diesel engines are turbocharged, have high mean indicated pressure,

extended expansion and low revolution. With increased efficiency of the energy conversion in the engine, the excitation forces per cylinder are increased too. Due to irregular nature of these forces, problems with the design of the propulsion systems and ships are also more likely. Even though the basic principles of the reciprocal internal combustion engines are not changed (with the improvement in the engine's design) it is still important to review the source of the engine-caused vibrations and to show how they are implemented in propulsion system design.

II.4.2. **Forces and Moments**

Forces and moments produced by reciprocating piston engine can be separated into two categories:

- gas pressure forces, or combustion forces, and
- inertia forces of the masses in rotational and translational motion.

These forces can be further divided, considering their place of action, into forces that are acting on:

- engine structure, and
- crankshaft.

II.4.2.1. *Forces Acting on the Engine Structure*

Forces acting on engine structure, and from there transmitted to the surrounding hull, are an important part of the overall ship information which is usually neglected in the early ship designs. Engine is not only generator of the exciting forces, but it also transmits propeller generated forces via thrust bearing (that is incorporated within engine structure), to the hull structure.

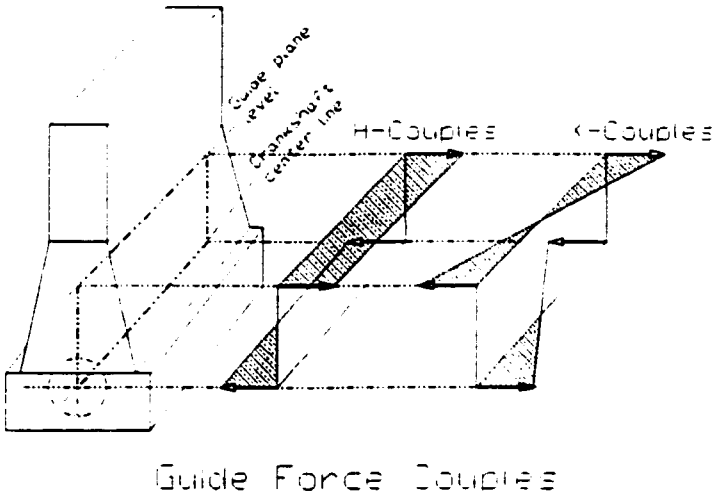

Figure II-4 Engine Guide Force Couples

Dominant forces acting on the engine structure originate from combustion process (so called Guide Force Couples - Figure II-4), and from inertia of masses in motion (external forces).

Guide force couples result from transverse reaction forces acting on the crosshead as shown in Figure II-4, and are the cause of rocking (H-couples), and twisting (X-couples) of the diesel engine. These forces can get into resonance with engine foundation structure. Solution for the possible vibrational problem is in installing

transverse stays (top bracing) that connect the engine top structure to the ship hull, stiffening the structure and increasing natural frequency of the assembly of the engine and engine's foundation, thus avoiding eventual resonance.

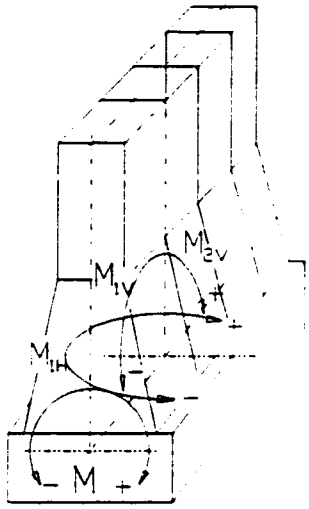

Figure II-5 Engine External Moments

Another important excitation is generated from engine unbalanced masses in motion. The first (M_{1V} and M_{1H}) and the second order forces (M_{2V}) only, are of importance. First order vertical and horizontal forces are produced by masses rotating with crankshaft speed, and second order forces are those of two times engine speed that are acting in vertical direction only. Both of these forces lose in intensity as the number of cylinders of the engine increases. For lower cylinder numbers, forces need to be balanced with additionally installed compensators. Detailed consideration of the structural forces and their effect on the ship hull is beyond the scope of this study.

For shafting design, however, only engine exciting forces acting on the crankshaft are of interest. Those forces are combustion and inertia forces, that cause

torsional, axial, and transverse vibrations, and moreover couple these three vibration forms.

II.4.2.2. *Forces Acting on the Crankshaft*

II.4.2.2.1. Combustion Forces

Combustion forces are in direct relationship with the quantity of fuel injected and burned in the cylinders during the combustion process. The fuel quantity burnt depend on the structural and thermal capability of the engine, to sustain forces developed during the fuel oxidation. The force on the crankshaft that is generated as a result of the combustion activity is partly reduced by friction. Force is transmitted from the combustion chamber via piston and crank mechanism to the crankshaft. The purpose of the crank mechanism is to enable transformation of the linear motion of the piston into rotational motion of the crankshaft. This mechanism has only one degree of freedom, which is piston translation.

For modern long stroke diesel engines the crankshaft mechanism consists of:

- piston,
- piston rod,
- cross-head,
- connecting rod, and
- crankshaft.

Force on crankshaft is divided into radial force and tangential force. Radial forces on the crankpin bearing are brought in equilibrium by reaction in main bearings of the engine, and are the cause of bending and axial vibration of the crankshaft. Tangential forces, and the corresponding torque produced by them, cause the circular motion of the crankshaft. Torque transmitted via line shafting is absorbed on the propeller and converted into axial movement of the ship.

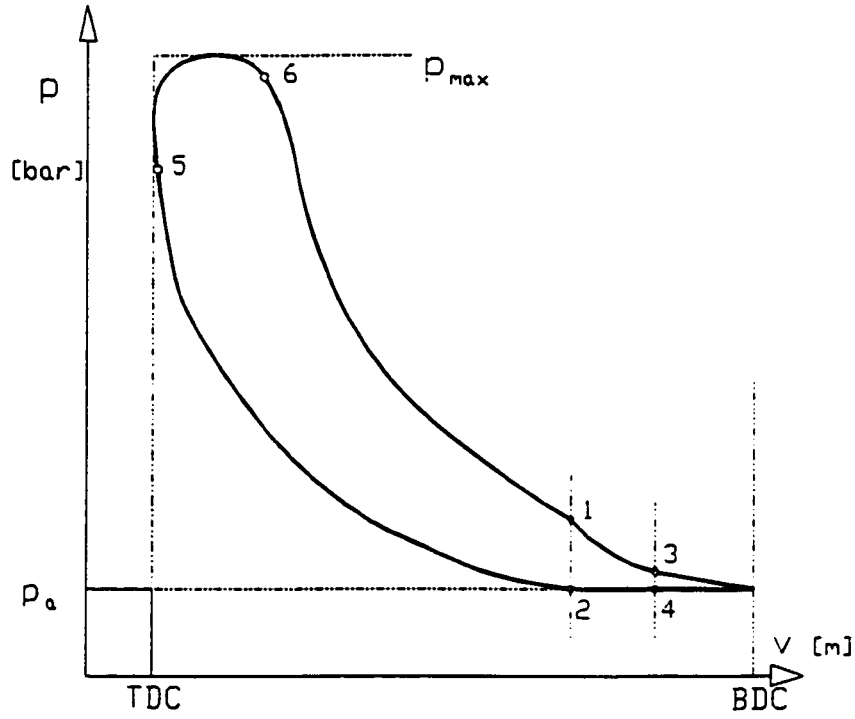

Figure II-6 Indicated Diagram for 2-stroke Diesel Engine

Tangential and radial forces acting at the crankpin are usually represented in the form of pressure; i.e. forces are divided with cylinder's cross section area. This is convenient, for the same excitation data (harmonic components) can be used for the

engines of the same series, which have different diameter of the cylinders and the same combustion pressures.

Harmonic Components. The engine excitation is of appreciable value, and it is usually presented in the form of "indicated" or *p-v* diagrams (Figure II-6 represents indicated diagram for a two stroke diesel engine).

Indicated diagrams have specific volume[3] on the abscissa, and indicated pressure on the ordinate. More detailed explanation about *p-v* diagrams follow.

Indicated diagrams are directly recorded from the engine for desired number of indicated pressures. These diagrams are then analyzed using Fourier spectral analysis, and data are usually presented in tabular, or polynomial form. Result of the spectral analysis provides harmonic forces that are reduced to the cylinder area; i.e. harmonic pressures. Reduced harmonic forces are presented as a function of the chosen number of harmonic orders, by Fourier analysis. Number of harmonic orders will depend on the particular exciter. For low speed diesel engines considered in this thesis, the highest harmonic order that has some influence on the response of the vibrating system, is the 16^{th} harmonic. The case may be different for different types of exciters.

[3] Specific volume is cylinder's volume reduced to piston area.

Mean indicated pressure[4] is related to the engine speed (see next section). This relationship is enforced by the engine's governor which controls engine performance and regulates engine load depending on its speed.

For the ship propulsion installation relationship between mean indicated pressure and engine speed is a quadratic function[5], and it is called "propeller low".

II.4.2.3. Forces Acting on the Crankshaft - Mathematical Formulation

II.4.2.3.1. Gas Forces

The force produced in cylinder by gas expansion (Figure II-7) during the power stroke is equal to:

---

[4] Instead of mean indicated pressure, the mean effective pressure may be considered when mechanical losses are taken into account.

[5] Engine power to speed relationship is a cubic function for propulsion installation:

$$\frac{P_1}{P_2} = \left(\frac{n_1}{n_2}\right)^3 \quad , \quad \left[\frac{kW}{kW}\right]$$

Power to mean pressure relation is linearly dependent on the engine speed and therefore relationship between pressure and speed is quadratic:

$$\frac{p_{mep_1}}{p_{mep_2}} = \left(\frac{n_1}{n_2}\right)^2 \quad , \quad \left[\frac{bar}{bar}\right]$$

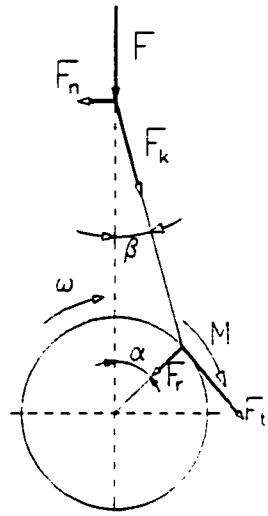

Figure II-7 Combustion forces

$$F = p_g \frac{d^2 \pi}{4} \tag{II-1}$$

where p_g is gas pressure, and d is cylinder diameter.

This force is broken down into:

- normal component F_n which is a result of piston's interaction with cylinder, and crosshead interaction with crosshead guide

$$F_n = F \tan \beta \tag{II-2}$$

- and a component acting along the connecting rod.

$$F_k = \frac{F}{\cos \beta} \tag{II-3}$$

The component acting along the connecting rod (F_k) can be further partitioned into its:

- tangential part that is causing torsional motion

$$F_t = F \frac{\sin(\alpha + \beta)}{\cos \beta} \qquad \text{(II-4)}$$

- and radial part that is resulting in bending and elongation of the shaft

$$F_r = F \frac{\cos(\alpha + \beta)}{\cos \beta} \qquad \text{(II-5)}$$

Torque on the crankpin produced by tangential force is given by:

$$T = F r \frac{\sin(\alpha + \beta)}{\cos \beta} \qquad \text{(II-6)}$$

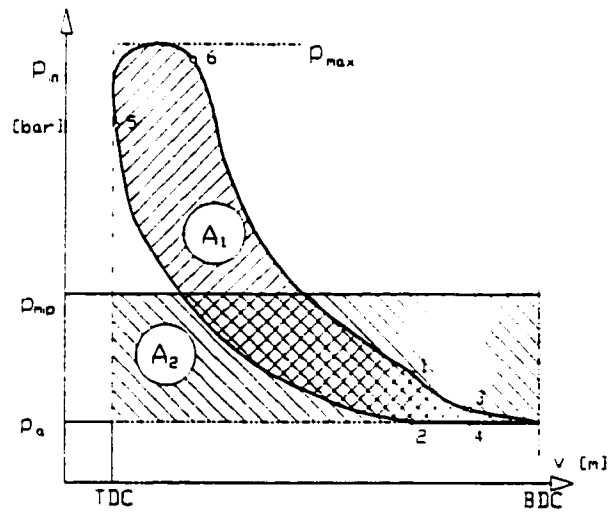

Figure II-8 Work-done during combustion process

Gas pressure is not constant during an engine cycle. Its value changes with piston stroke. In order to simplify selection of the harmonic components for the selected operating condition, mean indicated pressure is introduced (Figure II-8).

Mean indicated pressure covers the same area (rectangular area A_2) in the *p-v* diagram as a real indicated pressure does (area A_1). This means that the work done by real forces will be equal to the work done by the mean forces. Mean indicated pressure is constant over one complete engine cycle and because of this property it is a convenient parameter to relate engine revolution to the developed output.

As mentioned above, the area below the curve of a developed *p-v* diagram corresponds to the energy released in the combustion process. A number of such diagrams are taken in order to cover whole engine speed range. Each diagram, for each speed (mean indicated pressure) is thus valid for one steady-state engine condition.

Moreover, indicated pressure developed in the cylinder, is usually reduced to the equivalent tangential and radial 'pressure' acting on the crankpin. Benefits of this are to get harmonic components that are ready to use for torsional, axial, or transverse vibration analysis. Harmonic components are now easily accessible for vibration analysis, and for each speed corresponding to one mean indicated pressure, harmonic component can be selected.

II.4.2.3.2. Inertia Forces of Reciprocating Masses

Inertia forces of the reciprocating masses can also be reduced to:

- tangential, and

- radial forces acting at the crankpin (similarly to the gas forces).

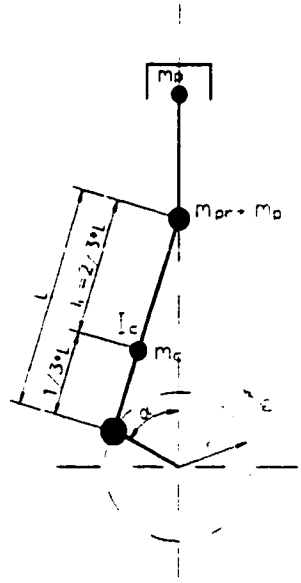

Figure II-9 Reciprocating inertia forces

The reciprocating mass is accelerating during the engine revolution and the intensity of inertia force is changing with acceleration. The process is repeated with each revolution of the shaft.

Reciprocating masses consist of:

- piston mass (plus piston rings and pistons journal) (m_p)

- piston rod mass (m_{pr}), and

- portion of the connecting rod mass that is performing translatory motion (m_{cr}).

- connecting rod mass (m_c)

The connecting rod mass participating in reciprocating motion can be approximated by (Jeras (1975)):

Total mass in reciprocating motion is then:

$$m_{cr} \approx \frac{1}{3} m_c \tag{II-7}$$

$$m_r = m_p + m_{pr} + m_{cr} \tag{II-8}$$

The piston's distance from top dead center (TDC) h is expressed in terms of angular crankshaft displacement α:

$$h = r[(1 - \cos\alpha) + \frac{\lambda}{4}(1 - \cos 2\alpha)] \tag{II-9}$$

where λ = r/L, h=h(t), and $\alpha=\alpha(t)$.

Differentiating the distance h twice with respect to time, acceleration is found to be:

$$a = r\omega^2(\cos\alpha + \lambda\cos 2\alpha) \tag{II-10}$$

where $\omega=d\alpha/dt$.

Therefore, force produced by reciprocating masses is:

$$F_{in} = -m_r r\omega^2(\cos\alpha + \lambda\cos 2\alpha) \tag{II-11}$$

The sign of the force is negative, i.e. it has the opposite direction to the acceleration that causes it. As with the gas forces, inertia forces of the reciprocating masses can be reduced at the crankpin position, and partitioned into their tangential (II-12) and radial components (II-13):

$$F_{in}^{t} = F_{in} \frac{\sin(\alpha + \beta)}{\cos\beta} \qquad \text{(II-12)}$$

$$F_{in}^{r} = F_{in} \frac{\cos(\alpha + \beta)}{\cos\beta} \qquad \text{(II-13)}$$

For the torsional vibration analysis, the torque on the crankshaft is of interest. Therefore, the torque on the crankpin produced by tangential force is obtained by simple multiplication by the crank-throw radius:

$$T_{in} = F^{t}_{in} r \qquad \text{(II-14)}$$

Expanding these forces into harmonic components using Fourier analysis, and adding them to the gas forces results in total engine excitation.

II.4.3. **Expansion of the Excitation into Harmonic Series**

Fourier Analysis. A periodic function can be expanded into series of sine and cosine elements:

$$f(t) = A_o + \sum_{n=1}^{\infty} \left(A_n \cos(n\omega t) + B_n \sin(n\omega t) \right) \qquad \text{(II-15)}$$

Coefficients A_n and B_n are amplitudes of vibration at frequency $n\omega$, and purpose of harmonic analysis is to define these coefficients.

$$A_o = \frac{1}{T} \int_{-T/2}^{T/2} f(t)\, dt \qquad \text{(II-17)}$$

$$A_n = \frac{2}{T} \int_{-T/2}^{T/2} f(t) \cos(n\omega t)\, dt$$

$$B_n = \frac{2}{T} \int_{-T/2}^{T/2} f(t) \sin(n\omega t)\, dt \qquad \text{(II-16)}$$

where T is time period.

After coefficients are calculated, sine and cosine components are known, and computation of the vibrational response can be performed by using harmonic analysis.

II.4.4. **Response Summation, Synthesis**

Synthesis. Summation of individual responses to the complex excitation should be done geometrically; i.e. superimposing separately responses to sine and to cosine components of excitation. Moreover, it is usually the case that more than one exciter exists in the system. For example, diesel engine is considered to have as many exciters

as it has cylinders. In such a case cylinders' excitations are equally distributed within one complete engine cycle (one revolution of the crankshaft for two stroke engines). This phase shift is usually represented by phase angle diagrams (Figure II-10).

For a two stroke, 5 cylinder engine there will be five power-strokes in one revolution of the shaft, and spacing between cylinders that are firing will be 72 degrees. Depending on firing order, phase angle will vary for each cylinder in reference to cylinder number one.

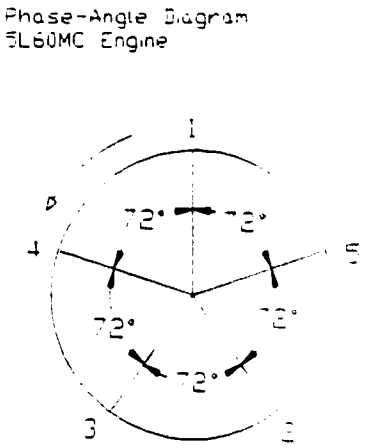

Figure II-10 Phase angle diagram for MAN-B&W 5L60MC engine

Excitations are simultaneously applied to all cylinders considering their phase shift, and the response (displacements, forces, and stresses) is obtained for each harmonic of excitation force. If the number of the harmonic-excitation-order p is a whole-number multiple of the number of cylinders, then the product of the p and phase angle will be the whole-number multiple of π. This means responses to the engine excitation can be summed as if the phase lag is zero (cosine to cosine, sine to sine). Thus, the frequencies

of these harmonics will be the most dangerous operating frequencies for the propulsion system.

II.5. PROPELLER CHARACTERISTICS

The exact excitation of the propeller would not be known until the sea trial of the ship is over and appropriate measurements are taken. Propeller is tailor made for a particular ship, and its performance is tested only on scaled models. Moreover, it is not only the propeller itself that defines its performance, it is also the ship's design that influences it.

In propeller design stage its diameter, pitch, blade section and developed thrust are defined so that propeller is able to absorb power delivered from the engine, and to maintain required speed of the ship. These parameters are derived from the scale model tests in the tunnels, and for common ship structures and propellers, results are accurate with low error margin.

Moreover, the theory describing propeller excitation is well established for the standard propeller types, with numerous research data available to support it.

Therefore, there are no exact numerical data which define propeller excitation (similar to the engine's) available, and in the design stage of the ship theoretical means need to be used to define it.

Propeller efficiency is increased in modern propulsion installations; efficiency is higher when the propeller revolution is lower. This matches perfectly with the modern low revolution diesel engines and would have given an ideal propulsion system, except for the increased excitation of the engine and higher structural vibration of the ship. Moreover, performance of propellers with low revolution and, therefore, bigger diameter is better because of lower possibility of occurrence of the cavitation.

Historically, the propeller excitation was considered less important than the excitation of the engine. Nowadays it is receiving more attention, particularly with heavy coupling effect of the torsional and axial vibrations. In modern commercial ocean going ships propeller excitation deserves at least the same attention as does the engine. In the following, the propeller thrust fluctuation generated by propeller will be examined in detail from the point of view of different shaft designs.

II.6 PROPELLER EXCITATION

II.6.1. Assumptions

The following assumptions need to be taken into account when considering presented data and equations:

- Propulsion is achieved with single-screw operating abaft the ship
- Fluid in which the propeller operates is considered ideal and incompressible
- Propeller operates with constant speed of revolution (i.e. steady condition)

- Propeller is assumed to be a rigid body

- The wake field is spatially nonuniform and time invariant

- Variations of the angle of attack of the propeller is considered to be small, which allows for application of linear theory

- Thickness of the blade is neglected

- The Cartesian coordinate system considers positive horizontal axis along the shaft center line in the direction of motion of the ship

II.6.2. **General**

The propeller that operates abaft the ship in a nonuniform wake field generates vibratory forces and moments. These dynamic forces and moments can be of high intensity causing damage to propellers, excessive vibration of the hull and machinery, and affecting the efficiency of the crew in performing their duties. Therefore it is of crucial importance to consider these forces when designing the ship. Unfortunately this is still not standard practice for most shipbuilders.

Propellers are nowadays recognized to play at least the same, if not a more important role as diesel engines do, in causing vibrations of the ship. Propeller can be set into vibration by its surroundings and can itself generate vibratory forces and moments. Moreover, due to the hydrodynamic environment in which operates the

propeller, it can couple torsional and axial vibrations producing additional forces and moments.

From the point of view of the interaction with the surrounding, the propeller generated forces can be divided into:

- Hull forces; directly affecting the hull structure via propeller excited surrounding fluid and
- Propeller forces; transmitted through the line shafting system and bearings to the machinery and indirectly to the ship structure.

It is important to know, predict, and measure direction and intensity of forces acting on propeller and forces generated by it, in order to use this information for:

- propeller design,
- design of the line shafting and machinery elements (bearings in particular), and
- ship hull design.

This study will deal only with propeller forces which influence line shafting vibrations and, indirectly, the hull. The impact of the propeller generated forces on propeller design will not be discussed.

The propeller forces originate in part from its steady rotation in a non-uniform wake field, and partly from forces generated by propeller's own vibrations in homogeneous flow; i.e.:

- propeller that rotates in nonuniform inflow will be forced to vibrate with intensity that is a function of the character of forces generated on propeller by inflow and

- propeller's own vibrations are those induced by the main drive through line shafting.

A number of different analyses and numerous experimental measurements have been conducted in order to explore and explain propeller's behavior, to develop appropriate tool for its design and to define forces and moments that are generated by it. Due to complexity of the problem none of the methods are universally applicable.

Adopted data and formulae used to explain propeller behavior in this thesis, are based on the Lifting Surface Theory which is presently considered to be the best available tool for propeller analysis and design. However, comprehensive explanation of the origin of adopted methodology used for vibratory forces calculation, as well as details of the Lifting Surface Theory itself, is beyond the scope of this thesis and it will not be discussed in detail.

The aim of this thesis is to consider the coupling of torsional and axial vibration of the line shafting through the propeller and to incorporate this in shafting design. This is made possible by adopting the lifting surface theory formulation which can define the relationship between different forms of propeller vibrations.

The performed computation in the following text regards propeller as a rigid body in the homogeneous inflow. The analysis performed considers the coupling effect

between torsional and axial vibrations that takes place on the propeller and results in oscillation of the propeller thrust force.

II.6.3. **Physical Characteristics of the Propeller**

The purpose of the propeller is to produce needed thrust for required speed of the ship. Optimal propeller would be the one which produces required thrust and has maximum possible diameter and lowest revolution; i.e. which has maximum efficiency. Propeller's speed and diameter depend on characteristics of the main drive and structural design of the ship respectively; i.e. ship's aperture influences propeller geometry limiting its maximum diameter, and the main drive defines its speed.

Generally speaking, an optimum propeller would need to be tailor made for the ship, and its exact performance would not be known until measurements are performed on the real ship. This fact has lead to the search for propeller design methods that will give reasonably accurate, and easy to calculate information about propeller performance and forces generated by it.

Modern computational methods can provide relatively reliable and close to optimal propeller design that can be classified as "conventional" (see Hadler and Cheng (1965)). Still, for new ship forms which do not have sufficient measurements, these theories may not be very accurate.

Therefore, it is common practice in propeller selection to choose the propeller geometry from the well known and established propeller design Series, such as:

- the Netherlands Ship Model Basin (NSMB), Troost and Van Manen series,
- Admiralty Experimental Works (A.E.W.), Gawn series,
- King's College Newcastle (KCN) series,

and others (see O'Brien (1962)). The Series have well established reputation and proven performance record and represent, therefore, a conservative approach in selection of the propeller. Choosing the propeller a propeller series means to restrict the design to already predefined geometry, such as cross section characteristics and hub radius. However, main propeller parameters need to be defined for each vessel in accordance with required thrust and ship speed.

In this thesis propeller design is chosen from the NSMB Wageningen B4 series (see Van Lammeren, Van Manen and Oosserveld (1969)). The reasons are the following:

- this is a frequently used series for merchant ships and there is high expectation that Wageningen B4 will be used for the category of ships considered in this study
- numerous research, experimental and measurement data are available for this series
- the actual ship that is used as example in this thesis has the same series propeller (Wageningen B4)

The Wageningen B-Screw series have airfoil blade section near the hub which gives better performance than those propellers of circular-back section, or elliptic ones.

However, in order to reduce cavitation, blade tips are wider, and circular-back section is adopted near the blade tips.

II.6.4. **Propeller Forces and Moments**

Positive direction of forces and moments generated by the propeller are displayed in Figure II-11.

Apart from the mean thrust produced by propeller, there are vibratory forces and moments that are generated by its operation in nonuniform wake field[6], and those generated by its own vibrations. Due to propeller rotation in nonuniform inflow, which is considered to be time invariant and periodical, angle of attack will vary and therefore pressure distribution over the blades will be periodical and unsteady. Unsteady pressure causes load variation on blades and vibration of the propeller. Moreover, variation of the angle of attack on the propeller blades due to its vibration in homogeneous wake field results from propeller's elastic connection to the main drive, and it is analyzed in detail in Chapter IV.

Two distinct types of behavior of the propeller reactions with its surrounding will, therefore, be distinguished:

- propeller response to operation in nonuniform wake field when it rotates at a steady speed and

---

[6] Hydrodynamic coefficients are adopted from Hylarides and Van Gent (1979).

- reactions generated by its own vibrations in steady and homogeneous inflow.

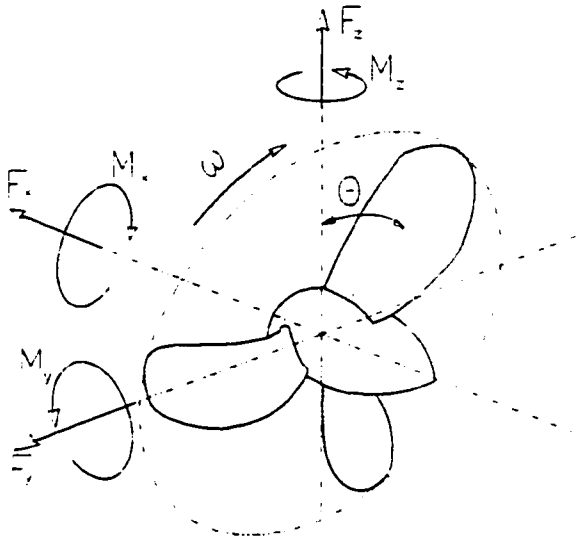

Figure II-11 Propeller forces and moments

These forces, as a hydrodynamic load on blades, have resulted from variation of the angle of attack of the propeller blades. When variation of angular amplitudes of the propeller blades around equilibrium are small, linear theory can be applied, and propeller forces can be separately estimated, and finally simply superimposed over the other.

Propeller excitation appears in the form of forces in directions of the three main axis, and also in the form of torque and moments around these axes. Secondly, it is of importance for this thesis that the hydrodynamic reactions cause coupling between different vibrating forms.

The intensity of interaction among vibrations in different directions is not equal. For merchant ocean going ships, and propellers of Wageningen B, or similar

series, significant vibration interaction is found between torsional and axial vibrations; i.e. there is a significant coupling effect that causes torsional vibrations to induce additional axial vibrations. Reciprocal interaction between axial and torsional vibration, as well as other coupling effects, do not exist, or are not significant to be considered for conventional design merchant ship. However, this may not be the case for some other propeller and ship designs.

Hydrodynamic response to the propeller vibrations causes the following effects on the propeller:

- virtual rise of the propeller's mass; added mass
- virtual rise in rotary inertia; added inertia, and
- resistance to the vibration; damping.

In order to be able to associate each of the hydrodynamic reaction to the propeller vibration, so called *hydrodynamic coefficients* are introduced.

II.6.4.1. *Hydrodynamic Coefficients*

Hydrodynamic coefficients are propeller forces and moments that are respectively reduced to the unit acceleration and unit velocity of the vibrating propeller.

It is assumed that propeller performs linear vibrations, fluid is homogeneous and undisturbed, and amplitudes are small. The linearized vibrating

condition implies that the hydrodynamic coefficients behave as proportionality factors, meaning that the propeller forces can be calculated by simple multiplication of the particular coefficient with vibration acceleration or velocity.

Hydrodynamic coefficients that are calculated from forces and moments reduced to the unit acceleration are called added mass and added inertia, respectively. Forces and moments that are reduced to the unit velocity are called damping coefficients.

Units of measure for propeller coefficients will be as tabulated below:

	ISO Units
Added Mass	[kg]
Added Inertia	[kgm^2]
Longitudinal Damping	[Ns/m]
Transverse Damping	[Ns/m]
Torsional Damping	[Nms/rad]

II.6.4.1.1. Added Mass and Inertia Matrix

Hydrodynamic coefficients related to acceleration can be arranged in a six by six matrix, which is called virtual, or added mass (inertia) matrix. Matrix is symmetric around main diagonal (with exception of four coefficients which are of same intensity but opposite sign), and it has the form as shown in Equation II-17.

$$[A] = \begin{bmatrix} a_{xx} & 0 & 0 & a_{x\theta_x} & 0 & 0 \\ 0 & a_{yy} & a_{yz} & 0 & a_{y\theta_y} & a_{y\theta_z} \\ 0 & a_{zy} & a_{zz} & 0 & a_{z\theta_y} & a_{z\theta_z} \\ a_{\theta_x x} & 0 & 0 & a_{\theta_x\theta_x} & 0 & 0 \\ 0 & a_{\theta_y y} & a_{\theta_y z} & 0 & a_{\theta_y\theta_y} & a_{\theta_y\theta_z} \\ 0 & a_{\theta_z y} & a_{\theta_z z} & 0 & a_{\theta_z\theta_y} & a_{\theta_z\theta_z} \end{bmatrix} \quad \text{(II-17)}$$

$a_{\Theta z\Theta z} = a_{\Theta y\Theta y}$

$a_{zy} = -a_{yz}$

$a_{\Theta zY} = -a_{Y\Theta z}$

$a_{Z\Theta y} = -a_{\Theta yZ}$

$a_{\Theta z\Theta y} = -a_{\Theta y\Theta z}$

Notation in this matrix is as follows:

- a stands for mass and mass moment of inertia

- indices x, y, and z are direction of translations along coordinate axis, and

- indices Θ_x, Θ_y, and Θ_z are directions of rotations around coordinate axis

Indices define which linear motions are coupled along and around the main coordinate directions. The first index shows the direction of added mass/inertia action, and the second index defines from which direction it originates.

First three diagonal terms in the matrix represent added mass in three main directions, and the following three are added mass-moment of inertia around the same axis. The other nonzero elements define coupling effects between different coordinate

directions; i.e. increment of virtual mass, or inertia in one coordinate direction due to the existence of the virtual mass/inertia in the other. Some terms in the matrix are zero which means that there is no interaction between added masses in these directions.

This virtual-mass matrix is to be added to the real mass and inertia matrix of the propeller (Equation (II-18)).

$$[M] = \begin{bmatrix} m & 0 & 0 & 0 & 0 & 0 \\ 0 & m & 0 & 0 & 0 & 0 \\ 0 & 0 & m & 0 & 0 & 0 \\ 0 & 0 & 0 & I_x & 0 & 0 \\ 0 & 0 & 0 & 0 & I_y & 0 \\ 0 & 0 & 0 & 0 & 0 & I_z \end{bmatrix} \qquad \textbf{(II-18)}$$

II.6.4.1.2. Damping Matrix

Hydrodynamic coefficients related to vibration velocity are called *Damping*, and are also arranged as a 6x6 matrix. Matrix form is similar to the virtual mass-inertia matrix. Matrix is also symmetrical around main diagonal with the exception of two pairs of coefficients which are of opposite sign.

$$c_{\theta z \theta z} = c_{\theta y \theta y}$$

$$c_{zy} = -c_{yz}$$

$$c_{\theta z Y} = -c_{Y \theta z}$$

$$c_{Z \theta y} = -c_{\theta y Z}$$

$$[C] = \begin{bmatrix} c_{xx} & 0 & 0 & c_{x\theta_x} & 0 & 0 \\ 0 & c_{yy} & c_{yz} & 0 & c_{y\theta_y} & c_{y\theta_z} \\ 0 & c_{zy} & c_{zz} & 0 & c_{z\theta_y} & c_{z\theta_z} \\ c_{\theta_x x} & 0 & 0 & c_{\theta_x\theta_x} & 0 & 0 \\ 0 & c_{\theta_y y} & c_{\theta_y z} & 0 & c_{\theta_y\theta_y} & c_{\theta_y\theta_z} \\ 0 & c_{\theta_z y} & c_{\theta_z z} & 0 & c_{\theta_z\theta_y} & c_{\theta_z\theta_z} \end{bmatrix} \quad \text{(II-19)}$$

$c_{\theta z \theta y} = -c_{\theta y \theta z}$

Notation in this matrix is as follows:

- c stands for damping coefficient
- indices x, y, and z are direction of translations along coordinate axis
- indices Θ_x, Θ_y, and Θ_z are directions of rotations around coordinate axis

The diagonal elements of the matrix represent damping along and around the three main coordinate directions. Other, off-diagonal nonzero terms represent damping coupling between different coordinate directions.

Elements, or coefficients of the added-mass matrix and damping matrix, are determined by applying the lifting surface theory. Each of the matrices contains 36 coefficients, some of which are zero.

Propeller symmetry in y-z plane (transverse plane) makes following coefficients equal:

$$a_{yy} = a_{zz} \qquad c_{yy} = c_{zz}$$
$$a_{\theta_y y} = a_{\theta_z z} \qquad c_{y\theta_y} = c_{z\theta_z} \tag{II-20}$$
$$a_{y\theta_y} = a_{\theta_y y} \qquad c_{y\theta_y} = c_{\theta_y y}$$

For the other nonzero-elements the reciprocal interaction between same axis makes them equal:

$$a_{y\theta_y} = a_{\theta_y y} \qquad c_{y\theta_y} = c_{\theta_y y} \tag{II-21}$$

Negative signs in [A] and [C] matrices define only different direction of action, of otherwise the same coupling coefficients. Zero coefficients in the rows means that there is no coupling between directions that correspond to zero-coefficient's indices.

From a practical point of view, each of the matrices [A] and [C] can be divided into two matrices defining two independent systems:

- the first system will be symmetrical around the diagonal, and define only axial and torsional vibrations and
- the other system will define transverse vibrations only. Transverse vibrations are coupled horizontal and vertical vibrations (whirling) which, besides the hydrodynamic reactions on the propeller, have origins in bearings' oil film coupling and gyroscopy of the propeller.

Detailed derivation of the propeller coefficients is presented in section II.6.5.1.

II.6.4.2. Wake Field

For definition of forces and moments generated on the propeller when it operates at steady speed in nonuniform wake field, it is particularly important to measure, calculate or estimate wake field produced by the ship with certain accuracy. The best method to assess wake field is to measure it. However, for new designs in early stages, wake measurements are not available, and therefore need to be either calculated or estimated.

Analysis of the wake field is not an easy task. It is costly, time consuming, and at the end not always reliable enough. Thus, the only recourse for the designer in this early project stage is to rely on experimental estimates; i.e on data that are readily available from the stock propellers with conservative margin of accuracy.

Ship's wake field is caused by friction between ship hull and surrounding water, increased pressure around the stern tube to streamline flow, and waves generated by ship movement through water.

Wake can be expressed in the form of a coefficient w:

$$w = \frac{V - V_A}{V} \qquad \text{(II-22)}$$

where V is ship speed, and V_A is propeller advance speed or wake speed.

Wake distribution around the propeller is circumferentially nonuniform. This uneven wake inflow velocity on the propeller causes periodic change in angle of attack on the blades that results in longitudinal and transverse propeller vibration.

II.6.4.2.1. Wake Generated Forces

Applying the procedure of Van Manen and Van Oossanen in Lewis (1988), page 147, and Hadler and Cheng (1965), simple calculation can be performed in order to estimate wake forces produced by propeller, as shown below.

Due to its periodic nature, wake can be expanded in a series of sine and cosine functions by applying Fourier series expansion. Thus wake in longitudinal direction is equal to:

$$w_x = \sum_{k=0}^{K} \left[a_k(r) \cos(k\Phi) + b_k(r) \sin(k\Phi) \right] \qquad \text{(II-23)}$$

Coefficients a_k and b_k are k-th harmonic amplitudes of the wake, defined at any point on the blade by its radial position r and angle Φ.

Vibratory forces generated by nonuniform wake field can be derived from Equation (II-27) by applying simple formulation for lift of the blade[7] as proposed by Lewis (1988):

$$L = \frac{1}{2} c_l \rho A v^2 \qquad \textbf{(II-24)}$$

where L is a lift, c_l is lift coefficient, ρ is density of the fluid, A is observed area on the propeller, and v is inflow velocity.

For small hydrodynamic pitch angles β, lift coefficient is approximated as shown below:

$$c_l = 2 \pi \beta \qquad \textbf{(II-25)}$$

Considering inflow velocity v to be composed of rotational speed and forward speed, we have

$$v^2 = (\omega r)^2 + [V(1 - w_x)]^2 \qquad \textbf{(II-26)}$$

[7] Basic lift data are generally derived from airfoil tests in the wind tunnels.

Assuming that axial wake is symmetrical, w_x in Equation (II-23) will consist only of cosine terms, and with substitution of (II-23) into (II-26) and (II-25), following equation for thrust variation can be obtained:

$$f_x = z \sum_{k=0}^{K} F_{kz} \cos(kz\omega t - \Phi_{kz}) \qquad \textbf{(II-27)}$$

where z represent the number of blades.

Similar procedure can be applied do derive wake varying torque, and bending moments, as shown in Equations (II-28), and (II-29).

$$T = z \sum_{k=0}^{K} T_{kz} \cos(kz\omega t - \varphi_{kz}) \qquad \textbf{(II-28)}$$

$$M_z = \frac{z}{2} \sum_{k=0}^{K} [\, F_{kz+1} \sin(kz\omega t - \vartheta_{kz+1}) - F_{kz-1} \sin(kz\omega t - \vartheta_{kz-1}) \,] \qquad \textbf{(II-29)}$$

$$M_y = -\frac{z}{2} \sum_{k=0}^{K} [\, F_{kz-1} \sin(kz\omega t - \vartheta_{kz-1}) + F_{kz+1} \sin(kz\omega t - \vartheta_{kz+1}) \,]$$

f, T, and M are time dependent functions and Φ_{kz}, φ_{kz}, ϑ_{kz} are k-th harmonic phase angles of the z-th blade, for longitudinal force, torque and bending moment, respectively.

If wake data are not readily available for preliminary computation at early design stage, the following (based on Van Manen's tests on some 40 ship models) may be assumed (data are restricted to prismatic coefficients between *0.73* and *0.79*):

- For four-blade propellers

  There exists *80%* probability that:

  first harmonic of the torque fluctuation will be *6.5%* of the mean torque, and

  first harmonic of the thrust fluctuation will be *10%* of the mean thrust.

- For five-blade propellers with same probability there is

  1.5% torque fluctuation of the mean torque, and

  2% thrust fluctuation of the mean thrust for the first harmonic.

Vibratory thrust and torque, as presented in Equations (II-27) and (II-28), are integer multiples of the blade number. The first harmonic (which for thrust and torque fluctuation coincides with blade number) is dominant in the response, and it is usually sufficient for such preliminary analysis. In wake data analysis presented by Hadler and Cheng (1965) it is shown that higher order wake forces are significantly lower than forces generated by first order excitation.

For analysis of the bending vibrations, the fluctuating bending moments in vertical and horizontal direction in the propeller plane will be integer multiples of the *(kz+1)* and *(kz-1)* harmonics, respectively.

II.6.4.3. Equation of Motion

For the purpose of obtaining the forces on the propeller, it is considered to be rigid body and is isolated from its surroundings. The influence of the elasticity of the line shafting can be included into analysis by adding a stiffness matrix into the formulation below.

$$[M]\{\ddot{u}_i\} = [A]\{\ddot{u}_i\} + [C]\{\dot{u}_i\} + \sum_{i=1}^{n}\{Q_i\} \qquad \text{(II-30)}$$

$$([M] - [A])[\ddot{u}] - [C][\dot{u}] = [Q]$$

Displacement vector {u}, and its velocity and acceleration, consists of three translatory motions, and three rotary motions along and around coordinate axis.

$$\{u\} = [x, y, z, \Theta_x, \Theta_y, \Theta_z]^T \qquad \text{(II-31)}$$

The vectors of the *n* vibratory thrust force and moments acting on the propeller are grouped together as matrix [Q]. The total response {u} will then be a sum of particular responses to each $\{Q_i\}$.

II.6.5. **Determination of Reaction Forces due to Propeller Vibration**

For propeller design and determination of its excitation, two and three dimensional models and adequately developed theories are in use today. These theories are still not generally applicable and are restricted to certain propeller series. Only a brief introduction of the theories in use is given here.

Two dimensional modelling such as:

- Thin Foil Theory, and
- Lifting Line Theory

are still in use. If three dimensional approach is required, as needed in propeller design, lifting line theory can be applied more successfully when additional corrections are done in order to approximate 3-D models. However, when it is necessary to define load over propeller blade surface three dimensional modelling is necessary.

Propeller is treated as a helicoidal surface of zero thickness, constant pitch and no rake. Its interaction with the surrounding is defined through a finite number of angular equidistant lifting surfaces on blade's helicoidal plane (Van Gent (1975)).

$$\theta - \frac{x}{P} 2\pi - \omega t - \frac{k}{Z} 2\pi = 0 \qquad \textbf{(II-32)}$$

θ - angular coordinate

ω - angular velocity

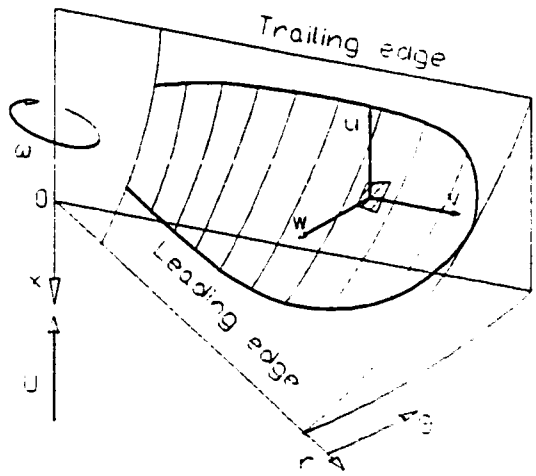

Figure II-12 Blade modeling

t - time

k - blade number

z - number of blades

x - axial coordinate

P - pitch

Equidistant helicoidal surfaces, as presented in Figure II-12, can be mathematically formulated as in Equation (II-32) (Van Gent (1975), page 277). The following sign convention is adopted here:

- positive axial direction is opposite to the direction of the inflow, and
- positive angular coordinate is in the direction opposite to the rotation of the propeller.

Irrespective of the applied theory the equations of propeller's vibrational motion and blade load can be determined as presented below.

Main flow velocity on the helicoidal surface, can be decomposed into components in three main directions, i.e. axial, tangential and radial. Radial component can be neglected for small disturbances of the inflow and for small pitch variations. Disturbance of the inflow can now be formulated as:

$$d = u\cos\varphi - w\sin\varphi$$
$$\tan\varphi = \frac{p}{2\pi r} \qquad \text{(II-33)}$$

General equations of vibrational motions of the propeller blade can be expressed with the following relations:

$$\begin{aligned} \delta_i &= A_i \sin(\nu\,\omega\,t) & \theta_i &= B_i \sin(\nu\,\omega\,t) \\ \dot{\delta}_i &= \nu\,\omega A_i \cos(\nu\,\omega\,t) & \dot{\theta}_i &= \nu\,\omega B_i \cos(\nu\,\omega\,t) \\ \ddot{\delta}_i &= -\nu^2\omega^2 A_i \sin(\nu\,\omega\,t) & \ddot{\theta}_i &= -\nu^2\omega^2 B_i \sin(\nu\,\omega\,t) \end{aligned} \qquad \text{(II-34)}$$

where i takes values of 1, 2, 3 for x, y, and z coordinate axes and respectively, represents displacement, velocity and acceleration in longitudinal, transverse and vertical direction. Coefficients A_i and B_i are respective amplitudes of displacement, and ν represents order of the angular frequency ω.

Considering propeller to be a rigid body reacting with its surrounding, corresponding fluid velocities relative to the propeller blade will be of equal intensity but in opposite directions. Therefore velocity components of the disturbance of the inflow, equation (II-33), can be rewritten for each direction separately considering appropriate values of the axial and tangential velocities. However, in transverse plane, propeller vibration can be considered only in one direction and thus only two displacement amplitudes are necessary; i.e. A_2 and B_2 (A_3 and B_3 yield from these two).

The blade loads generated by propeller motion described above can be presented as in following equation:

$$\begin{aligned} l_{1/2} &= d_{1/2}\cos(\nu\,\omega\,t) \\ l_{3/4} &= d^{-}_{3/4}\sin((\nu-1)\,\omega\,t+\alpha^{-}_{3/4}) + d^{+}_{3/4}\sin((\nu+1)\,\omega\,t+\alpha^{+}_{3/4}) \end{aligned} \qquad \textbf{(II-35)}$$

Indices 1 and 2 correspond to the axial and torsional flow disturbances d_1 and d_2, and indices 3 and 4 correspond to the transverse inflow disturbances d_3 and d_4.

II.6.5.1. Lifting Surface Theory

In contrast to the wing theory, where two dimensional approach is appropriate, for accurate analysis of propeller blade it is necessary to follow a three dimensional approach. In wing theory, when it moves through a gust flow, the wing load is uniform along its span. Therefore, 2-D theories can be applied with high accuracy.

For the propeller the case is different and 3-D approach is necessary. Propeller operates in nonuniform inflow, which in general varies spatially and with time. Temporal variation is generally stochastic and it is neglected here assuming that no temporal changes will occur for ship on a straight course with steady speed.

For the purpose of defining reaction forces generated by propeller vibration in uniform wake field, the following assumptions are made:

- propeller blade pitch is considered constant,
- blade thickness is neglected, and
- rake of the blade is assumed to be zero.

As shown in Van Gent (1975), Tsakonas, Jacobs and Ali (1973) and Sparenberg (1960), the propeller coefficients can be defined from the relations for propeller motion and propeller load by using Lifting Surface Theory. Propeller excitation frequency which is a multiple of the propeller blade number is the dominant frequency, and it produces the highest response.

The propeller chosen in the example in this thesis is:

- Wageningen B4-40-80

- Number of blades, 4

- Expanded area ratio, A/Ao=0.4

- Pitch ratio P/D=0.8

- Propeller diameter D=6.15 [m]

- Nominal frequency of rotation f = 1.85 [1/s]

- Sea water density ρ = 1025 [kg/m^3]

The propeller coefficients in this case are as tabulated below (data are adopted from Hylarides and Van Gent (1979)). Three tables are presented below, showing propeller coefficients for:

- torsional-axial vibration,

- transverse vibration with parallel vectors for load and motion, and

- transverse vibration with vectors for load and motion mutually perpendicular.

The first column in tables represents mathematical formulation of the propeller coefficients (as calculated by Hylarides and Van Gent in (1974)), the second column represents coefficients as shown in the matrices Equation (II-17) and (II-19). The third column are dimensionless propeller coefficients.

TORSIONAL AND AXIAL VIBRATION COEFFICIENTS

$F_x/\dot{\delta}_x$	$\frac{c_{xx}}{\rho f D^3}$	-0.595	*linear damping*
$F_x/\ddot{\delta}_x$	$\frac{a_{xx}}{\rho D^3}$	-0.0274	*added mass*
$F_x/\dot{\phi}_x$	$\frac{c_{x\theta_x}}{\rho f D^4}$	0.0758	*damping coupling*
$F_x/\ddot{\phi}_x$	$\frac{a_{x\theta_x}}{\rho D^4}$	0.00348	*inertia coupling*
$T_x/\dot{\delta}_x$	$\frac{c_{\theta_x x}}{\rho f D^4}$	0.0758	*damping coupling*
$T_x/\ddot{\delta}_x$	$\frac{a_{\theta_x x}}{\rho D^4}$	0.00348	*inertia coupling*
$T_x/\dot{\phi}_x$	$\frac{c_{\theta_x\theta_x}}{\rho f D^5}$	-0.00965	*torsional damping*
$T_x/\ddot{\phi}_x$	$\frac{a_{\theta_x\theta_x}}{\rho D^5}$	-0.000443	*added inertia*

Table II.6.-1 Torsional and axial vibration coefficients

TRANSVERSE VIBRATION COEFFICIENTS ; PARALLEL

$F_y/\dot{\delta}_y$	$\frac{c_{yy}}{\rho f D^3}$	-0.0556	*linear damping*
$F_y/\ddot{\delta}_y$	$\frac{a_{yy}}{\rho D^3}$	-0.00356	*added mass*
$F_y/\dot{\phi}_y$	$\frac{c_{y\theta_z}}{\rho f D^4}$	-0.0355	*damping coupling*
$F_y/\ddot{\phi}_y$	$\frac{a_{y\theta_z}}{\rho D^4}$	-0.00193	*inertia coupling*
$M_y/\dot{\delta}_y$	$\frac{c_{\theta y}}{\rho f D^4}$	-0.0364	*damping coupling*
$M_y/\ddot{\delta}_y$	$\frac{a_{\theta y}}{\rho D^4}$	-0.00188	*inertia coupling*
$M_y/\dot{\phi}_y$	$\frac{c_{\theta\theta_z}}{\rho f D^5}$	-0.0326	*damping*
$M_y/\ddot{\phi}_y$	$\frac{a_{\theta\theta_z}}{\rho D^5}$	-0.00151	*added inertia*

Table II.6.-2 Transverse vibration coefficients; with parallel load and motion vectors

TRANSVERSE VIBRATION COEFFICIENTS ; PERPENDICULAR

$F_z/\dot{\delta}_y$	$\frac{c_{zz}}{\rho f D^3}$	2.23e-3	*linear damping*
$F_z/\ddot{\delta}_y$	$\frac{a_{zz}}{\rho D^3}$	-6.45e-5	*added mass*
$F_z/\dot{\phi}_y$	$\frac{c_{z\theta_z}}{\rho f D^4}$	0.0124	*damping coupling*
$F_z/\ddot{\phi}_y$	$\frac{a_{z\theta_z}}{\rho D^4}$	2.75e-4	*inertia coupling*
$M_z/\dot{\delta}_y$	$\frac{c_{\theta_z z}}{\rho f D^4}$	-0.00607	*damping coupling*
$M_z/\ddot{\delta}_y$	$\frac{a_{\theta_z z}}{\rho D^4}$	-5.27e-4	*inertia coupling*
$M_z/\dot{\phi}_y$	$\frac{c_{\theta_z\theta_z}}{\rho f D^5}$	0.00264	*damping*
$M_z/\ddot{\phi}_y$	$\frac{a_{\theta_z\theta_z}}{\rho D^5}$	-1.53e-4	*added inertia*

Table II.6.-3 Transverse vibration coefficients - with mutually perpendicular load and motion vectors

The next chapter describes the conventional line shafting design approach wherein the torsional and axial vibrations are considered separately in design.

CHAPTER III

CONVENTIONAL LINE SHAFTING DESIGN

III.1. GENERAL

Conventional shafting design presumes propulsion system detached from its physical environment, and use of conservative analysis procedures and practices in its design. These analysis and practices are often defined in Classification Society Rules and are used by ship builders as a guidance and minimum requirement for line shafting design.

New technologies and advances in computational capabilities have pushed ship design up to its structural limits by reducing thickness of the hull structure and installing high powered main drives. At the same time most shipbuilders did not apply the same level of high standards in defining excitations which is also higher and more thoroughly defined with modern techniques. This discrepancy in treatment of excitation and hull design can be a reason for increased reduction in ship lifetime and worse overall ship design.

Unfortunately, rules for shafting design established by Classification Societies are not enforcing requirements for more thorough calculations. Rules are often outdated and technically do not follow trends in modern shipbuilding. There is however a commercial

trend that they follow because the Classification Societies do not want to lose their clientele by imposing stringent rules and asking for additional and more comprehensive analysis. They want to attract ship owners and not to disturb shipbuilders at the same time. The end results of these practices are non-demanding rules that can also reflect in the quality of the ship and propulsion system.

For merchant ocean going ships, Classification Societies typically require only torsional vibration analysis. From the shafting strength point of view this is usually sufficient requirement, because torsional stationary and dynamic torques are far greater than other excitations. However, in cases where it may be reasonably suspected that longitudinal and transverse vibration can produce significant dynamic response (based on previous experiences from similar line shafting designs), analysis of these two vibration forms may be required too. For longitudinal and transverse analysis, only natural frequency calculation will be considered satisfactory if frequencies are sufficiently distant from resonant torsional ones. If there is no proximity of the torsional, axial and transverse vibration natural frequencies, forced longitudinal and transverse vibrations are not required for calculation by classification societies. Axial and transverse vibrations have usually low intensity and do not significantly influence the response. Axial vibrations have also negligible contribution to the line shafting strength, but due to the propeller's capability to couple torsional and axial vibrations, and significant axial thrust developed due to the coupling, axial excitation cannot be avoided.

Nevertheless, it is important to focus on the main engine and the propeller and their influence on shafting design.

Modern engines have:

- low number of cylinders

- low operational speed

- rigid connection to the propeller via line shafting[1]

- high stiffness of the shafting resulting from the engine's position on the ship (engine is pushed as close as possible to the aft peak of the ship in order to give maximum possible space to the cargo).

The above are the reasons that engine excitation is brought into, or close to, the resonance with hull structures. Natural frequencies of the propulsion system have increased and approached the ship hull structural frequencies which were already lowered due to hull's reduced thickness.

Propeller design is also changing in order to accommodate requirements for propulsion with given main engine. As the engines are becoming slower, the propellers are getting bigger and heavier to ensure enough thrust for required speed of the ship. These changes influence propeller response to the vibration and its behavior in the wake flow behind the ship. For the propulsion efficiency this is better, but for the shafting design higher inertia means higher amplitudes and stresses in the shafts.

As the shafting system is an integral part of the ship structure its impact on the surrounding structure cannot be neglected in its design. This changes the whole picture of the shaft design and, contrary to the conventional shafting design (explained below), it is of crucial importance to analyze shafting design considering in particular coupling

---

[1] An elastic coupling is not desired, because of its high price, in the low speed propulsion systems.

between torsional and axial vibrations. Ship hull vibration measurements (Appendix E) show the significance of the shafting design for the vibration intensity at the superstructure of the ship.

III.1.1. **Methods For Shafting Vibration Computation**

A number of computational methods can be applied for shafting vibration analysis. Moreover, what was once restricted only to highly expensive mainframe computers, is today easy to run on almost equally capable low cost personal computers. Therefore, less accurate approximate methods that calculated only resonant stresses (such as those based on energy principles), are not attractive any more.

Among methods that can achieve high accuracy, the following three equally reliable methods are mostly in use:

- transfer matrix,
- stiffness (flexibility) matrix, and
- finite element method.

Transfer Matrix Method is chosen here for conventional analysis of shafting vibration. This method is well suited for purposes such as torsional, axial and transverse vibration analysis of ship propulsion installation, where simple successive multiplication of matrices is needed. The other benefit of this method is that the order of the matrices is very small, not memory demanding, and that matrices maintain same order whatever

the degree of freedom of the system. Besides, for applications of this kind, with relatively small number of system elements, there is less concern about possible error accumulation, which can affect huge systems.

Stiffness Matrix Method is also a reliable and accurate tool for shafting vibration analysis and, although there are pros and cons for both the transfer matrix and the stiffness matrix method, it is more convenient to apply transfer matrix method for computation on personal computers.

Finite Element Method is used to investigate the vibration interaction between torsional and longitudinal modes.

III.1.2. **Allowable Stresses**

Endurance stresses are dependent on geometry (stress distribution and concentration) and physical properties of the material. Classification Societies have proposed semi empirical methods which can be easily applied to propulsion shafting in order to arrive at the stress limits with significant safety margin. These limits are only imposed for torsional vibration. Allowable stress limits are different for different Classification Societies, but variations between them are not significant.

Fatigue life of the shafting will depend on the load intensity and on the number of dynamic cycles to which the shaft is exposed. Therefore, two stress curves

are provided, one limiting the allowable stresses for continuous operation[2] and the other limiting the same transient condition. Both curves present functional relation between torsional stress (or torque in some cases) and revolution of the shaft.(See Figure III-1).

Continuous operation limit bears no restriction on the propulsion system operation in the whole range of operational speeds only if torsional stresses are below the limit. For the propulsion installation where developed stresses are above limit for continuous operation, while still below that defining transient condition, operation of the installation will be limited only to fast passing through this range of speeds (so called Barred Speed Range - BSR). However, transient condition is restricted only to the shafting revolutions that are reasonably below[3] nominal operational speeds of the propulsion system.

Information required for definition of the limits is only the shaft diameter, tensile strength of the shaft material, and position of the shaft in the propulsion system. These requirements are improving today by including additional design factors which take into account stress concentration.

The most advanced IACS (International Association of Classification Societies) Rules take into account a number of factors that allow more realistic limits to be applied; e.g. some of these factors are: the maximum number of dynamic cycles that shafting is expected to be exposed to, notch coefficient, material fibre direction, etc.

---

[2] Continuous operation stress limit implies infinite fatigue life of the structure if the structure operates below this limit. Fatigue life is expressed in number of accumulated dynamic cycles, and it is considered to be infinite when number of cycles exceeds 10^7.

[3] BSR is normally not acceptable for speeds that are greater than 0.8 of the nominal operation speed.

Although some Classification Societies were fast in adopting these kinds of changes, like DNV (Det Norske Veritas) for example, IACS rules are still not endorsed by most of them.

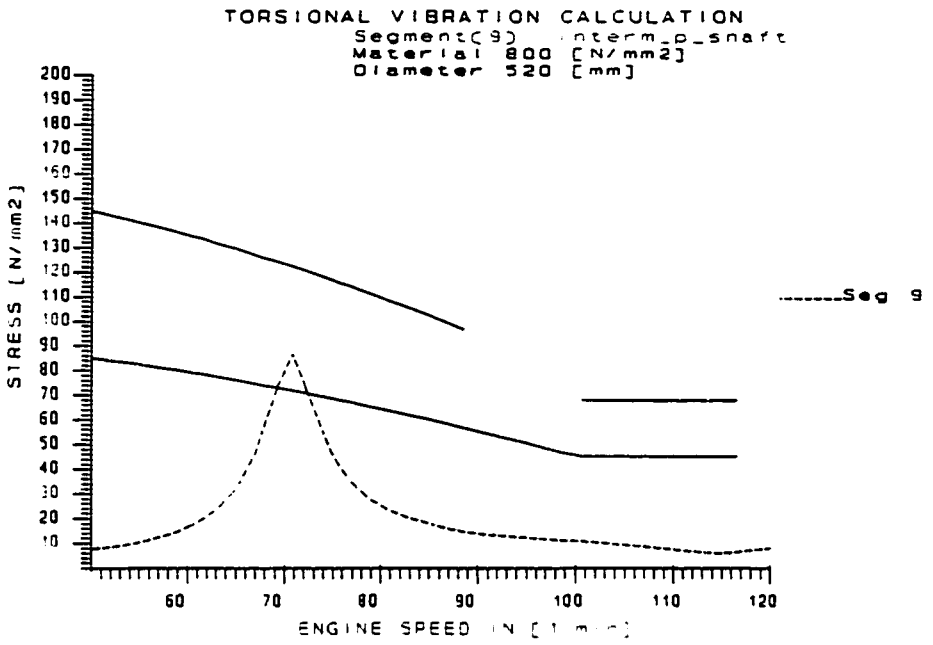

Figure III-1 An example of the T/V stress diagram with ABS stress limits

In this study ABS (American Bureau of Shipping) Rules are adopted. As shown in presented stress diagram (Figure III-1) ABS stress limits consist of three full line curves:

- The lower curve represents limit for single harmonic continuous operation without restrictions. It becomes a straight line between 90-105% of engine nominal speed.

- For synthesis calculation, limits in range of speed between 90-105% of rated speed are increased by 50%. This is shown on the diagram as a straight line parallel to the one for single harmonic.

- The uppermost curve that goes up to 80% of rated speed is the limit for transient operation.

The dashed line in Figure III-1 represents an example of the torsional stress curve. The curve connects all stresses calculated for steady state conditions at different engine speeds.

III.1.3. **Vibration Control**

When vibrations exceed allowable limits, measures must be taken in order to reduce them. In case the vibrations are over the limit for continuous operation and below the limit for transient operation, barred speed range may be introduced. In some applications BSR may not be acceptable. In that case, as well as in cases where vibratory stresses are beyond transient limit, vibrations must be reduced by installing either detuners or vibration dampers.

Detuners reduce natural frequency of the system and stabilize the vibratory torque which reduces the stress in the shafting. They are effective only for overcritical solutions. Detuners are usually only additional inertias added to the system.

On the other hand, dampers are designed to reduce vibratory amplitude by absorption of vibratory energy. For propulsion systems of ocean-going merchant ships only viscous dampers are found to be in use. Viscous dampers can be further classified as tuned and untuned. Tuned dampers have springs that operate in viscous fluid (silicone usually). Spring stiffness is adjusted to resonant frequency that is to be tuned. These are high efficiency dampers, relatively small in size. Untuned dampers consist of seismic masses that float in viscous fluid. Dampers of this type are large in size, but simple in design, and therefore less expensive than tuned dampers.

Vibration problem solutions with vibration dampers are not desirable. They are costly, need extra maintenance and any malfunction can have severe consequences on propulsion systems.

III.1.4. **Example**

The procedure of the conventional propulsion system design is shown on the example of a 40,000 DWT cargo ship, with a 5 cylinder engine. The reasons for choosing this type of ship and engine as an example are:

- large number of ships in service[4]
- problems related to torsional and axial vibration interaction are found to be particularly intense on this type of vessels, and

[4] Only partial statistic (restricted to MAN B&W engines) shows that more than one hundred ships with five cylinder B&W engines that can fall into the category of 40,000 DWT or so, were built and in operation since 1994 (MAN B&W List of Reference(1994)).

- available vibration measurement data.

Problems with vibration coupling are also found on other types of ships; ships with different load capacity and different engine types. However, ships in the chosen category are more likely to experience excessive effects of torsional and axial vibration coupling than the others.

III.2. TORSIONAL VIBRATION ANALYSIS

III.2.1. General

Sources of torsional vibration of the line shafting are main engine and propeller. As explained in Chapter II, the main engine generates vibratory torque due to the irregularity in combustion process and acceleration or deceleration of the masses in reciprocating motion. On the other hand, the propeller excites shafting torsionally as it operates in circumferentially non-uniform wake field created by the presence of the hull.

The main engine contribution in total torsional response is dominant and therefore propeller response can be neglected in most cases. In computer programs developed in this thesis propeller excitation can be included in response analysis.

Total engine excitation is the sum of particular excitations generated in each of the cylinders. Normally, due to imperfection in engine construction and uneven fuel

injection into cylinders, combustion process will deviate from cylinder to cylinder. Such deviations will contribute to higher irregularity in vibratory torque and must be considered in software developed for computation of torsional vibration. Deviation in excitation between cylinders, if expressed in form of indicated pressure, can be taken approximately 5% of its mean value for the selected revolution. This percentage depends on deterioration of the engine and proper adjustment of the fuel injection. Deviation will be smaller for a new engine.

III.2.2. **Initial Line Shafting Parameters**

III.2.2.1. *Propeller Shaft and Intermediate Shaft*

Shafting length is defined when ship hull design and position of the engine are known, leaving very little room (if any) to influence the stiffness of the shafting by changing its length. Therefore, for the fixed length of the shafting, only shafting diameters and material properties can be changed in order to define the stiffness and allowable stresses in the shafting.

According to adopted ABS Rules, the least shafting diameters must be defined by the following empirical relation:

$$d = 100\,K\left(\frac{P}{n}\,\frac{c_1}{U + c_2}\right)^{1/3}$$

where,

d - shaft diameter [mm]

K - shaft design factor is chosen from ABS Rules. Factor depends on the type of propulsion, propeller attachment, stern tube configuration, shafting connections, etc.

P - power at rated speed [kW]

n - rpm at rated speed [rpm]

c_1- material factor [N/mm^2]

c_2- material factor [N/mm^2]

U - minimum specified tensile strength [N/mm^2]

Therefore, for diesel engine output of P = 7830 [kW] at n = 111 [rpm], with the following characteristics of the propulsion system:

- oil lubricated stern tube bearing
- keyless, shrink fitted propeller
- integral flanges
- and material factors

c_1 = 560 [N/mm^2]

c_2 = 160 [N/mm^2]

the propeller shaft is characterized with

$K = 1.22$

$U = 400\ [N/mm^2]$

and the minimum diameter must be

$d_p = 505\ [mm]$

Similarly for the intermediate shaft

$K = 1$

$U = 400\ [N/mm^2]$

and the minimum diameter must be

$d_i = 415\ [mm]$

Minimum allowable ultimate tensile strength[5] is used here to define preliminary shafting diameters. Maximum value of ultimate tensile strength is also limited by Class; the reason for this limitation is the lower elongation as the tensile strength gets higher.

Having defined diameters, the stiffness and mass moment of inertia of the shafting can be calculated. Stiffness and inertia of the shafting is calculated for each segment[6] of the physical shaft, taking into consideration that shaft segments can be plain, hollow, tapered, or a combination of these. These calculations will be performed by a computer program which will preprocess "raw" data in a form suitable for torsional

[5] ABS requires minimum ultimate tensile strength to be 400 [N/mm^2].

[6] The segment of the physical shaft is usually chosen to be the portion of the shaft where diameters (inner and/or outer) change.

vibration analysis by transfer matrix method. Inertia of each discretized massless shaft segment will be evenly divided and added to corresponding shaft segment's end masses.

The torsional stiffness c, areal polar moment of inertia I, and mass moment of inertia J of the shaft segment are given by (Timoshenko (1972)):

$$c = \frac{G I_p}{l} \quad , \; I_p = \frac{(D^4 - d^4)}{D} \pi$$

$$J = \frac{1}{2}\left[\left(\frac{D}{2}\right)^4 - \left(\frac{d}{2}\right)^4\right] \pi \varrho \, l \qquad \text{(III-2)}$$

For tapered shaft, formulation is similar.

III.2.2.2. *Diesel Engine Inertia-Elastic System*

Diesel engine inertia-elastic system (i.e. thrust shaft and crankshaft) is chosen as per original makers design. If original (engine maker) data for crankshaft stiffness are not available, torsional stiffness can be determined as proposed by Jeon and Tsuda (1974). Inertias, diameters, stiffness, and main particulars of the engine are as listed below.

Diesel engine parameters are

- Engine Type 5L60MC MAN_B&W
- Rated Power 7830.0 [kW]
- Rated Speed 111.0 [rpm]

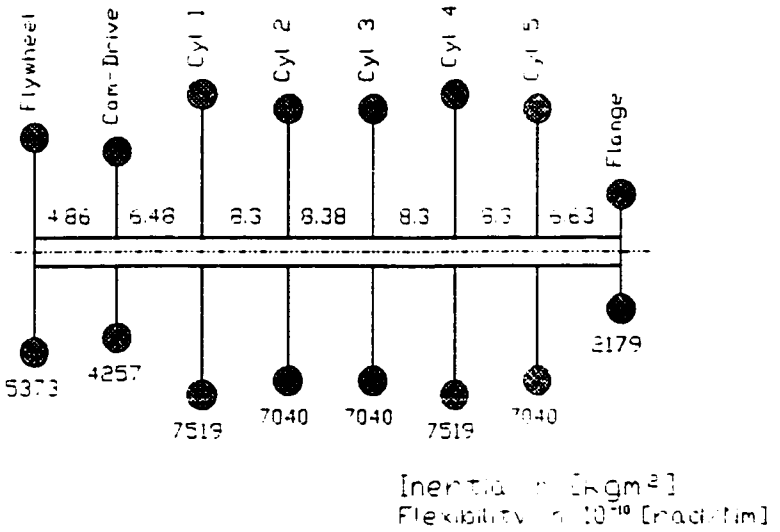

Figure III-2 Inertia-elastic diagram for MAN B&W 5L60MC engine

MASS-ELASTIC SYSTEM

Inertia	Abs.Damp.	Tor.Flex.	Shaft-Dia[m]		Descrip.
kgm2	%	rad/Nm	out	in	
2179	0.5	6.630E-10	0.672	0.115	Flange
7040	0.85	8.300E-10	0.672	0.322	Cyl_1
7519	0.85	8.300E-10	0.672	0.115	Cyl_2
7040	0.85	8.380E-10	0.672	0.322	Cyl_3
7040	0.85	8.300E-10	0.672	0.322	Cyl_4
7519	0.85	6.480E-10	0.672	0.115	Cyl_5
4257	0.5	4.860E-10	0.672	0.115	Cam-drive
3700	0.5				Flywheel

Table III-1 MAN B&W 5L60MC engine mass elastic system

Inertia designated as a 'Flange' in Figure III-2 includes forward second order moment compensator too, and inertia designated as a 'Cam-Drive' includes camshaft drive mass moment of inertia as well as inertia of the after second order moment compensators. Installation of these two second order moment compensators is optional. They are chosen for this engine in order to eliminate free 2nd order moment generated by the engine.

Flywheel inertia is a parameter that can be adjusted according to the torsional vibration requirements. Minimum flywheel inertia for MAN B&W 5L60MC engine is 3700 [kgm^2]. Minimum and maximum flywheel inertias are limited by engine maker. Limit for maximum inertia is permissible load on the engine's main bearing, and criterion for minimum inertia is degree of irregularity of the engine generated torque.

In presented torsional vibration calculation, flywheel inertia is not kept at the minimum, but adjusted to the higher values in order to reduce crankshaft stresses and control position of the main resonance.

According to the engine maker's experience, the damping factor per cylinder, expressed as percentage of critical damping, can be taken as:

$$\zeta = \frac{c}{c_c} 100 = 0.85\ \%$$

Moreover, damping factor on the forward and the after second-order moment compensator is 0.85%, and on the flywheel 0.5%.

ENGINE EXCITATION DATA

Harmonic Components: As per Engine Maker

Firing Order : 1-4-3-2-5

Cylinder Diameter : 0.600 [m]

Piston Stroke : 1.944 [m]

Connecting Rod Length : 2.340 [m]

Reciprocating Mass/Cyl. : 5389 [kg]

Mechanical Efficiency : 100 [%]

Load Deviation : 0 [%]

Engine Speed Range from 30 [rpm] to 111 [rpm]

Harmonics Range from 1.0 to 16.0 with increment 1.0

PROPELLER DATA:

- Type: Wageningen B4-40-80
- number of blades: 4
- expanded area ratio A/Ao=0.4
- pitch ration P/D=0.8
- diameter: 6150 [mm]
- mass: 15410 [kg]
- mass moment of inertia in air 28515 [kgm2]
- inertia of the added water 34975 [kgm2]

Added water and propeller damping can be obtained from the basin model measurements, or calculated using Lifting Surface Theory.

III.2.3. **Results**

Torsional stiffness of the shafting can be defined for each of its segments once the diameters are chosen. Stiffness computation is performed by data preprocessing computer routine for the given shafting geometry . The number of shafting segments for propeller shaft and intermediate shaft are chosen arbitrarily.

Physical propeller shaft has been divided into four segments, one outside the stern tube and three inside the stern tube. For segment outside the stern tube, criteria for intermediate shaft need to be applied. Three segments inside the stern tube are divided into:

- portion of the shaft between propeller and the stern tube
- portion inside the stern tube, and
- portion in front of the stern tube.

The reason for such division of propeller shaft is because some classes (IACS and DNV for example) are applying different criteria for stress limit calculation for different shaft segments, that gives the designer a better tool to optimize the shafting. ABS Rules apply the same criteria for the whole propeller shaft.

The solution to the torsional vibration analysis depends on chosen shafting diameters (stiffness), and must satisfy the following criteria:

- stresses in all segments of the propulsion system must be below limits required by Classification Society

- if barred speed range exists it must be placed below 0.8 of the nominal speed of the engine

- BSR must be chosen not to interfere with normal operation of the ship (manoeuvring, operation in channels and rivers, etc).

For given criteria, two solutions of the problem are possible:

1. **Overcritical**, where rated speed of propulsion installation is located over the resonant speed of the main excitation harmonic. This holds good for shafts with small diameters.

2. **Undercritical,** where rated speed of propulsion installation is below the resonant speed of the main excitation harmonic. This holds good for shafts with large diameters.

Once shafting geometry is selected, analysis of torsional vibrations for both the overcritical and undercritical solutions will be performed according to the following procedure:

a) raw input data is preprocessed in order to create mass-elastic system useful for torsional vibration calculation

b) preprocessed data is printed into report file

c) natural frequencies are calculated in order to define more accurately location of resonances

d) modal vectors are printed in tabular form

e) resonant frequencies are calculated for all major orders which fall into operating speed range of the engine

f) response is calculated for each of selected resonant frequency (therefore no resonance within operating speeds is missed)

g) torsional amplitudes are calculated on all masses

h) torsional torque and stresses are calculated in all segments

i) amplitude, torque and stress diagrams are available as a screen output, and/or as a plot file (stress diagrams can have included stress limits too). Synthesis or order-by-order outputs are possible.

III.2.3.1. *Overcritical Solution*

Overcritical solution has main resonance within operating range of the propulsion installation. Therefore propulsion system when run at rated speed, will be said to operate *over* the *critical* speed.

For diesel engines with up to six cylinders, it is not possible to avoid barred speed range with least shafting diameter. Therefore, solution will have main resonance (5th order in the case of 5 cylinder engine) placed within operating speed of the installation and it will be considered valuable if:

- dominant resonance is below the limit for transient operation,

- main resonance occurs on the engine speeds below 88 [rpm], and

- there is no interference with required operational regimes of the propulsion installation.

In order to match these criteria least shafting diameter usually needs to be adjusted (increased).

If BSR is not acceptable, or stresses are over the transient limit, torsional vibration damper can be installed to reduce the stresses, or the problem needs to be solved as undercritical.

Two solutions to the overcritical case with the same shafting are presented. The first one is without damper, and another with a tuned type damper.

Schematics of the line shafting and discrete model for each shaft are given in Figures III-3 and III-4.

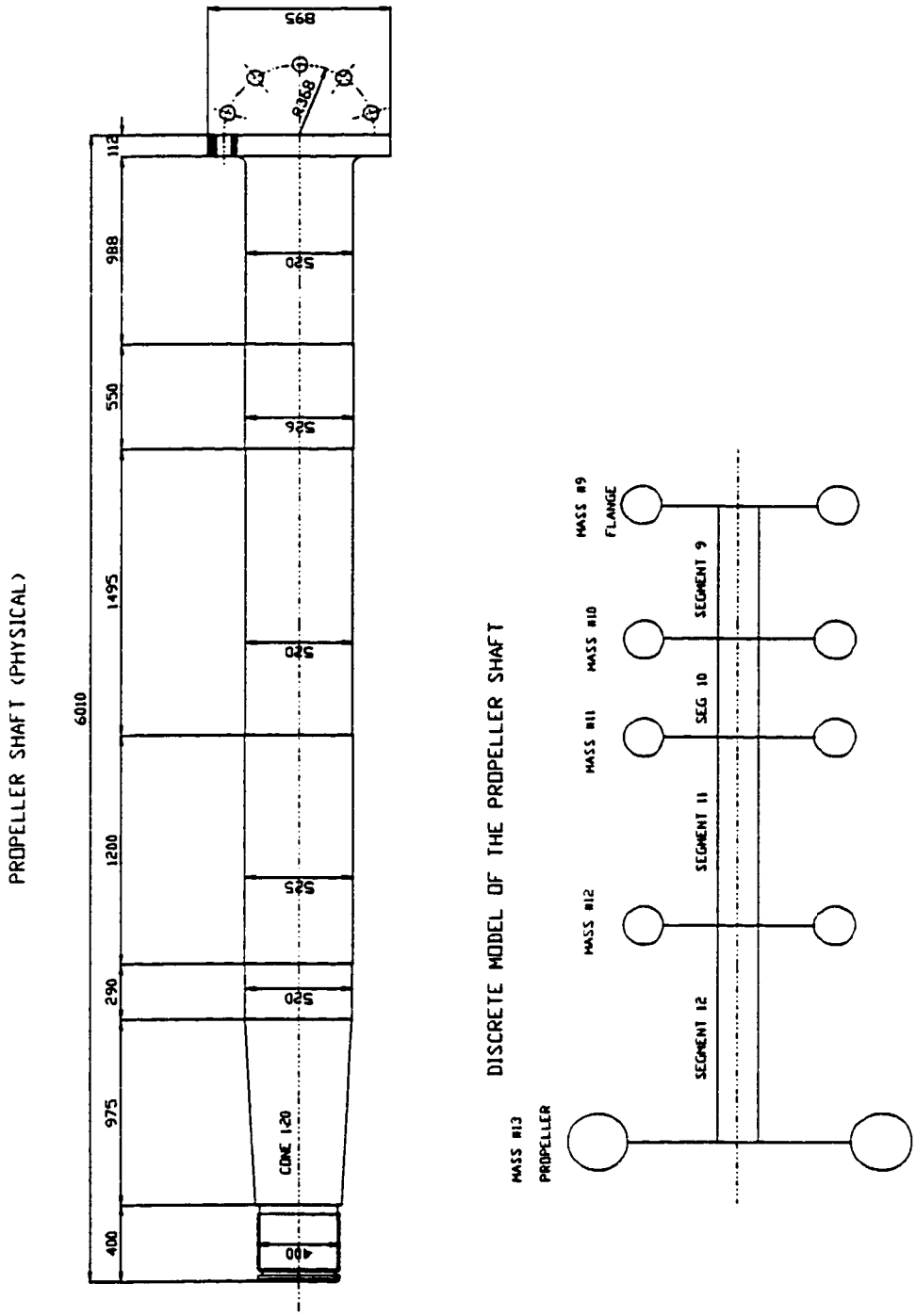

Figure III-3 Propeller shaft design - Overcritical solution

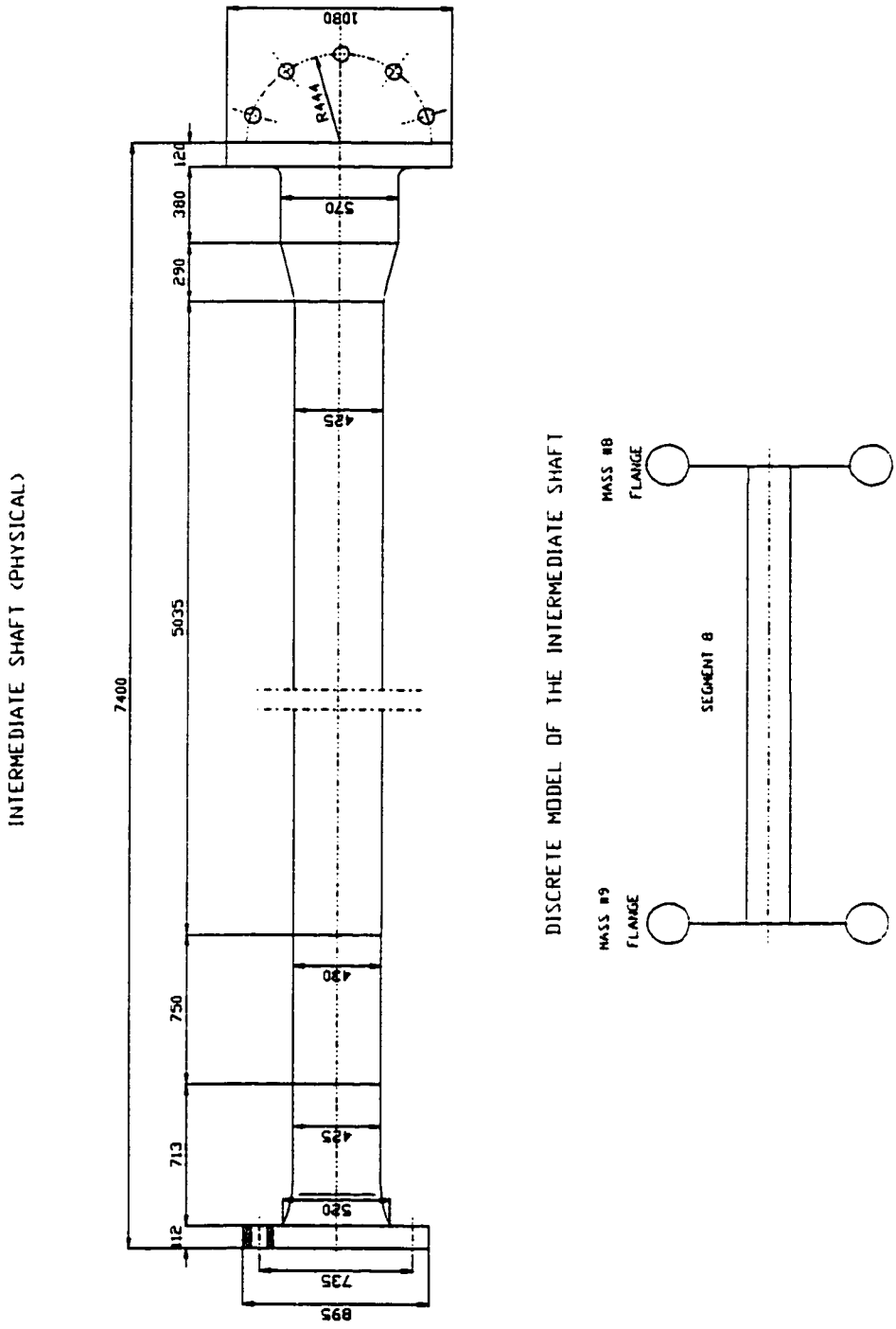

Figure III-4 Intermediate shaft design - Overcritical solution

Solution to OVERCRITICAL System Without Damper

Propulsion shafting diameter is enhanced for the purpose of stress reduction and adjustment of main resonance position:

- propeller shaft diameter is

d_p = 520 [mm]

- intermediate shaft diameter

d_i = 425 [mm]

Flywheel inertia is also increased to:

I = 4893 [kgm2]

Discrete model of the complete propulsion system is given in Figure III-5, and Table III-2.

Natural frequencies: First six natural frequencies are calculated, and their modal vectors are presented in Table III-3. Modal vector for one node vibration and frequency of 354 [1/min] (Table III-3) shows that node position is in intermediate shaft. It is therefore expected that the highest torsional stress occurs in intermediate shaft.

From the two and three node vibration (Table III-3), the second and the third natural frequencies are found in crankshaft and in propeller shaft, respectively. Effect of the first natural frequency is dominant, while for the other modes the following is valid: the higher the modal frequency, the lower its contribution to total response.

Response analysis is presented in Figures III-6 to III-17. Stress limits are presented with full curves and the calculated stresses by the dashed lines. An inspection of these figures indicates that the obtained solution does not satisfy required criteria for the following reasons. The fifth order main resonance has its peak at 69 [rpm] of the engine. Stresses at main resonance, in intermediate shaft Figure III-13, and propeller shaft segments Figures III-14 to III-17, are found to be over the limit for transient operation. Moreover stresses in crankshaft Segment #6 (Figure III-11), and in thrust shaft (Figure III-12) are above limit for continuous operation.

Conclusion: Solution to torsional vibration calculation, with minimum diameters of the line shafting and small flywheel, does not suit ABS requirements. Possible changes to reduce stresses to acceptable values are:

- installation of tuning wheel,
- installation of torsional vibration damper, or
- solving the problem as undercritical.

Solution With Tuning Wheel: Solution to fit installation below transient limit can be found by installing tuning wheel on the forward end of the engine (inertia #1). Tuning wheel needs to have inertia of:

$$I = 10{,}000 \text{ [kgm}^2\text{]}$$

and therefore total inertia on mass #1 would be:

$$I = 12{,}179 \text{ [kgm}^2\text{]}$$

Results of this computation are not presented because they are an intermediate solution. Although they satisfy Classification Rules with barred speed range, they are not considered as good a solution as the one with damper, or undercritical solution. Possible reasons are:

- improper operation of the installation with BSR is possible if appropriate equipment is not installed to prevent any human error
- very heavy masses (like, for example, a 10,000 [kgm^2] tuning wheel would be) can reduce life of the main bearings,
- additional bearing may be required to support heavy turning wheel,
- engine's response will be slower when manoeuvring (reversing),
- reduced load capacity.

Figure III-5 Inertia-elastic system - Overcritical solution

TORSIONAL VIBRATION CALCULATION

INPUT DATA FOR: Engine 5L60MC MAN_B&W Overcritical Solution

Rated Power 7830.0 [kW]
Rated Speed 111.0 [1/min]

MASS-ELASTIC SYSTEM

Mass No.	Inertia kgm2	A.Flex rad/Nm	A.Dmp. %	Sh.Flex. rad/Nm	R.Dmp. %	Shaft-Dia[m] out	in	Name
1	2179	0.000E+00	0.85	6.630E-10	0.00	0.672	0.115	flng
2	7040	0.000E+00	0.85	8.300E-10	0.00	0.672	0.322	cyl_1
3	7519	0.000E+00	0.85	8.300E-10	0.00	0.672	0.115	cyl_2
4	7040	0.000E+00	0.85	8.380E-10	0.00	0.672	0.322	cyl_3
5	7040	0.000E+00	0.85	8.300E-10	0.00	0.672	0.322	cyl_4
6	7519	0.000E+00	0.85	6.480E-10	0.00	0.672	0.115	cyl_5
7	4257	0.000E+00	0.50	4.860E-10	0.00	0.672	0.115	Cam
8	4893	0.000E+00	0.50	2.607E-08	0.00	0.425	0.000	Flywh
9	124	0.000E+00	0.00	1.743E-09	0.00	0.520	0.000	Flange
10	47	0.000E+00	0.00	9.148E-10	0.00	0.526	0.000	Pr.sh
11	58	0.000E+00	0.00	2.603E-09	0.00	0.520	0.000	Pr.sh
12	93	0.000E+00	0.00	3.141E-09	0.00	0.520	0.000	Pr.sh
13	35026	0.000E+00	5.50					Propeller

ENGINE EXCITATION DATA

Harmonic Components File: HCL60MC3
Firing Order : 1-4-3-2-5
Cylinder Diameter : 0.600 [m]
Piston Stroke : 1.944 [m]
Connecting Rod Length : 2.340 [m]
Reciprocating Mass/Cyl. : 5389 [kg]
Mechanical Efficiency : 100 [%]
Load Deviation : 0 [%]

Engine Speed Range from 30 [rpm] to 111 [rpm]
Harmonics Range from 1.0 to 16.0 with increment 1.0

Table III-2 Mass-elastic system for overcritical solution

TORSIONAL VIBRATION CALCULATION
NATURAL DAMPED FREQUENCIES

```
NATURAL FREQUENCY [ 1] =    37 [rad/s]
NATURAL FREQUENCY [ 2] =   197 [rad/s]
NATURAL FREQUENCY [ 3] =   387 [rad/s]
NATURAL FREQUENCY [ 4] =   545 [rad/s]
NATURAL FREQUENCY [ 5] =   674 [rad/s]
NATURAL FREQUENCY [ 6] =   779 [rad/s]
```

MODAL VECTORS

	1 Node 354 [1/min]	2 Node 1881 [1/min]	3 Node 3691 [1/min]
[1]	1.0000000E+00	1.0000000E+00	1.0000000E+00
[2]	9.9801558E-01	9.4393431E-01	7.8411555E-01
[3]	9.8752099E-01	6.5969467E-01	-1.7081724E-01
[4]	9.6856100E-01	2.1568048E-01	-9.6644830E-01
[5]	9.4156942E-01	-2.8199368E-01	-9.1773570E-01
[6]	9.0727824E-01	-7.1097031E-01	-6.8144151E-02
[7]	8.7443424E-01	-9.1144699E-01	6.4476657E-01
[8]	8.4731622E-01	-9.8862360E-01	9.8011026E-01
[9]	-7.5551310E-01	-2.3476480E-01	2.8672995E-01
[10]	-8.6245437E-01	-1.8239639E-01	2.3112737E-01
[11]	-9.1853997E-01	-1.5460085E-01	2.0044805E-01
[12]	-1.0779581E+00	-7.4588313E-02	1.0859036E-01
[13]	-1.2698798E+00	2.2803604E-02	-6.9997220E-03

	4 Node 5207 [1/min]	5 Node 6437 [1/min]	6 Node 7438[1/min]
[1]	1.0000000E+00	1.0000000E+00	1.0000000E+00
[2]	5.7047768E-01	3.4361070E-01	1.2352806E-01
[3]	-9.5830516E-01	-1.3903515E+00	-1.4116231E+00
[4]	-7.0898472E-01	8.1802127E-01	2.3979363E+00
[5]	7.8630393E-01	8.5501592E-01	2.3384392E+00
[6]	9.0130052E-01	-1.3782895E+00	1.2602020E+00
[7]	-3.1454772E-01	-7.0713105E-02	3.4460427E-01
[8]	-1.0329515E+00	9.7643990E-01	-7.7463558E-01
[9]	-3.9612259E-01	5.5858775E-01	-8.6651848E-01
[10]	-3.2813786E-01	4.7590069E-01	-7.5925400E-01
[11]	-2.8823669E-01	4.2315631E-01	-6.8305154E-01
[12]	-1.6166834E-01	2.4385214E-01	-4.0324856E-01
[13]	5.1310807E-03	-4.9547114E-03	6.0326678E-03

Table III-3 Eigenvalues for overcritical solution

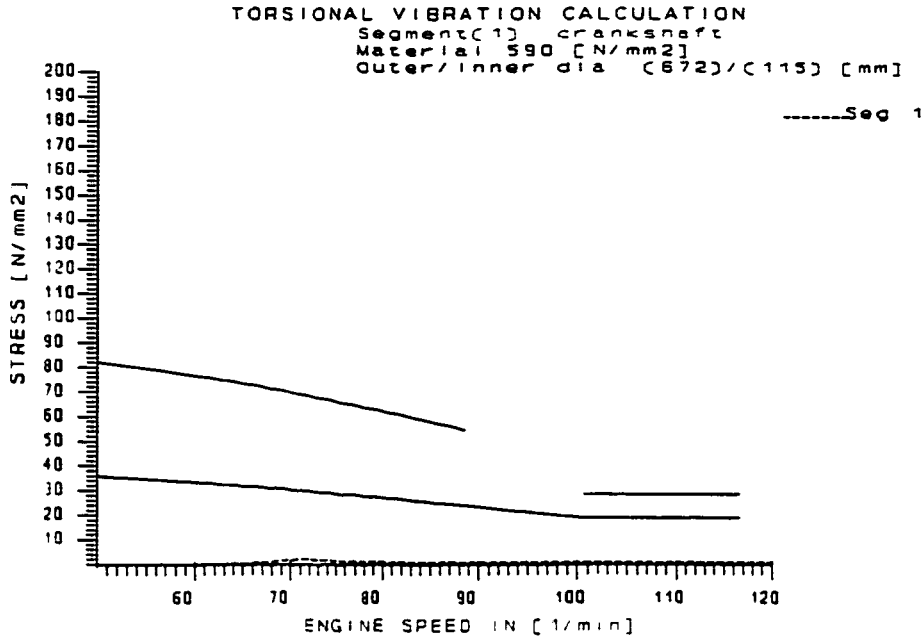

Figure III-6 T/V stress [N/mm2] in crankshaft - segment #1 - Overcritical solution

Upper full curve is ABS torsional stress limit for transient operation
Lower full curve is ABS torsional stress limit for continuous operation

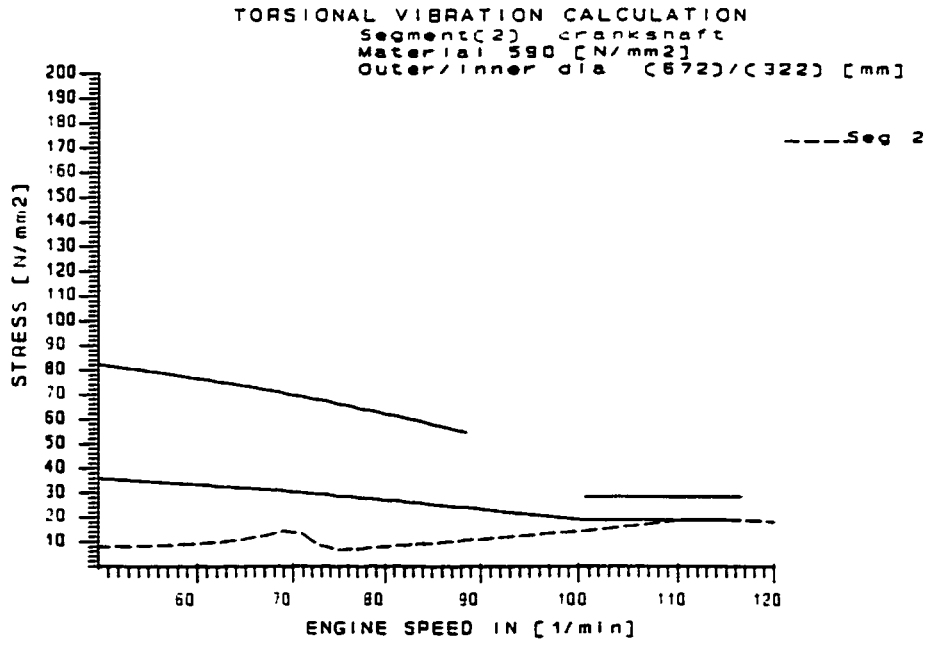

Figure III-7 T/V stress [N/mm2] in crankshaft - segment #2 - Overcritical solution

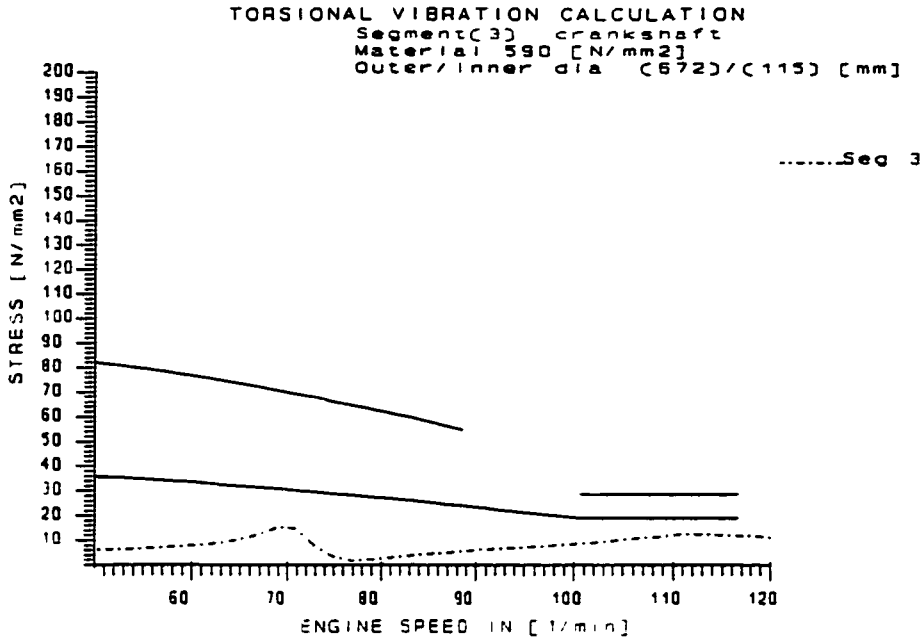

Figure III-8 T/V stress [N/mm2] in crankshaft - segment #3 - Overcritical solution

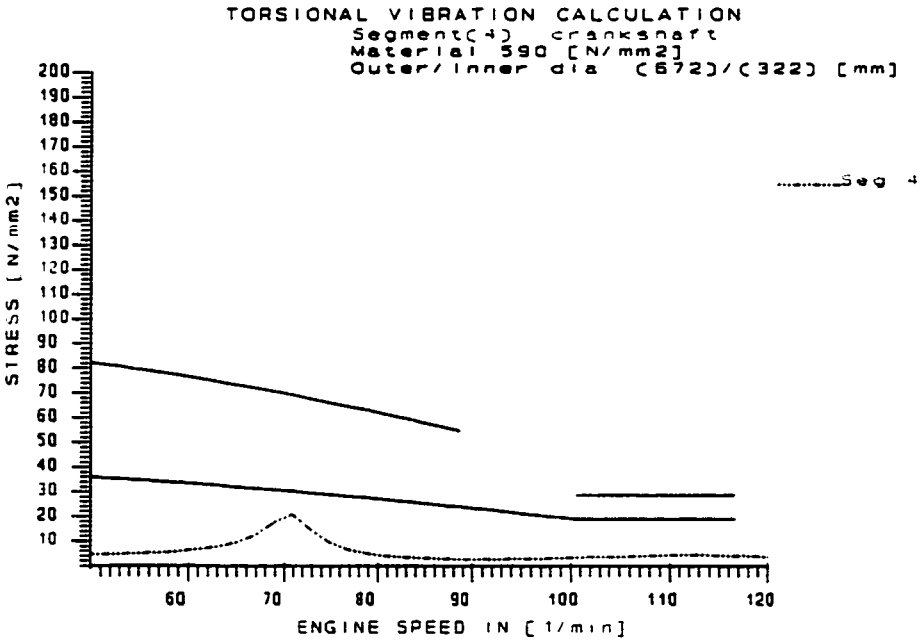

Figure III-9 T/V stress [N/mm2] in crankshaft - segment #4 - Overcritical solution

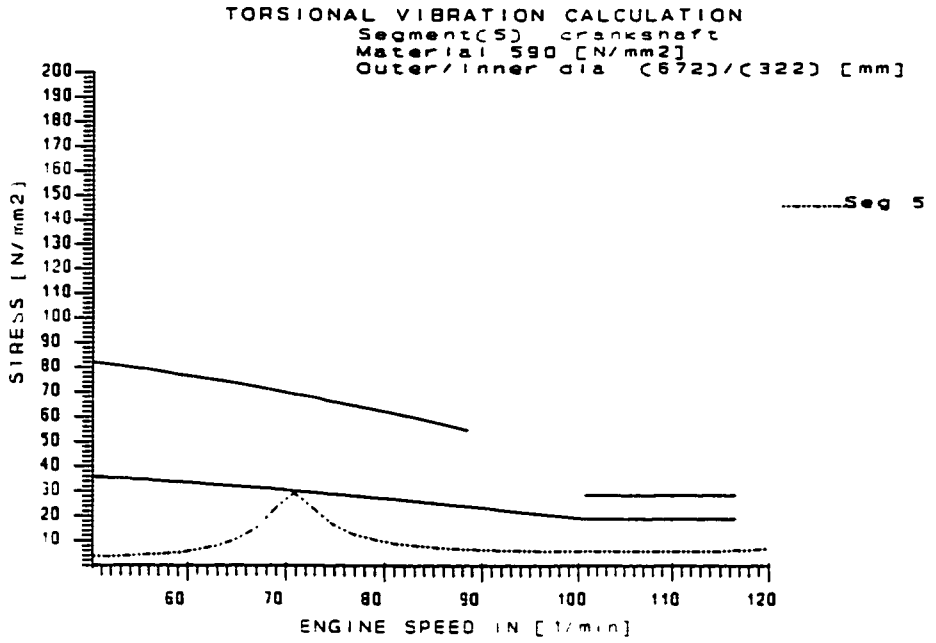

Figure III-10 T/V stress [N/mm2] in crankshaft - segment #5 - Overcritical solution

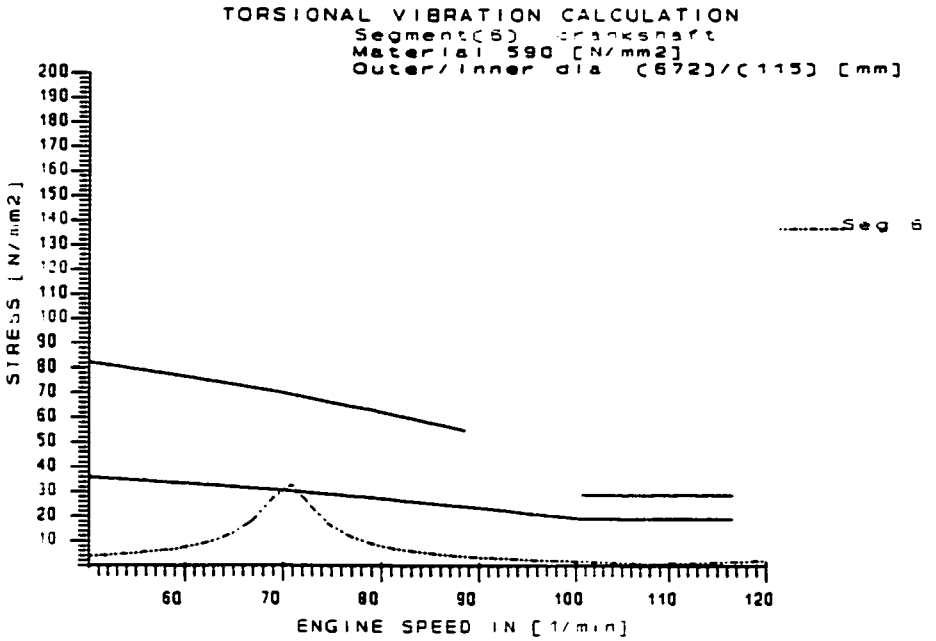

Figure III-11 T/V stress [N/mm2] in crankshaft - segment #6 - Overcritical solution

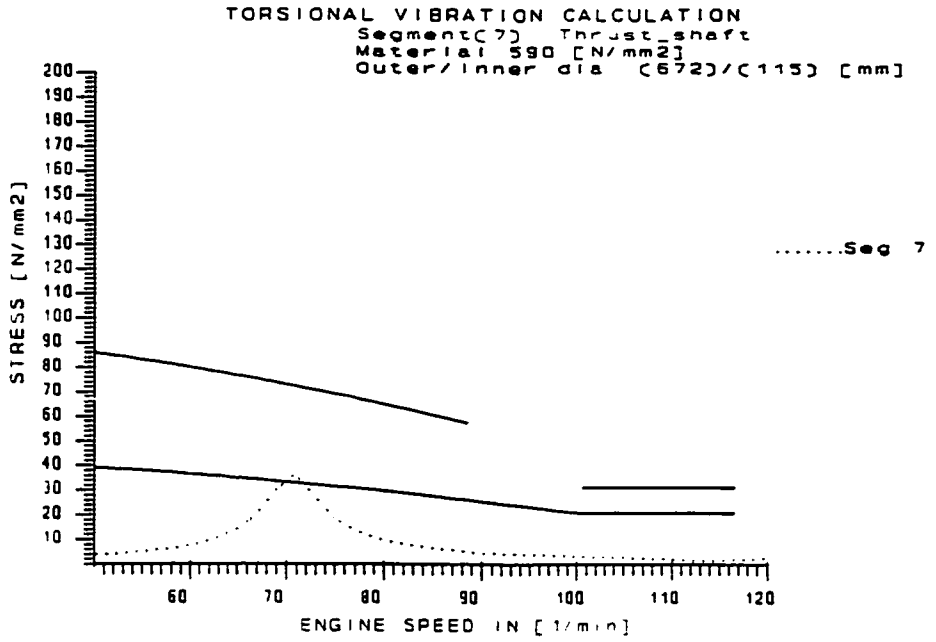

Figure III-12 T/V stress [N/mm2] in thrust shaft - segment #7 - Overcritical solution

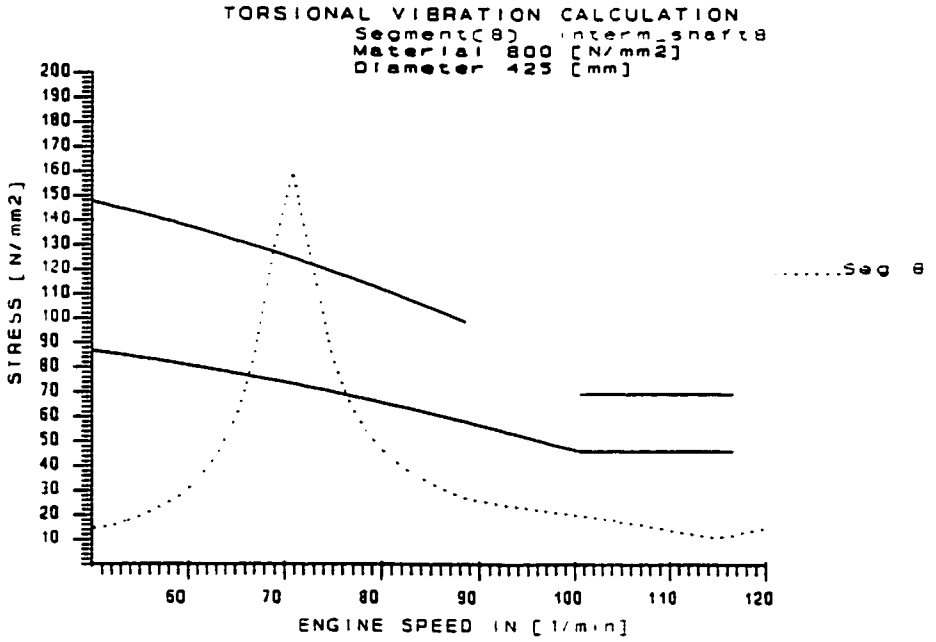

Figure III-13 T/V stress [N/mm2] in intermediate shaft - segment #8 - Overcritical solution

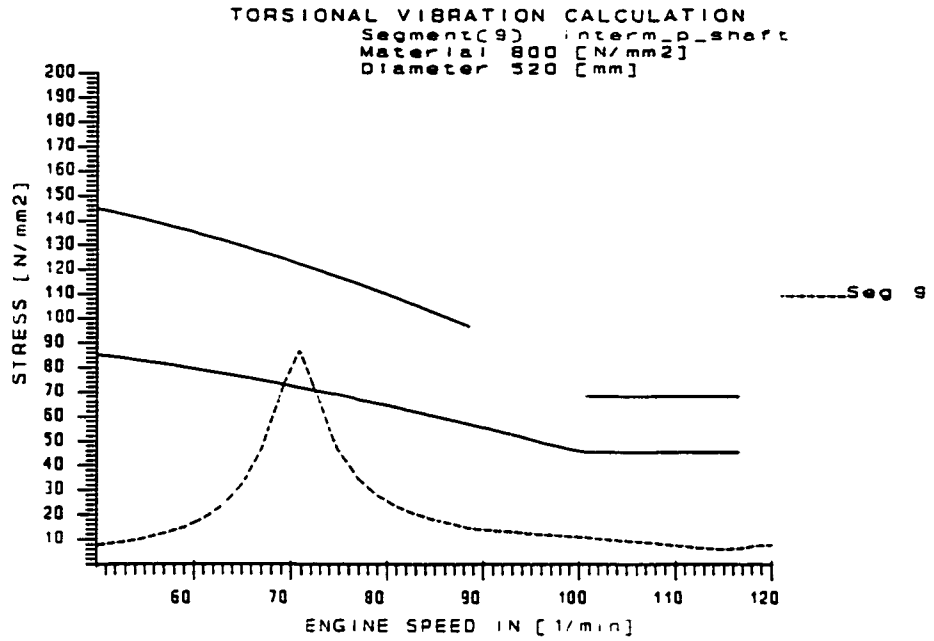

Figure III-14 T/V stress [N/mm2] in propeller shaft (intermediate) - segment #9 - Overcritical solution

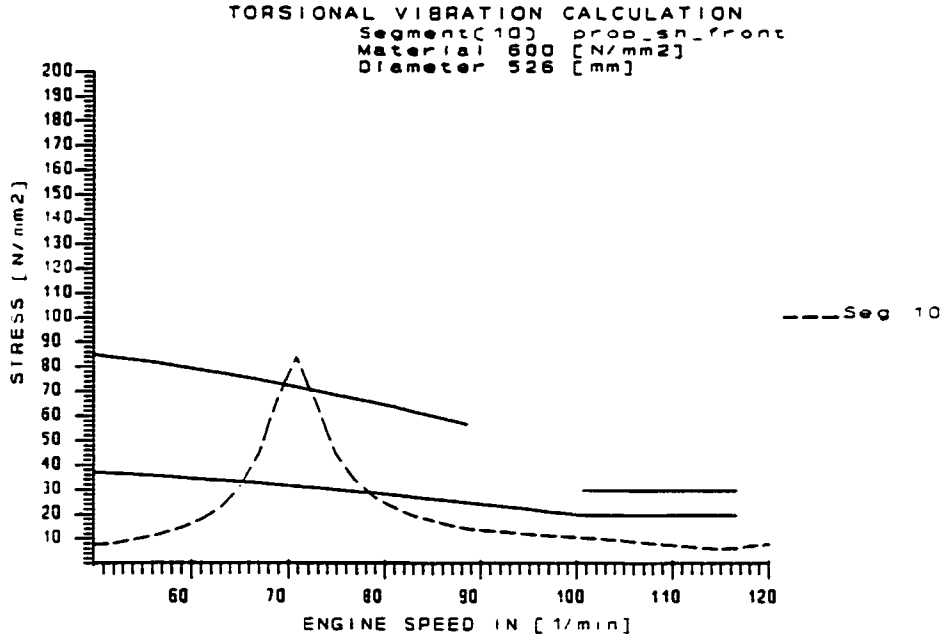

Figure III-15 T/V stress [N/mm2] in propeller shaft (front) - segment #10 - Overcritical solution

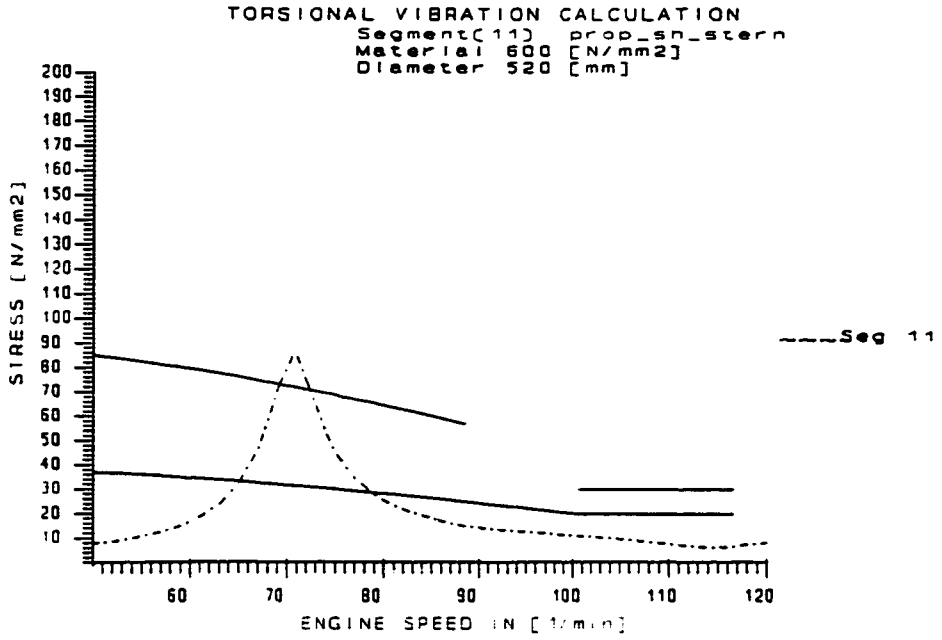

Figure III-16 T/V stress [N/mm2] in propeller shaft (stern) - segment #11 - Overcritical solution

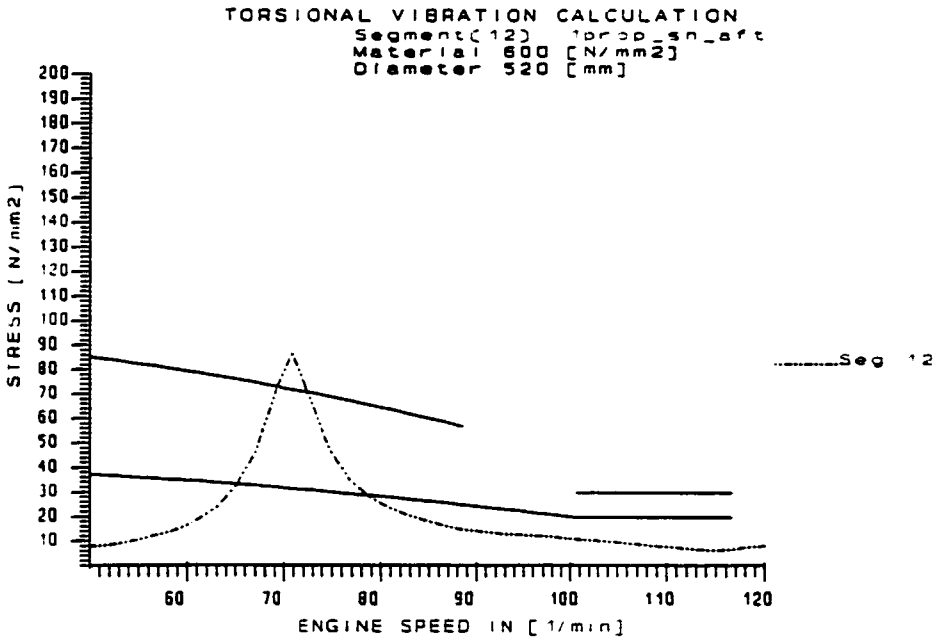

Figure III-17 T/V stress [N/mm2] in propeller shaft (aft) - segment #12 - Overcritical solution

Solution With Damper

This mass-elastic system differs from the previous one only in damper which is attached to the fore end of the crankshaft (mass #1 in Table III-4). The selected damper is a highly effective spring type tuned damper. Inertia of mass attached to the damper's secondary part is:

$$I = 5000 \ [kgm^2]$$

Stiffness of the damper is dependent on vibrating frequency. Damping factor is 0.28

Discrete model of the complete propulsion system is given in Figure III-18, and Table III-4.

Natural frequencies: First six natural frequencies are calculated as presented in Table III-5. One node vibration (frequency 335 [1/min]) shows that node is placed in intermediate shaft (Table III-5). From the 2 node vibration (frequency 426 [1/min]), second natural frequency is recognized to originate in the damper. Third and fourth frequencies originated in propeller shaft and crankshaft, respectively (Table III-5).

Response analysis is presented in Figures III-19 to III-31. These figures present the stress limits with full curves, and the calculated stresses and torque by the dashed lines. Main resonance from the solution without torsional vibration damper (Figures III-6 to III-17), has been divided in this analysis into two, significantly lower, resonant peaks. Stresses in intermediate shaft (Figure III-27), as well as in the propeller shaft segments (Figures III-28 to III-31) are placed below the limit for continuous

operation. Stresses in the crankshaft segments (Figures III-20 to III-25), and the thrust shaft (Figure III-21), are below the continuous operation limit as well. Figure III-19 shows a vibratory torque which a damper must be able to sustain. As inspection of these figures shows, in solution with tuned damper no restrictions are imposed on the propulsion system over the whole operating speed range.

The benefits of this solution are:

- lower cost of the shafting if diameters are small
- shafting bearings are also smaller and cheaper
- no restriction for running in whole engine speed range

Weak points of the solution with damper are:

- high cost of the damper
- additional equipment to monitor damper's performance
- maintenance cost

Conclusion: With installed tuned damper, vibration amplitudes are reduced below limits for continuous operation and therefore there is no restriction in operation. However, this type of vibration dampers are expensive and additional care and maintenance is required. Presented solution with big and tuned damper is not the only possible one. There is the possibility to install smaller and cheaper tuned or untuned dampers, which will only lower the amplitude below limit for transient operation, so BSR will be required. Although these alternative solutions can have commercial support, they are not technically justified.

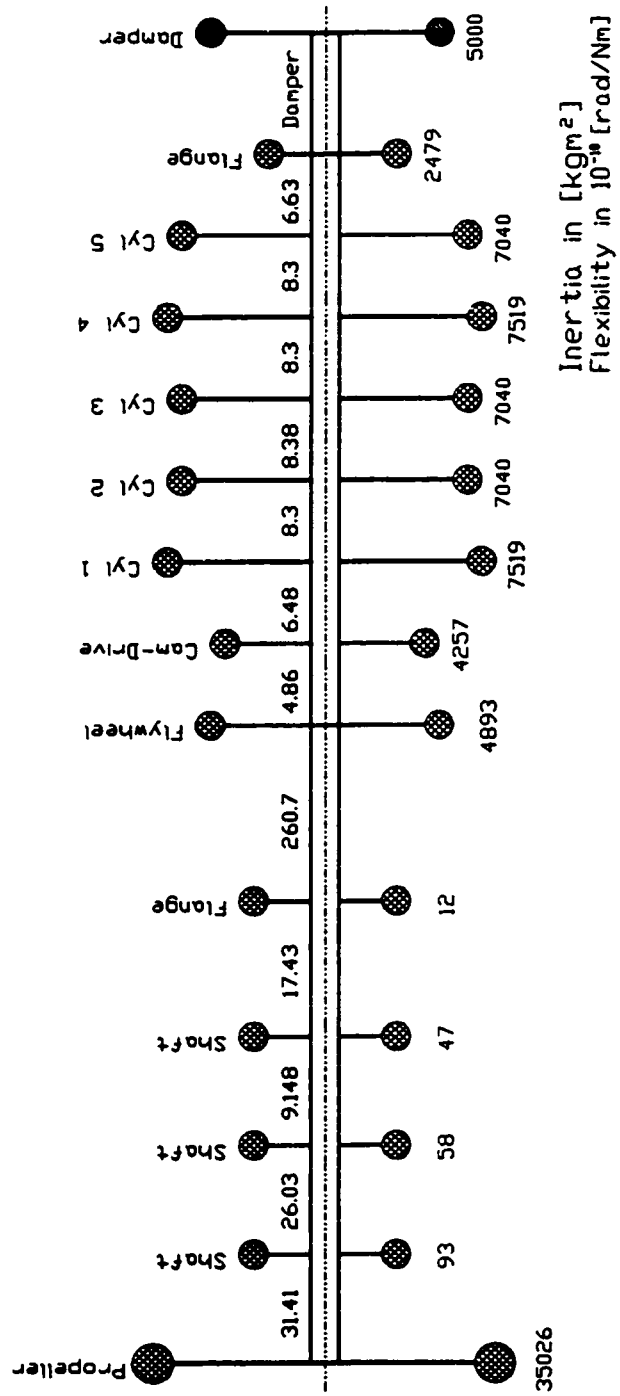

Figure III-18 Inertia-elastic system - Overcritical solution with damper

TORSIONAL VIBRATION CALCULATION

INPUT DATA FOR: Engine 5L60MC MAN_B&W-Overcritical-With DAMPER

Rated Power 7830.0 [kW]
Rated Speed 111.0 [1/min]

MASS-ELASTIC SYSTEM

Mass No.	Inertia kgm2	A.Flex rad/Nm	A.Dmp. %	Sh.Flex. rad/Nm	R.Dmp. %	Shaft-Dia[m] out	in	Name
1	5000	0.000E+00	0.00	<see damper spec. below>				DmpSec
2	2479	0.000E+00	0.00	6.630E-10	0.00	0.672	0.115	Dmp
3	7040	0.000E+00	0.85	8.300E-10	0.00	0.672	0.322	cyl_1
4	7519	0.000E+00	0.85	8.300E-10	0.00	0.672	0.115	cyl_2
5	7040	0.000E+00	0.85	8.380E-10	0.00	0.672	0.322	cyl_3
6	7040	0.000E+00	0.85	8.300E-10	0.00	0.672	0.322	cyl_4
7	7519	0.000E+00	0.85	6.480E-10	0.00	0.672	0.115	cyl_5
8	4257	0.000E+00	0.50	4.860E-10	0.00	0.672	0.115	Cam
9	4893	0.000E+00	0.50	2.607E-08	0.00	0.425	0.000	Flywh
10	124	0.000E+00	0.00	1.743E-09	0.00	0.520	0.000	flange
11	47	0.000E+00	0.00	9.148E-10	0.00	0.526	0.000	Pr.sh
12	58	0.000E+00	0.00	2.603E-09	0.00	0.520	0.000	Pr.sh
13	93	0.000E+00	0.00	3.141E-09	0.00	0.520	0.000	Pr.sh
14	35026	0.000E+00	5.50					Propell

DAMPER DATA

Damper Type : Damper
Undimens. Damping : 0.28
Max Power Loss : 39.3 [kW]
Max Damping Torque : 30000.0 [Nm/bar]
Linear viscous damping [Nms/rad], and damper stiffness [Nm/rad] are function of omega [rad/s]

ENGINE EXCITATION DATA

Harmonic Components File: HCL60MC3
Firing Order : 1-4-3-2-5
Cylinder Diameter : 0.600 [m]
Piston Stroke : 1.944 [m]
Connecting Rod Length : 2.340 [m]
Reciprocating Mass/Cyl. : 5389 [kg]
Mechanical Efficiency : 100 [%]
Load Deviation : 0 [%]

Engine Speed Range from 30 [rpm] to 111 [rpm]
Harmonics Range from 1.0 to 16.0 with increment 1.0

Table III-4 Mass-elastic system -Overcritical solution with damper

TORSIONAL VIBRATION CALCULATION
DAMPED NATURAL FREQUENCIES

NATURAL FREQUENCY	[1]	=	35 [rad/s]
NATURAL FREQUENCY	[2]	=	48 [rad/s]
NATURAL FREQUENCY	[3]	=	197 [rad/s]
NATURAL FREQUENCY	[4]	=	385 [rad/s]
NATURAL FREQUENCY	[5]	=	543 [rad/s]
NATURAL FREQUENCY	[6]	=	672 [rad/s]

MODAL VECTORS

	1 Node	2 Node	3 Node
	335 [1/min]	462 [1/min]	1880 [1/min]
[1]	1.0000000E+00	1.0000000E+00	1.0000000E+00
[2]	3.9036283E-01	-1.5951562E-01	-1.8222638E+01
[3]	3.8549812E-01	-1.6665471E-01	-1.7190031E+01
[4]	3.7663852E-01	-1.7331479E-01	-1.2003247E+01
[5]	3.6488691E-01	-1.7744548E-01	-3.9123462E+00
[6]	3.5037930E-01	-1.7916792E-01	5.1513503E+00
[7]	3.3349096E-01	-1.7842569E-01	1.2961578E+01
[8]	3.1830804E-01	-1.7581324E-01	1.6610870E+01
[9]	3.0611114E-01	-1.7300328E-01	1.8015516E+01
[10]	-3.9603353E-01	2.9296413E-02	4.2774618E+00
[11]	-4.4287388E-01	4.2807389E-02	3.3231622E+00
[12]	-4.6743829E-01	4.9895392E-02	2.8166563E+00
[13]	-5.3725701E-01	7.0048881E-02	1.3586432E+00
[14]	-6.2130748E-01	9.4318298E-02	-4.1604034E-01

	4 Node	5 Node	6 Node
	3675 [1/min]	5185 [1/min]	6417 [1/min]
[1]	1.0000000E+00	1.0000000E+00	1.0000000E+00
[2]	-7.2432741E+01	-1.4515803E+02	2.2291897E+02
[3]	-5.5292608E+01	-7.5808850E+01	-5.8956322E+01
[4]	1.4013761E+01	1.4158264E+02	3.0187986E+02
[5]	7.0367830E+01	9.8517671E+01	-1.8808396E+02
[6]	6.5783514E+01	-1.1628621E+02	-1.8167124E+02
[7]	4.3154982E+00	-1.2874639E+02	3.0407371E+02
[8]	-4.6787999E+01	4.6434256E+01	1.4239655E+01
[9]	-7.0779608E+01	1.4950156E+02	-2.1644027E+02
[10]	-2.0657692E+01	5.7031761E+01	-1.2274547E+02
[11]	-1.6646557E+01	4.7222616E+01	-1.0452304E+02
[12]	-1.4434503E+01	4.1472253E+01	-9.2918702E+01
[13]	-7.8146809E+00	2.3250868E+01	-5.3521082E+01
[14]	5.1190435E-01	-7.4300204E-01	1.0970196E+00

Table III-5 Eigenvalues - Overcritical solution with damper

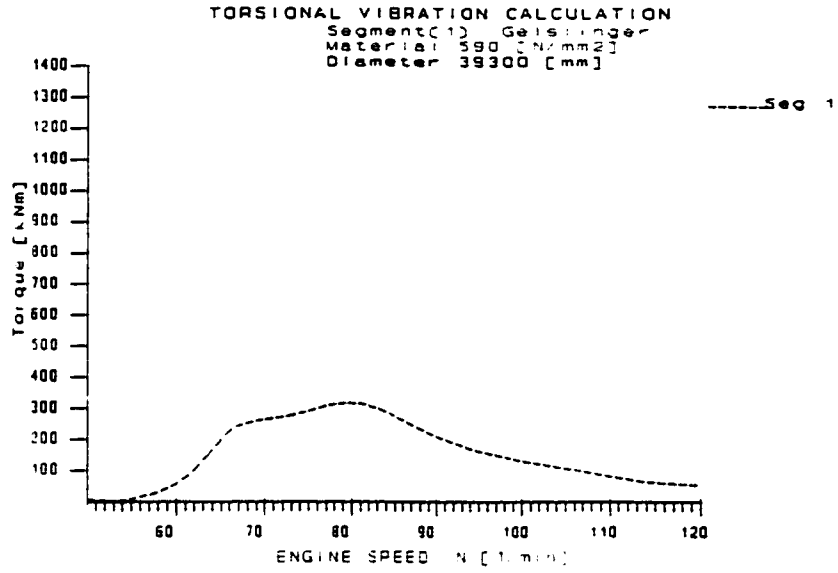

Figure III-19 - Total torque [kNm] in the damper - segment #1 - Overcritical solution with damper

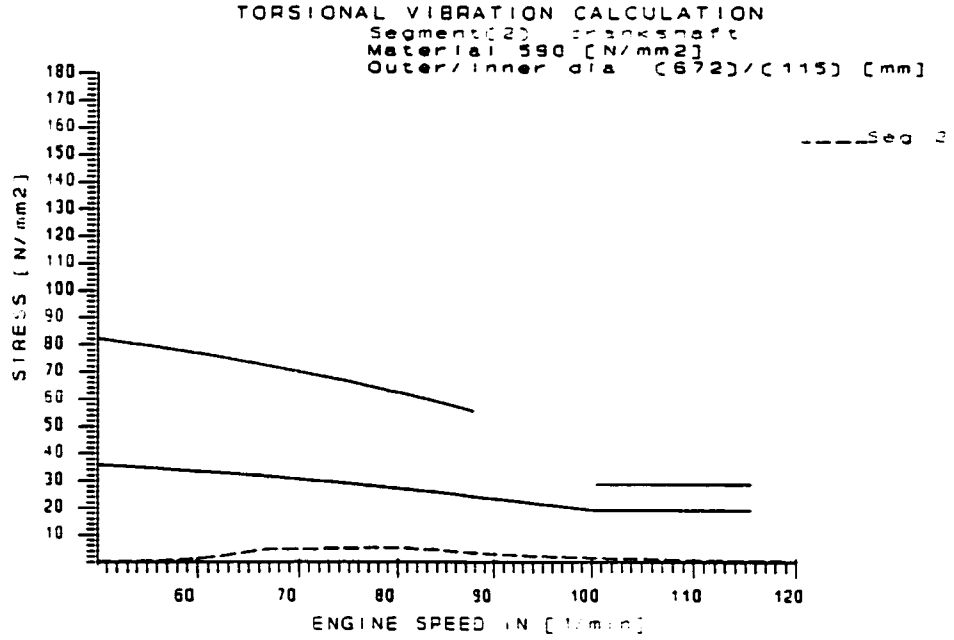

Figure III-20 T/V stress [N/mm2] in crankshaft - segment #2 - Overcritical solution with damper

Upper full curve is ABS torsional stress limit for transient operation
Lower full curve is ABS torsional stress limit for continuous operation

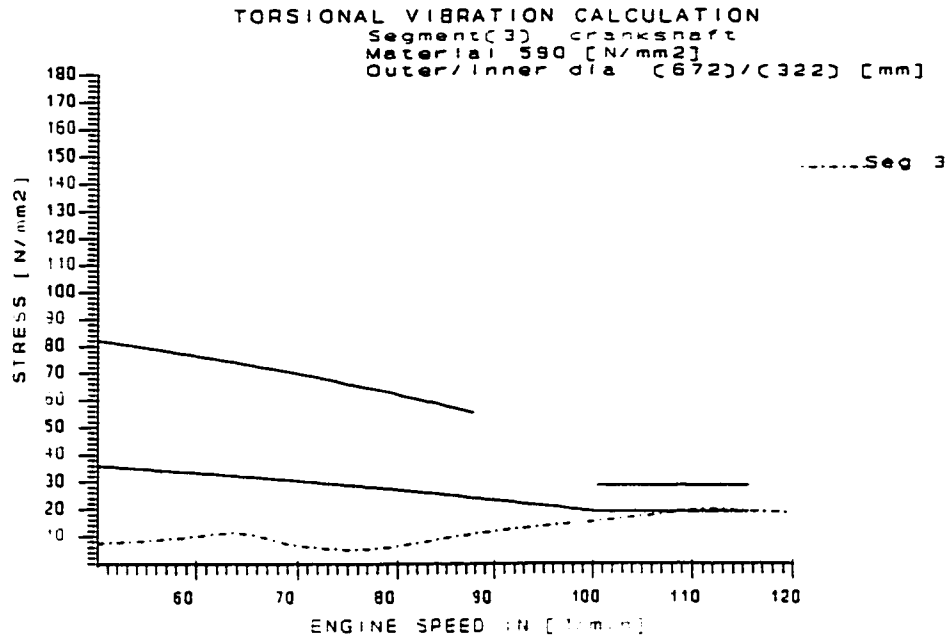

Figure III-21 T/V stress [N/mm2] in crankshaft - segment #3 - Overcritical solution with damper

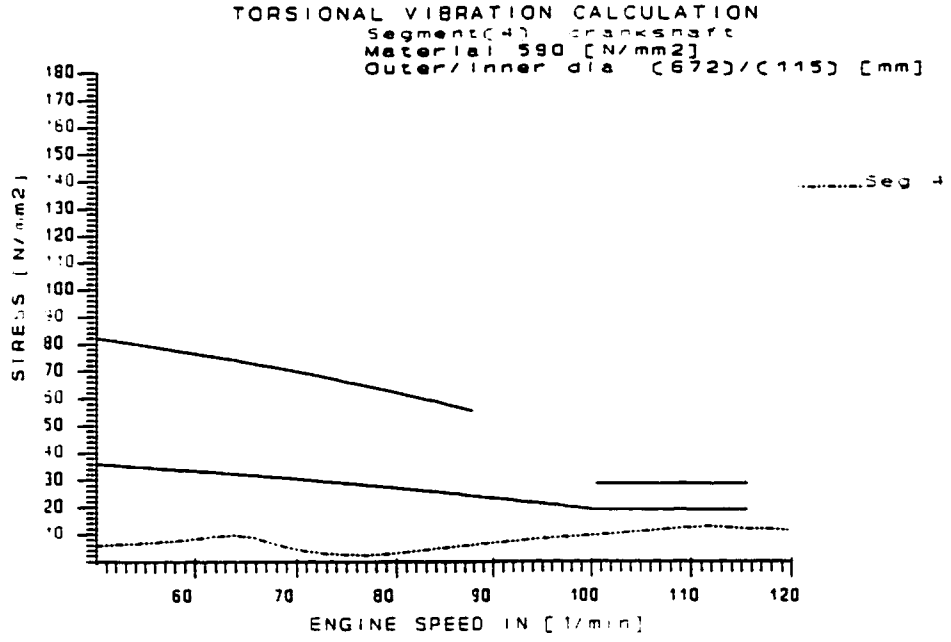

Figure III-22 T/V stress [N/mm2] in crankshaft - segment #4 - Overcritical solution with damper

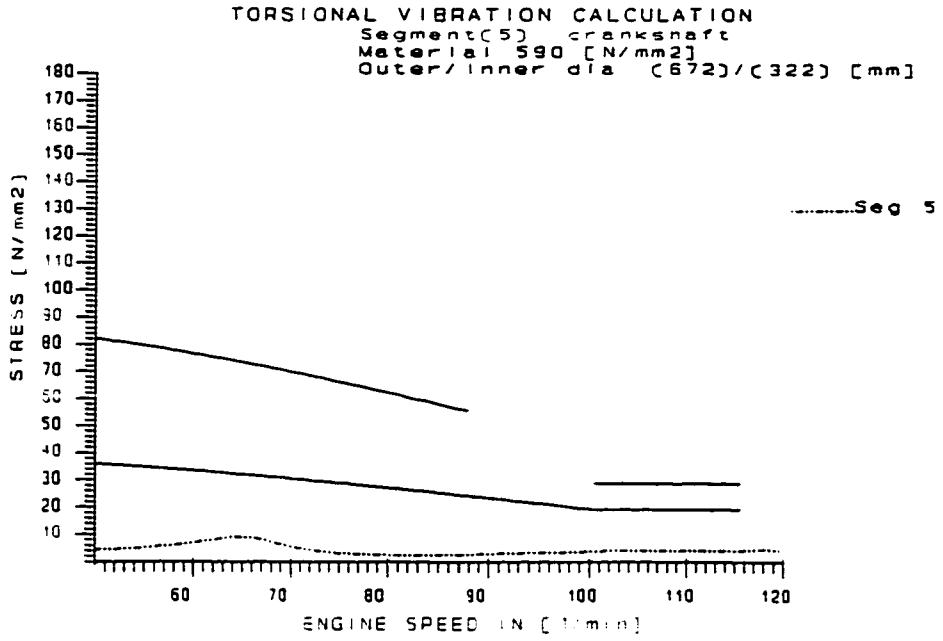

Figure III-23 T/V stress [N/mm2] in crankshaft - segment #5 - Overcritical solution with damper

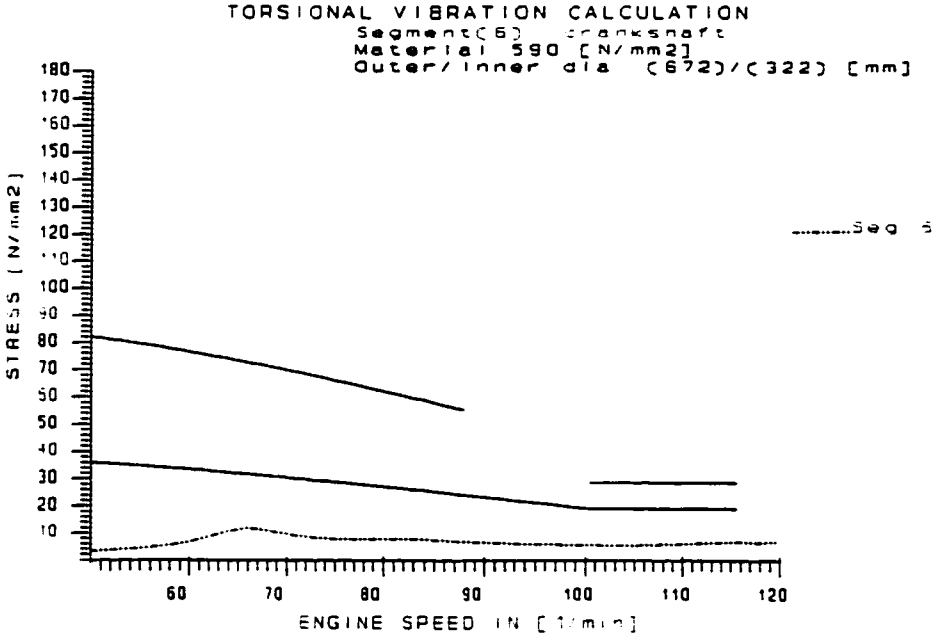

Figure III-24 T/V stress [N/mm2] in crankshaft - segment #6 - Overcritical solution with damper

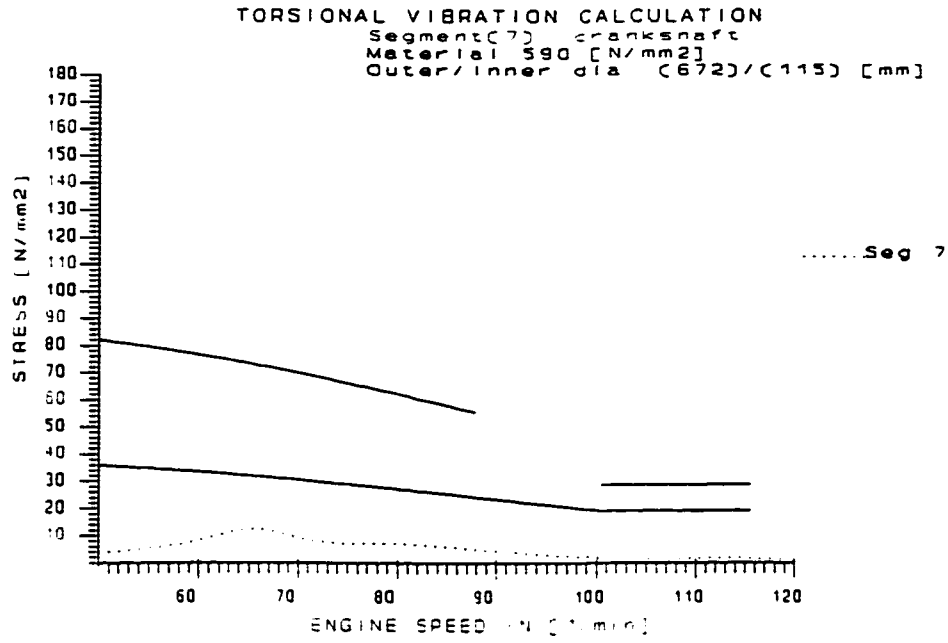

Figure III-25 T/V stress [N/mm2] in crankshaft - segment #7 - Overcritical solution with damper

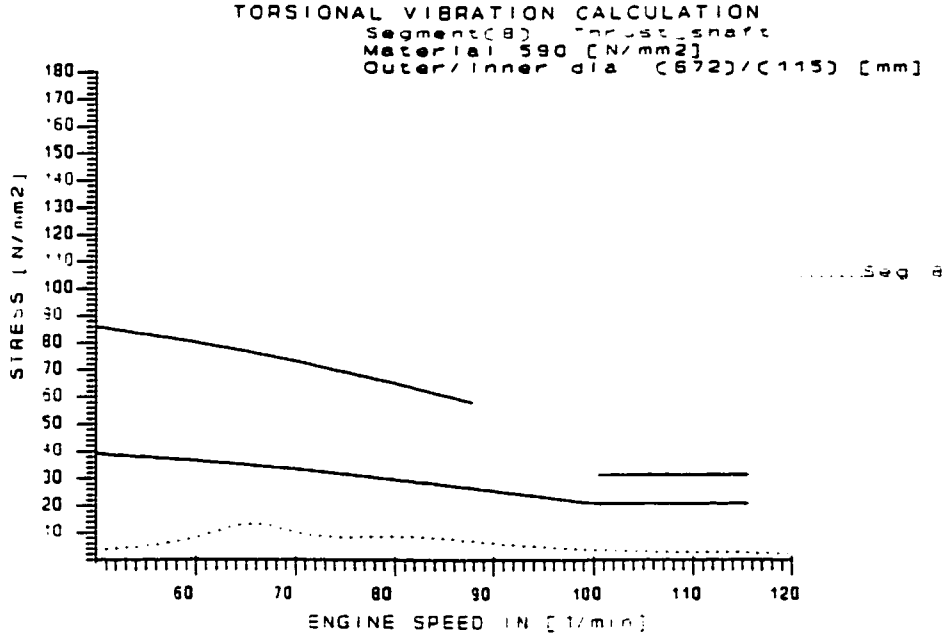

Figure III-26 T/V stress [N/mm2] in thrust-shaft - segment #8 - Overcritical solution with damper

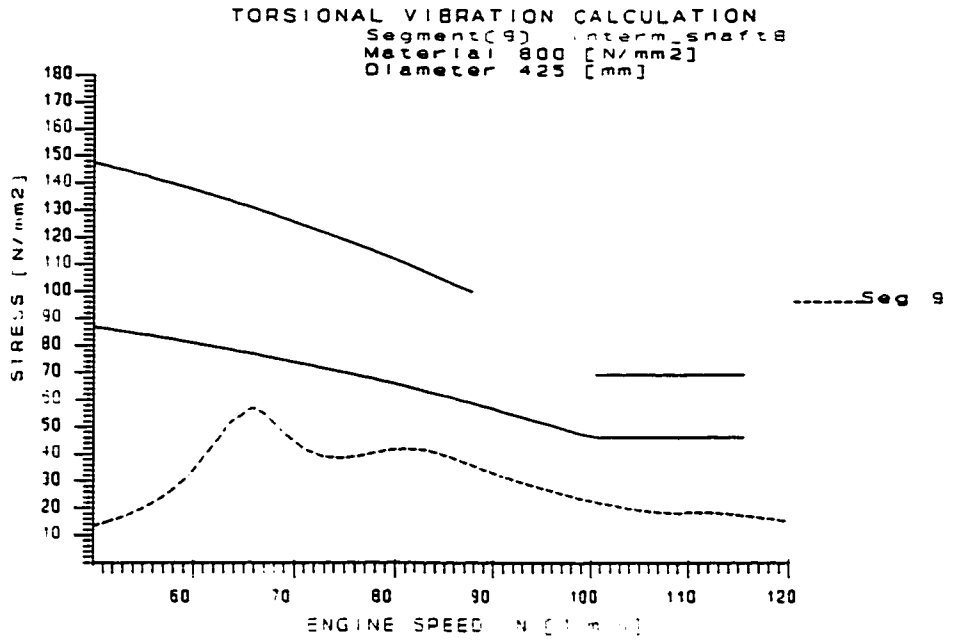

Figure III-27 T/V stress [N/mm2] in intermediate shaft - segment #9 - Overcritical solution with damper

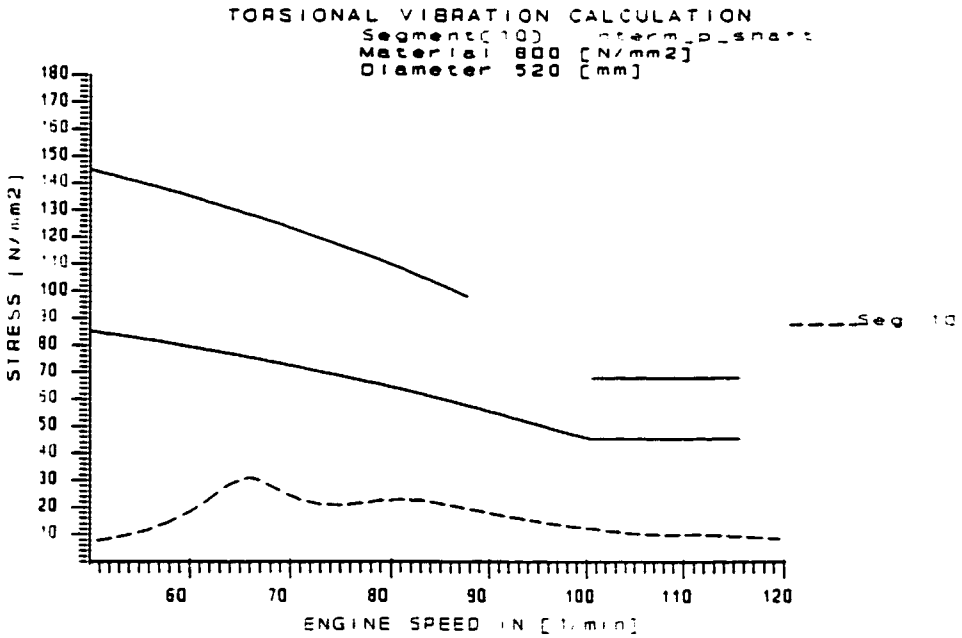

Figure III-28 T/V stress [N/mm2] in propeller shaft (int) - segment #10 - Overcritical solution with damper

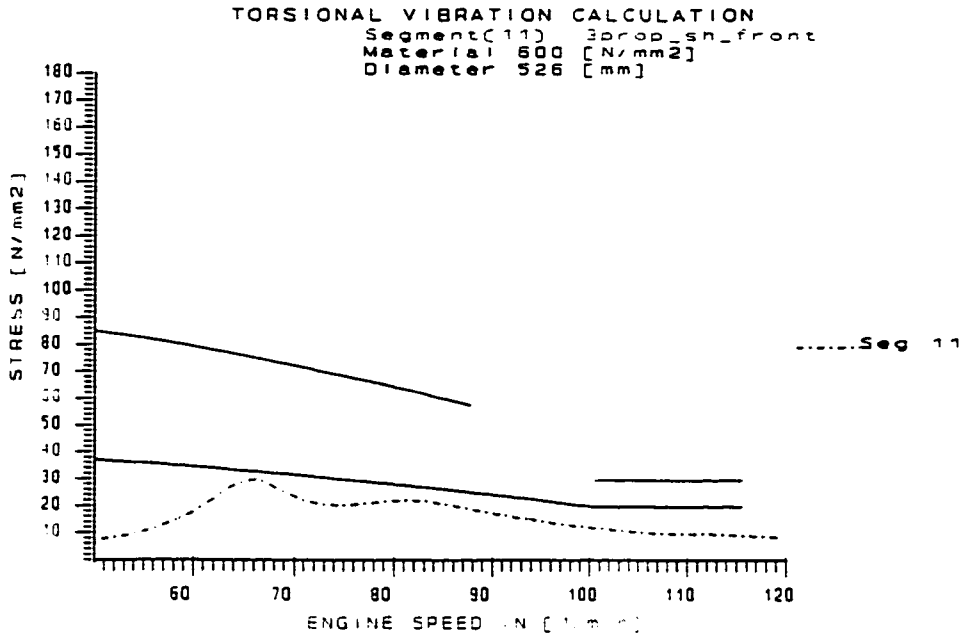

Figure III-29 T/V stress [N/mm2] in propeller shaft (front) - segment #11 - Overcritical solution with damper

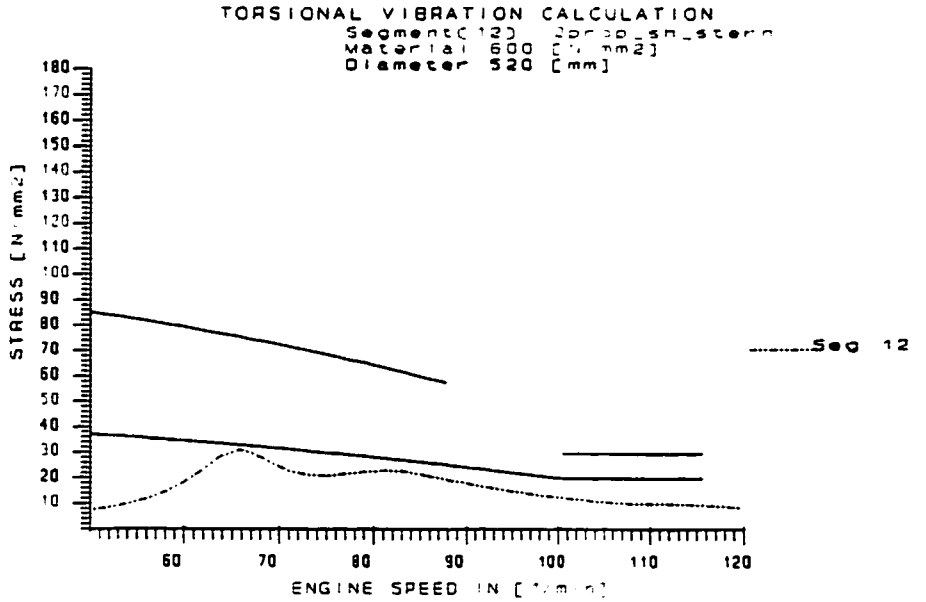

Figure III-30 T/V stress [N/mm2] in propeller shaft (stern) - segment #12 - Overcritical solution with damper

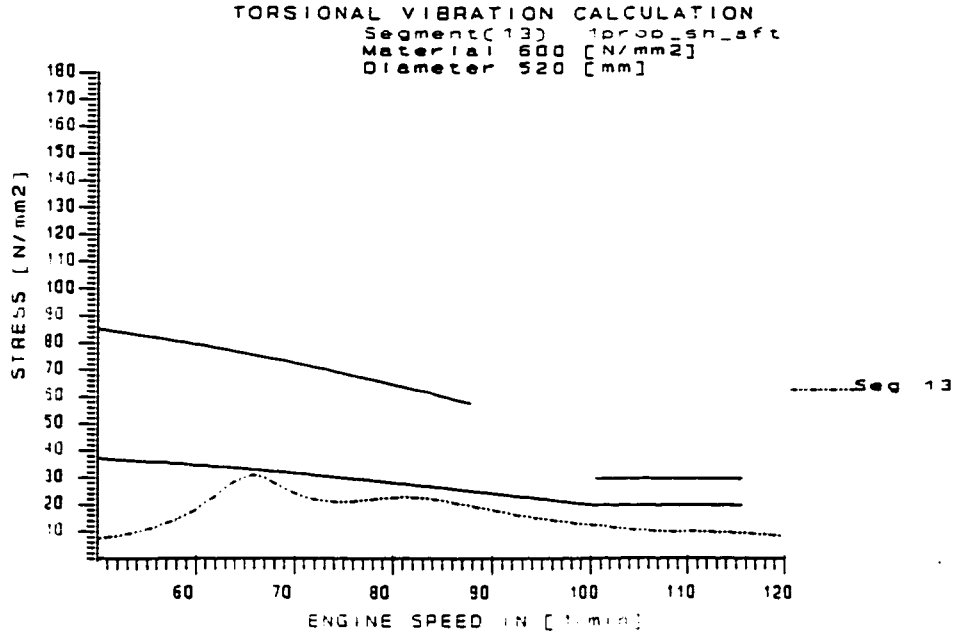

Figure III-31 T/V stress [N/mm2] in propeller shaft (aft) - segment #13 - Overcritical solution with damper

III.2.3.2. *Undercritical Solution*

Main resonance in undercritical solution is beyond the operating range of the propulsion installation. Therefore, propulsion system, when running at rated speed, will be said to operate under *undercritical* condition. Experience has shown that dominant order of the first natural frequency needs to have its resonance placed approximately at 35-45% over the nominal speed. The reason for pushing main resonance so far from nominal speed is to avoid the 5^{th} order main resonance to approach the rated speed.

Initial shafting design, chosen to meet the above criteria is as follows:

- propeller shaft diameter

  $d_p = 705$ [mm]

- intermediate shaft diameter

  $d_i = 670$ [mm]

- flywheel inertia

  $I = 5373$ [kgm^2]

Schematics and discrete models of the complete propulsion system are given in Figures III-32 to III-33. The mass-elastic system, and the table of natural frequencies are given in Tables III-6 and III-7, respectively.

Natural frequencies: First six natural frequencies are presented in Table III-7. Modal vector for one node vibration and frequency of 756 [1/min] shows node position in intermediate shaft (Table III-7). In the same table, from the two node vibration, second natural frequency of 1,999 [1/min] is originated in propeller shaft.

Response analysis is presented in Figures III-35 to III-46. These figures demonstrate the stress limits with full curves and the calculated stresses by dashed lines. An inspection of these figures shows that the obtained solution satisfies required ABS criteria without restrictions. The 5th order main resonance occurs at 151 [rpm], which is 36% of main engine nominal speed. This satisfies adopted criteria of the main resonance between 35-45% of nominal rpm. Enclosed stress calculation (Figures III-35 to III-46) shows that quite high stresses, still within the ABS limits, are developing in the crankshaft[7] segments (Figures III-35 to III-40)) as the installation is approaching the nominal speed. Stresses in all other segments of the propulsion system are below limits for continuous operation.

The benefits of this solution are:

- no restricted speed range
- there is no need for installation of additional equipment, and
- the solution is much cheaper than with installed damper.

Weak points of the solution are:

[7] Stress limits for crankshafts are usually defined by engine maker and Classification Societies normally accept it. Maker's limits are usually higher then ones required by Class. (However, if maker's limits are not available Class criteria need to be used, as is the case here).

- big diameter shafting

- more expensive bearings for big diameter shafting.

Conclusion: From the point of view of torsional vibration, solution with big diameter shafting is technically and commercially the best option. There is no restriction in operation anywhere in the whole speed range, and there is no need for torsional vibration dampers. However, analysis of the coupled axial and torsional vibration will show that high axial excitation that cannot be neglected, calls for the undercritical solutions.

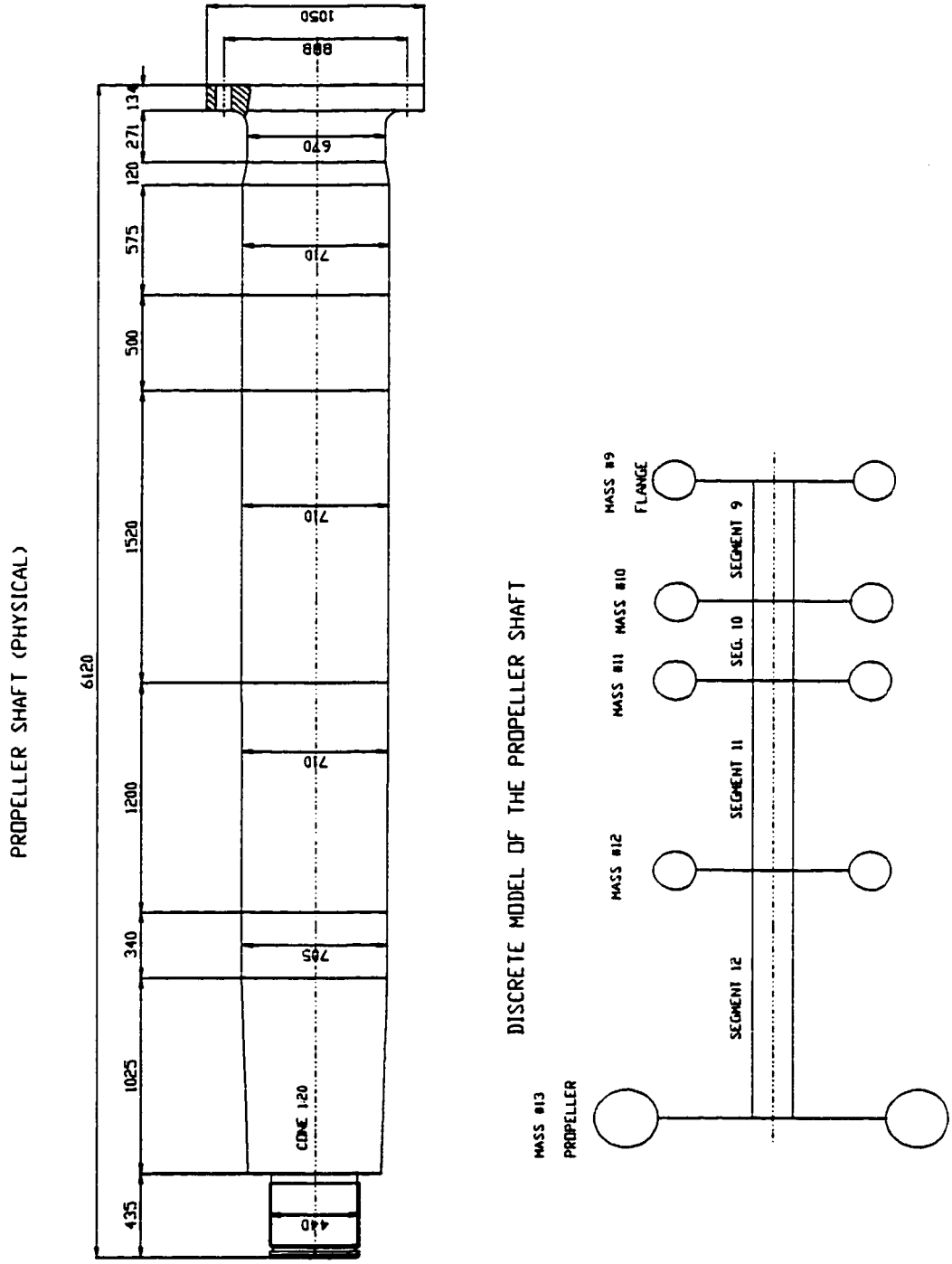

Figure III-32 Propeller shaft design - Undercritical solution

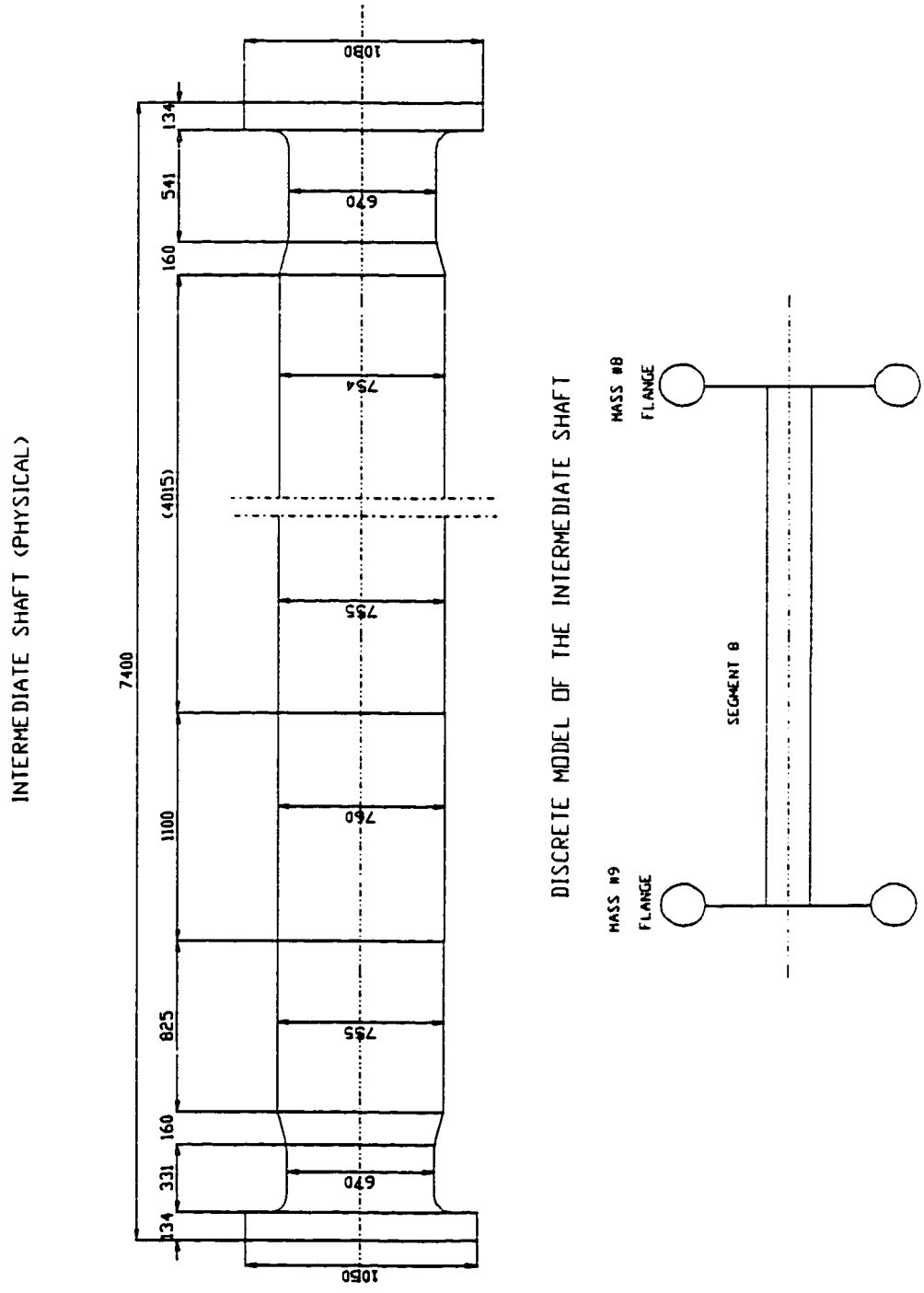

Figure III-33 Intermediate shaft design - Undercritical solution

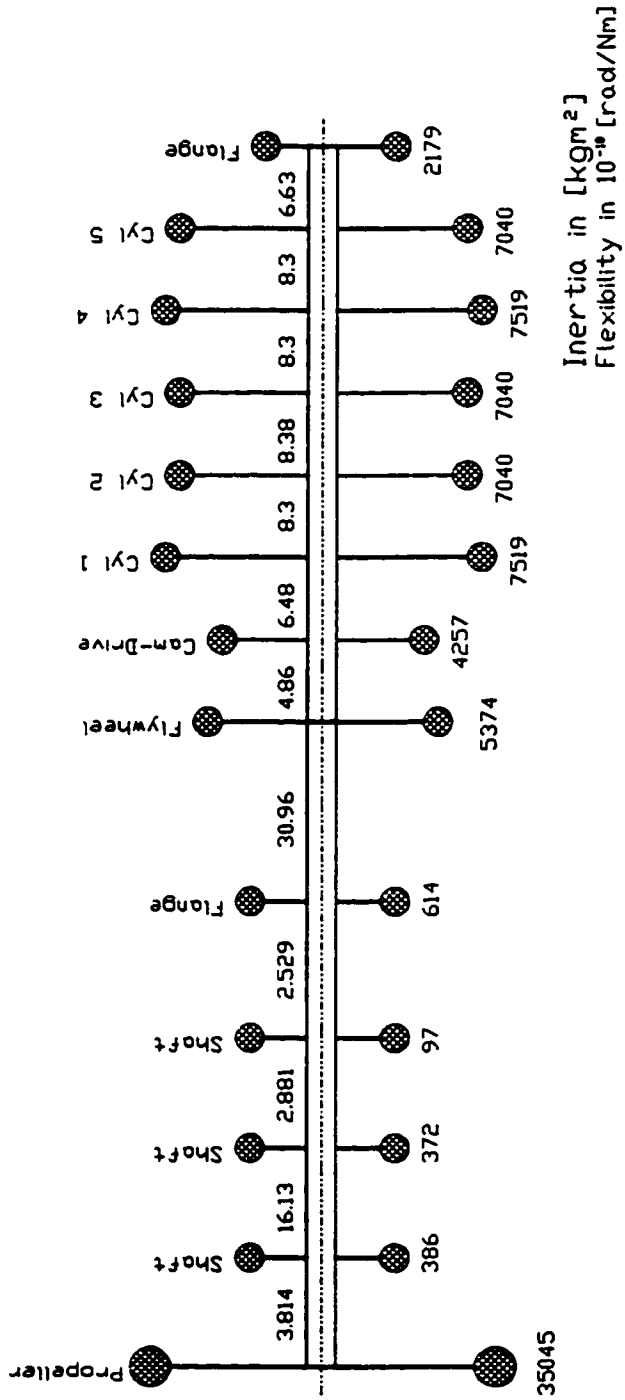

Figure III-34 Inertia-elastic system - Undercritical solution

TORSIONAL VIBRATION CALCULATION

INPUT DATA FOR: Engine 5L60MC MAN_B&W Undercritical Solution

Rated Power 7830.0 [kW]
Rated Speed 111.0 [1/min]

MASS-ELASTIC SYSTEM

Mass No.	Inertia kgm2	A.Flex rad/Nm	A.Dmp. %	Sh.Flex. rad/Nm	R.Dmp. %	Shaft-Dia[m] out	in	Name
1	2179	0.000E+00	0.50	6.630E-10	0.00	0.672	0.115	Fl+Cmp
2	7040	0.000E+00	0.85	8.300E-10	0.00	0.672	0.322	cyl_1
3	7519	0.000E+00	0.85	8.300E-10	0.00	0.672	0.115	cyl_2
4	7040	0.000E+00	0.85	8.380E-10	0.00	0.672	0.322	cyl_3
5	7040	0.000E+00	0.85	8.300E-10	0.00	0.672	0.322	cyl_4
6	7519	0.000E+00	0.85	6.480E-10	0.00	0.672	0.115	cyl_5
7	4257	0.000E+00	0.50	4.860E-10	0.00	0.672	0.115	Comp
8	5373	0.000E+00	0.50	3.096E-09	0.00	0.670	0.000	Flywh
9	614	0.000E+00	0.00	2.529E-10	0.00	0.670	0.000	flange
10	97	0.000E+00	0.00	2.881E-10	0.00	0.710	0.000	Pr_sh
11	372	0.000E+00	0.00	1.613E-09	0.00	0.710	0.000	Pr_sh
12	386	0.000E+00	0.00	3.814E-10	0.00	0.705	0.000	Pr_sh
13	35045	0.000E+00	5.50					Prop.

ENGINE EXCITATION DATA

Harmonic Components File: HCL60MC3
Firing Order : 1-4-3-2-5
Cylinder Diameter : 0.600 [m]
Piston Stroke : 1.944 [m]
Connecting Rod Length : 2.340 [m]
Reciprocating Mass/Cyl. : 5389 [kg]
Mechanical Efficiency : 100 [%]
Load Deviation : 0 [%]

Engine Speed Range from 30 [rpm] to 111 [rpm]
Harmonics Range from 1.0 to 16.0 with increment 1.0

Table III-6 Mass-elastic system for undercritical solution

TORSIONAL VIBRATION CALCULATION
NATURAL DAMPED FREQUENCIES

(1)	NATURAL FREQUENCY	[1] =	79	[rad/s]
(2)	NATURAL FREQUENCY	[2] =	209	[rad/s]
(3)	NATURAL FREQUENCY	[3] =	387	[rad/s]
(4)	NATURAL FREQUENCY	[4] =	540	[rad/s]
(5)	NATURAL FREQUENCY	[5] =	667	[rad/s]
(6)	NATURAL FREQUENCY	[6] =	773	[rad/s]

MODAL VECTORS

	1 Node 756 [1/min]	2 Node 1999 [1/min]	3 Node 3694 [1/min]
[1]	1.0000000E+00	1.0000000E+00	1.0000000E+00
[2]	9.9085849E-01	9.3607251E-01	7.8165071E-01
[3]	9.4252423E-01	6.1232521E-01	-1.8685673E-01
[4]	8.5671080E-01	1.1825880E-01	-9.7835762E-01
[5]	7.3786448E-01	-4.1175652E-01	-8.9940336E-01
[6]	5.9267686E-01	-8.2964151E-01	-2.0882185E-02
[7]	4.6092007E-01	-9.7587914E-01	6.8156107E-01
[8]	3.5606636E-01	-9.9622696E-01	9.9547737E-01
[9]	-3.4941470E-01	-3.9247886E-01	4.9298010E-01
[10]	-4.0669198E-01	-3.4050105E-01	4.4048899E-01
[11]	-4.7188040E-01	-2.8086221E-01	3.7883909E-01
[12]	-8.3500443E-01	6.0343685E-02	-2.2325755E-04
[13]	-9.2011584E-01	1.4065201E-01	-8.9868920E-02

	4 Node 5155 [1/min]	5 Node 6365 [1/min]	6 Node 7381 [1/min]
[1]	1.0000000E+00	1.0000000E+00	1.0000000E+00
[2]	5.7473849E-01	3.5172589E-01	1.2829768E-01
[3]	-9.5330299E-01	-1.3890353E+00	-1.4194752E+00
[4]	-7.1911095E-01	7.8578986E-01	2.4153167E+00
[5]	7.7654087E-01	8.9421739E-01	-2.3590324E+00
[6]	9.1586385E-01	-1.3652805E+00	1.2533649E+00
[7]	-2.9977475E-01	-1.2969976E-01	4.0852918E-01
[8]	-1.0298401E-01	9.1981780E-01	-7.4332446E-01
[9]	-6.4323286E-01	7.6505586E-01	-7.2385532E-01
[10]	-5.8255672E-01	6.9965141E-01	-6.5513574E-01
[11]	-5.0867628E-01	6.1643876E-01	-5.6589357E-01
[12]	-6.2814416E-03	-1.3477147E-02	1.3624391E-01
[13]	1.1280737E-01	-1.6157519E-01	2.9032866E-01

Table III-7 Eigenvalues for undercritical solution

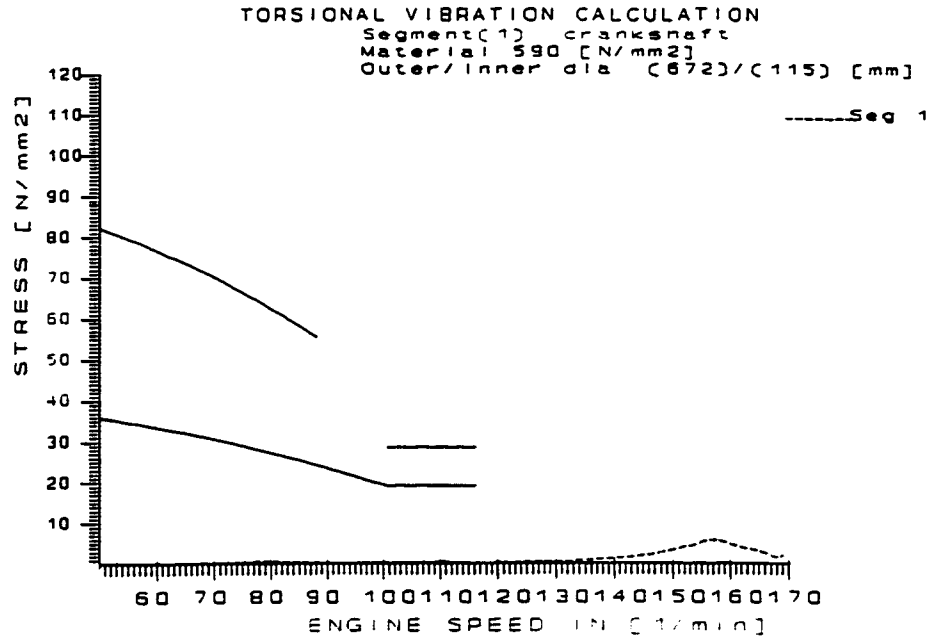

Figure III-35 T/V stress [N/mm2] in crankshaft - segment #1 - Undercritical solution

Upper full curve is ABS torsional stress limit for transient operation
Lower full curve is ABS torsional stress limit for continuous operation

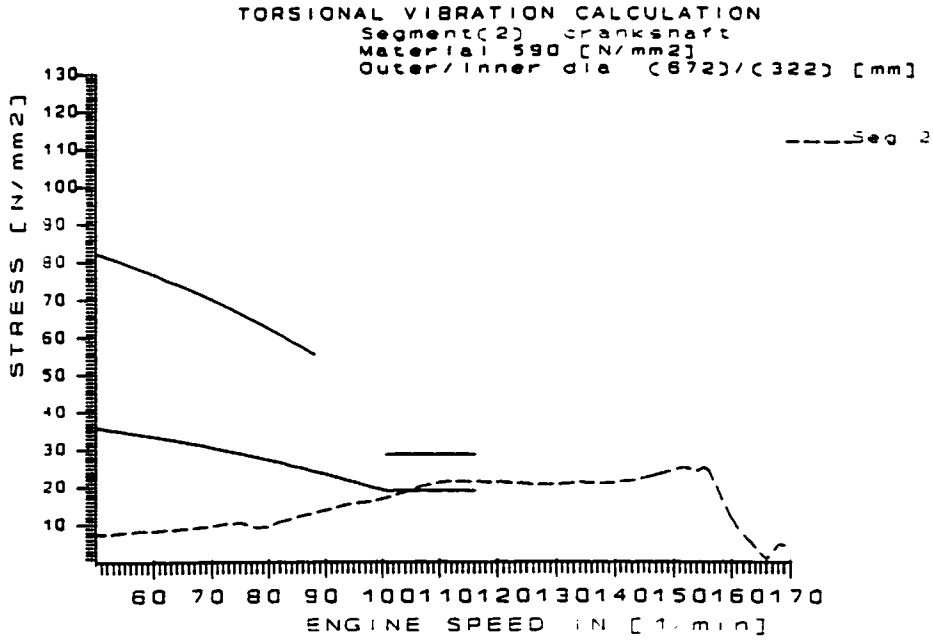

Figure III-36 T/V stress [N/mm2] in crankshaft - segment #2 - Undercritical solution

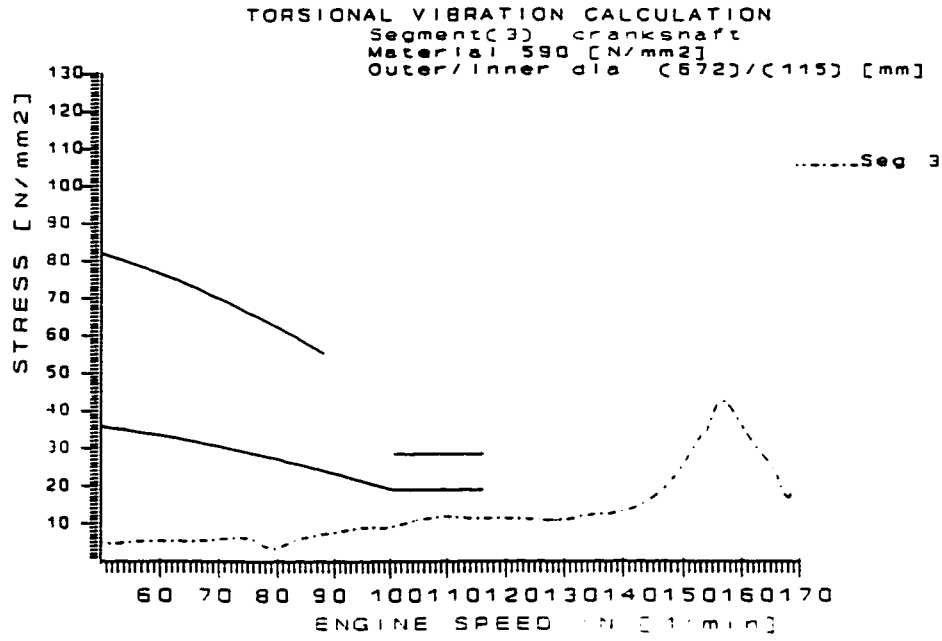

Figure III-37 T/V stress [N/mm2] in crankshaft - segment #3 - Undercritical solution

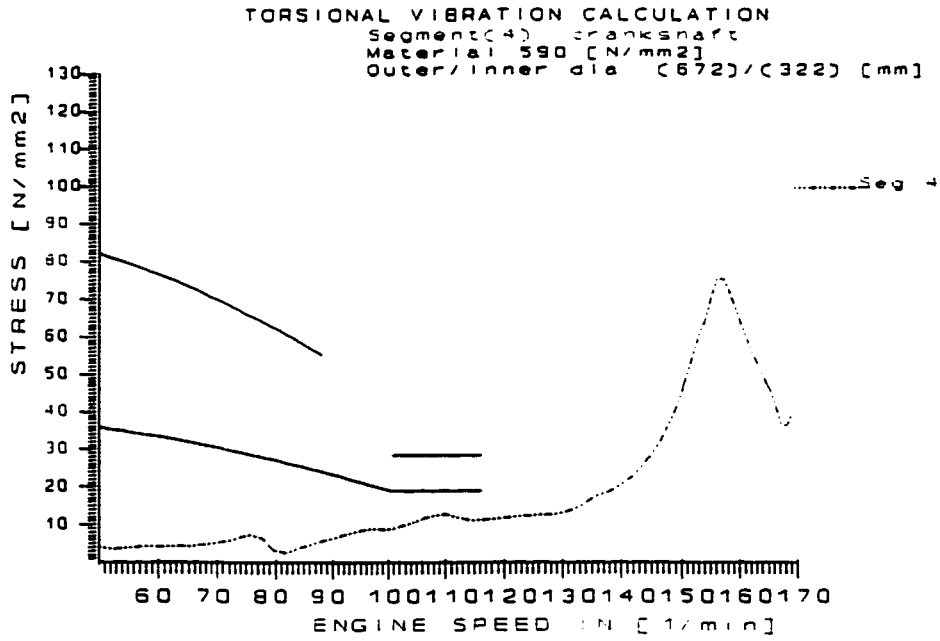

Figure III-38 T/V stress [N/mm2] in crankshaft - segment #4 - Undercritical solution

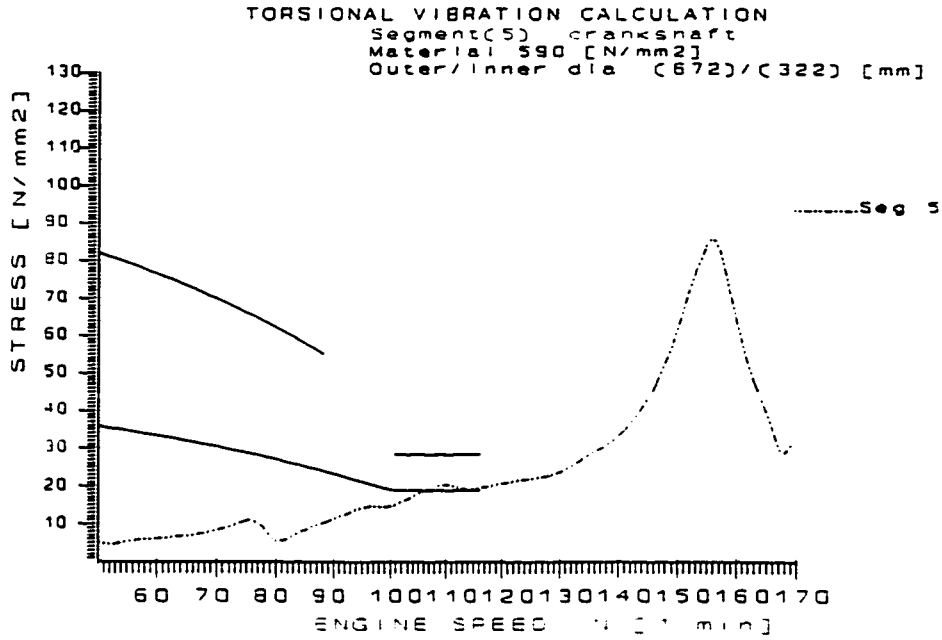

Figure III-39 T/V stress [N/mm2] in crankshaft - segment #5 - Undercritical solution

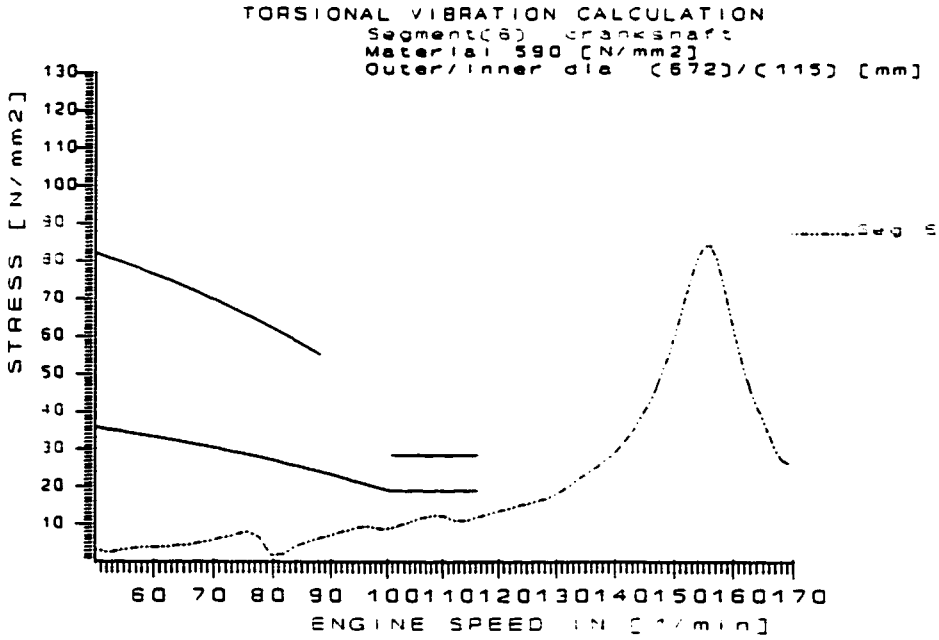

Figure III-40 T/V stress [N/mm2] in crankshaft - segment #6 - Undercritical solution

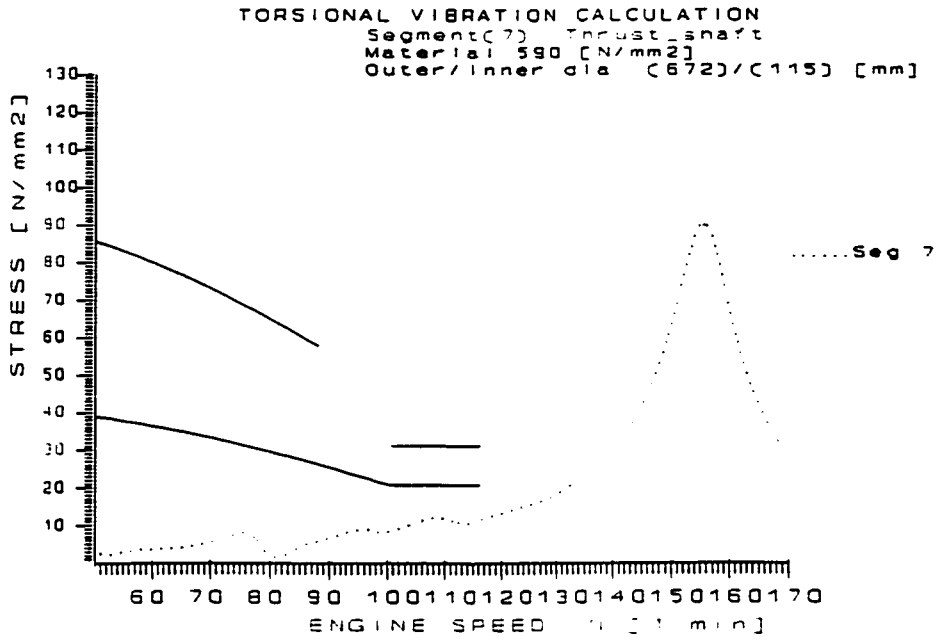

Figure III-41 T/V stress [N/mm2] in thrust shaft - segment #7 - Undercritical solution

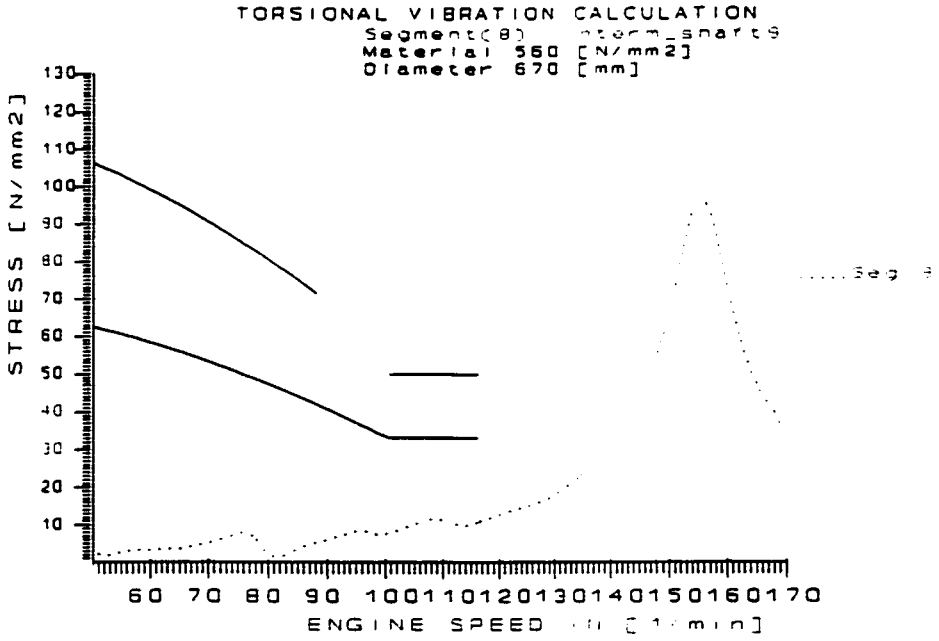

Figure III-42 T/V stress [N/mm2] in intermediate shaft - segment #8 - Undercritical solution

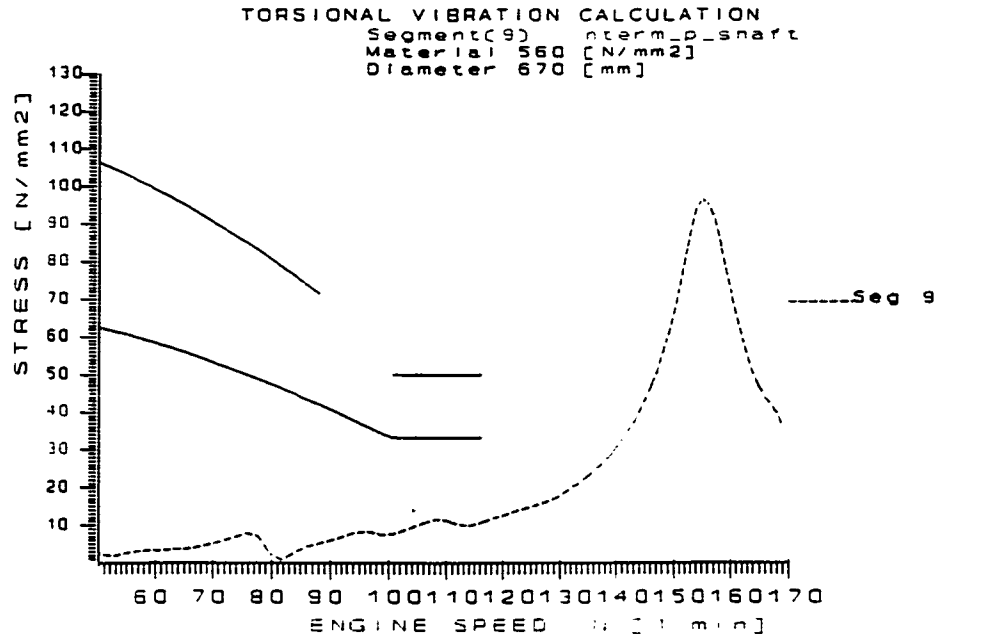

Figure III-43 T/V stress [N/mm2] in propeller shaft (intermediate) - segment #9 - Undercritical solution

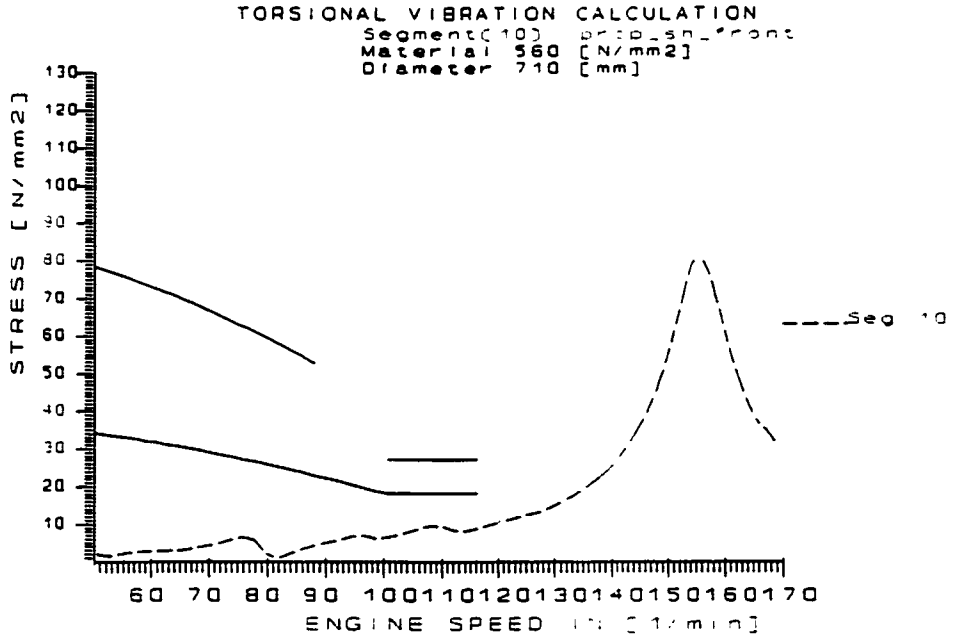

Figure III-44 T/V stress [N/mm2] in propeller shaft (front) - segment #7 - Undercritical solution

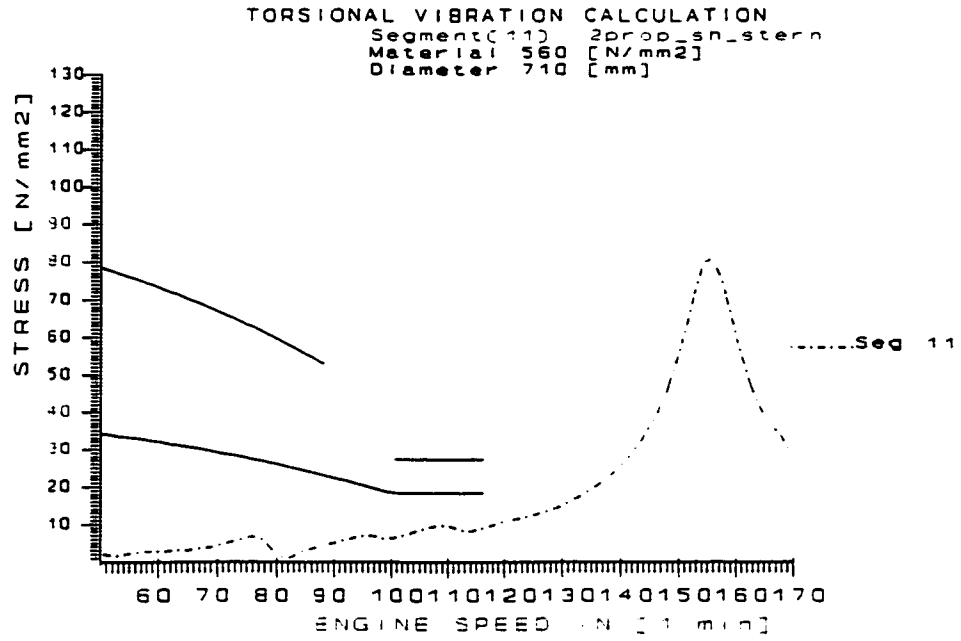

Figure III-45 T/V stress [N/mm2] in propeller shaft (stern) - segment #11 - Undercritical solution

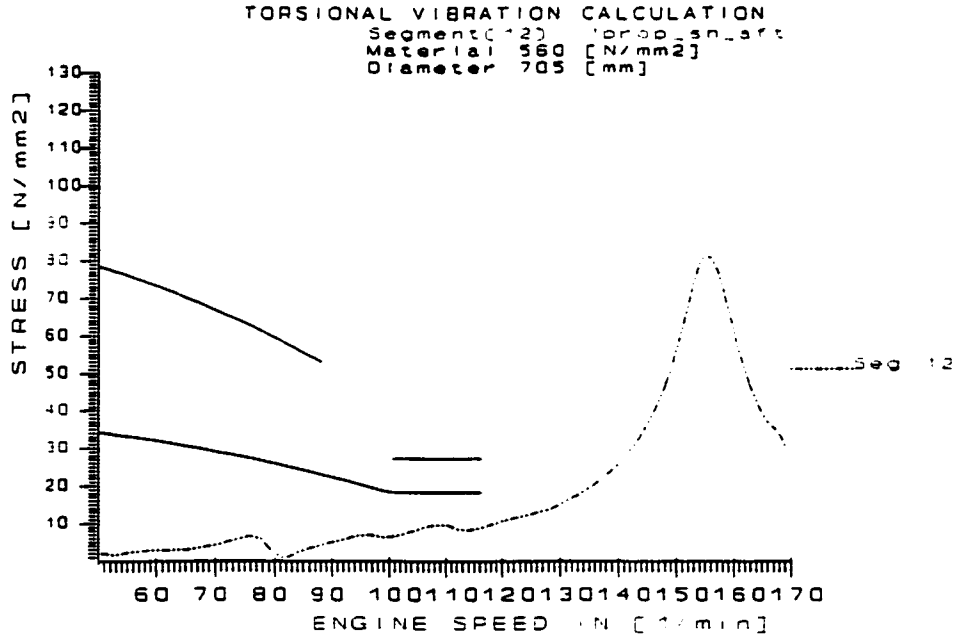

Figure III-46 T/V stress [N/mm2] in propeller shaft (aft) - segment #12 - Undercritical solution

III.3. AXIAL VIBRATION ANALYSIS

III.3.1. General

Sources of axial vibrations of the ship propulsion installation are propeller and main engine. However, in axial vibration analysis for ocean going merchant ships, when design of line shafting is considered, excitation of the main engine has no significant contribution. The reason for that is thrust bearing, which due to its high rigidity, physically divides axial system into the following two separate systems (see Figure III-47):

- line shafting, and
- crankshaft of the main engine.

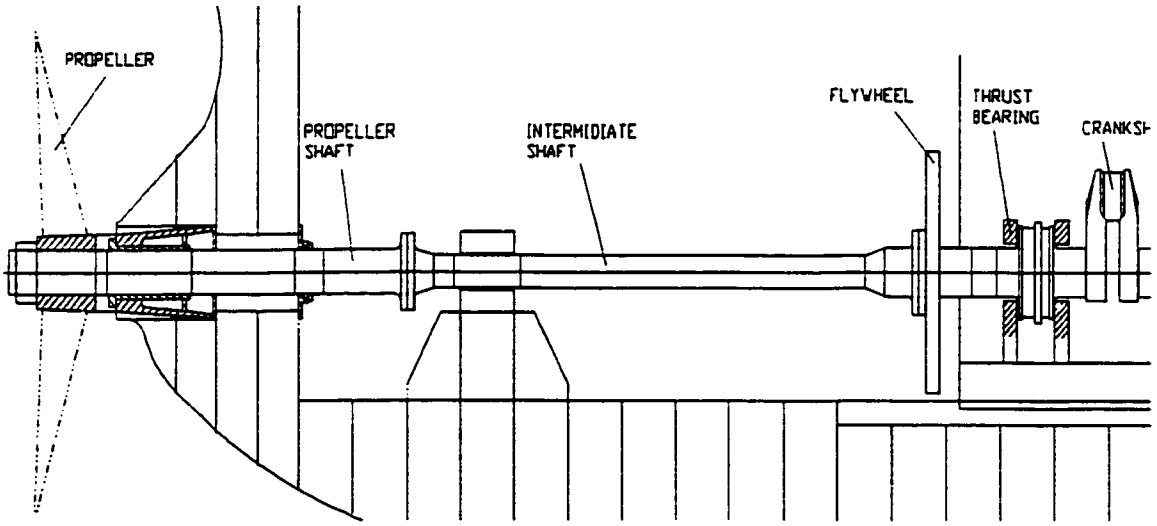

Figure III-47 Shafting arrangement

On the other hand, propeller caused axial excitation is also of low intensity and although propeller excitation could have some influence on the strength calculation of the "conventional" line shafting, this is usually negligibly small in comparison to the torsional vibrations. In cases where axial and torsional vibrations are strongly coupled and the resonances of their main orders are close, axial vibration can influence torsional resonant amplitude and significantly increase its response. Therefore, in order to check whether such a coincidence of torsional and axial vibration exists, the minimum requirement for analysis of the axial vibration is calculation of natural frequencies of the line shafting system. If such a coincidence does not exist for dominant orders[8], natural frequencies analysis would be a sufficient proof that installation is safe from axial vibrations.

Propeller main orders are integer multiples of its number of blades. Normally only the first order is taken into consideration, since higher orders are notably less influential.

In case the resonant frequencies of axial and torsional vibrations coincide, or are very close to each other, it is necessary to analyze forced axial vibrations for the line shafting. Axial vibration response is added to the torsional, and shafting strength must be checked for this composite value.

In this study forced axial vibrations are calculated for main order propeller excitation, although torsional and axial vibration do not coincide (as illustrated later on in this chapter). The response to this excitation is shown to be insignificant. For the

[8] For cases where main orders resonant frequencies are sufficiently far from each other.

second and higher orders of propeller excitation, for which excitation force is lower, and dominant resonance further above nominal engine revolution, response is expected to be even lower, and it is therefore not calculated.

III.3.2. **Axial Excitation**

As explained in Chapter II axial excitation on the propeller is caused by the propeller operation in the nonuniform wake field generated behind the ship. When propeller rotates in the nonuniform wake field its blades generate periodic forces and moments which can be measured and decomposed using Fourier decomposition (see Chapter II section 1.4).

In conventional design of the line shafting only thrust variation on the propeller will be of interest. However, wake data are not always available; this is especially true in early design stages when ship design cannot be classified as conventional. In that case rough approximation of the fluctuating forces can be adopted from the statistical data available for the similar category of ships. Such an analysis has been carried out by Van Manen and Van Oossanen in Lewis (1988), p.127, and its results are adopted here:

- 10% of the mean thrust; for the first excitation order that corresponds to propeller blade number.
- second order and higher order excitations have no significant impact on the response of the four blade propeller

Mean thrust can be obtained by:

$$T = \frac{P_E}{(1-t)\,V} \qquad \text{(IV-4a)}$$

$$T = \rho\, f^2\, D^4\, K_T \qquad \text{(VI-4b)}$$

For given nominal operating condition of the ship (i.e. ship nominal speed and power consumed on the propeller), and with known thrust deduction fraction t, the nominal thrust T can be defined. With known thrust, the coefficient K_T may be obtained from Equation (III-4b), where:

T - is mean thrust [N],

ρ - density of surrounding water = 1025 [kg/m^3],

f - propeller frequency of revolution = 0.5 to 1.85 [1/s]

D - propeller diameter = 6.15 [m]

K_T - thrust coefficient

P_E - effective power consumed by propeller

t - thrust deduction fraction

V - ship service speed

III.3.3. **Example**

In the chosen example it is assumed that there are no losses in power transmission from the main engine to the propeller[9]. Therefore, propeller will consume 6765 kW at 111 rpm (power and propeller revolution are related via propeller curve).

Thrust deduction fraction t is calculated from Taylor's formula, as given in Van Manen (1957), and Lewis (1988) p.127. For single screw propeller, wake coefficient w , and t are:

$$w = -0.05 + 0.5\,C_b = 0.325$$
$$t = k\,w = 0.21 \qquad \text{(III-5)}$$

C_b = 0.75 ,ship block coefficient

k = 0.5 to 0.7 - rudder design factor. For streamlined slender rudder k = *0.5*, for streamlined thick rudders k = *0.7*. In this case k is chosen to be 0.65.

Ship speed at nominal engine output of 7830 [kW] at revolution of 111 [rpm] is 7.2 [m/s] (14 knots). If basin data are not available, ship speed can be roughly related to the propeller revolution as shown in Figure II-3.

After substitution of known data into (III-4a) and (III-4b) the thrust developed by propeller at nominal operating conditions, and thrust coefficient are:

T = 1376.3 [kN]

---

[9] Assuming mechanical losses to be zero will give higher value of the thrust and therefore increase safety margin.

$K_T = 0.27$

The same results can be achieved using open-water test results for the chosen propeller. In that case the thrust coefficient is selected for given speed of advance and advance coefficient.

$V_A=(1-w)V = 4.86$ [m/sec]

$J= V_A/(nD) = 0.633$

where V is ship speed of advance, w is wake coefficient, n is propeller speed of rotation, and D is propeller diameter.

From the open-water test diagram for B4-40 screw series (see reference Van Lammerman, Van Manen, and Oossterveld (1969), Fig. 5)

$K_T = 0.27$

which confirms the previous result.

In order to calculate axial dynamic response of propulsion system through whole operating speed range of the installation, it is necessary to express the vibratory propeller thrust as a function of the propeller frequency of revolution. Therefore, the propeller thrust will vary with square change of propeller revolution (Equation (III-4b)). For presented example this relation will be $T(f) = 402,061\, f^2$ [kN].

III.3.3.1. *Main Propeller Parameters*

Propeller type Wageneingen B4-40-80

Diameter D = 6.15 [m]

Pitch ratio P/D = 0.8

Expanded area ratio Ae/Ao = 0.4

Mass in the air m = 15400 [kg]

Specific gravity of the surrounding water ρ = 1025 [kg/m3]

III.3.3.2. *Thrust Variation*

Thrust variation on the propeller is defined by Equation (II-27) in Chapter II:

$$f_x = z\sum_{k=0}^{K} T_{kz}^{(10\%)} \cos(kz\omega t - \Phi_{kz}) \qquad \text{(III-6)}$$

Axial varying force is sum of forces over K blades ($k=0$ corresponds to stationary propeller thrust, $k=1$ will correspond to the 4th order of the propeller blade frequency, etc.). $T_{kz}^{(10\%)}$ is 10% of the mean thrust; z represents number of the blades, and phase angle Φ is the blade angle of $k*z$ order; ω is propeller excitation angular frequency [rad/sec].

For propeller chosen in this study thrust variation will be:

$T^{10\%}$ = 137.63 [kN]

or expressed as a function of propeller frequency of revolution:

$T(f)^{10\%}$ = 40.206 f^2 [kN]

III.3.3.3. *Propeller Added Water*

Propeller added water is virtual increase of the propeller mass due to its vibration in the surrounding fluid. It is calculated from the Propeller Coefficients as presented in Chapter II.

Propeller coefficient that corresponds to the added water is the one related to acceleration of the vibrating propeller (III-7)[10].

$$\frac{F_x}{\ddot{\delta}_x} = 0.0274$$

$$m_a = \rho D^3 \frac{F_x}{\ddot{\delta}_x} = 6533 \ [kg] \qquad \text{(III-7)}$$

Added mass m_a is transformed into dimensional value by simple multiplication with specific gravity of the fluid and propeller diameter to the power of 3, which gives virtual rise of the propeller mass to:

- $m_p = 21933$ [kg]

This mass will additionally be increased by half of the mass of the propeller shaft, as the propulsion system is discretised for Transfer Matrix Method analysis.

[10] In case that propeller coefficients are not available, a good approximation of the mass of the added water would be to add approximately 50% to the propeller mass in the air.

III.3.3.4. *Axial Stiffness and Mass of the Shafting*

Axial stiffness and mass of the shafting can be easily calculated (III-8) knowing shafting geometry and specific gravity.

$$k = \frac{EA}{L} \quad [N/m]$$

$$m = A\,L\,\rho_s \quad [kg] \qquad \text{(III-8)}$$

However, computation of these values is performed automatically by a computer program for given geometry of the shafting.

III.3.4. **Axial Vibration Eigen-Values and Response**

As mentioned above, the natural frequency calculation for the given system is performed first in order to check whether there is coincidence of torsional and axial vibration resonances. Next, the axial forced vibration computation is performed considering only propeller generated axial excitation. Forced vibration confirms that axial dynamical stresses are not influencing strength of the line shafting. Analysis is performed for two cases of shafting geometry, undercritical with big shaft diameter, and overcritical with relatively small diameters, as defined by Torsional Vibration Analysis.

III.3.4.1. *Undercritical Solution*

In undercritical solution with big shafting diameter the 4th order[11] of axial vibration dominant modes is found to be far above torsional resonance of the dominant 5th and 10th orders, and far above engine nominal speed. The Campbell diagram in Figure III-48 shows that 199 [1/min] resonance, which corresponds to the 4th order (0 node) first natural frequency of the axial vibration, is far above the nominal engine speed range, and main torsional resonances of the 5th and 10th order. The 8th order propeller axial resonance is not significant because of negligible excitation. Therefore, no interaction between torsional and axial resonances is expected. (Inclined lines in Campbell diagram represent engine speed lines of order of 1, 2, 3, and 4 times the engine revolution.)

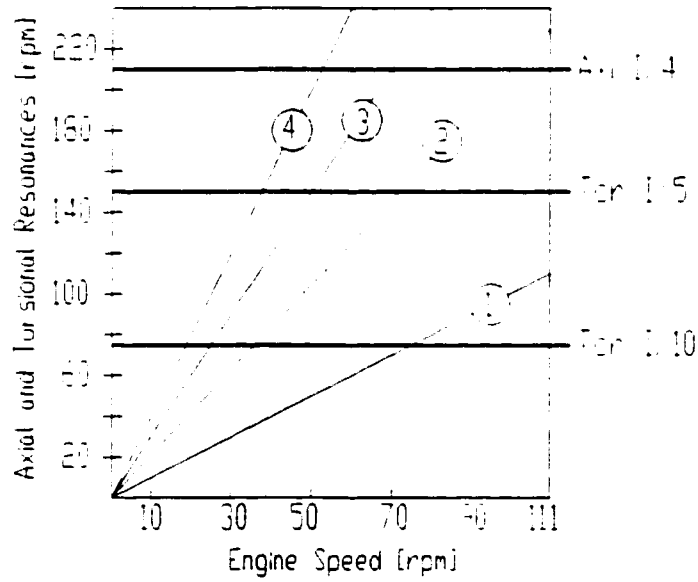

Figure III-48 Campbell diagram for undercritical solution

[11] For 4 blade propeller the order of excitation will be integer multiple of the propeller blade number; i.e. 4, 8, etc.

Response of the system to the axial excitation caused by propeller is presented by diagrams in Figures III-49 to III-52. Figure III-49 shows stresses in all segments of the system. The stress distribution in intermediate shaft is shown in Figure III-50. This diagram is extracted from the aggregate display because maximal stress in the line shafting occurs in segment 9.

The stresses in Figures III-49 and III-50 are shown on the vertical axis in [N/mm^2] as a function of the propeller's revolution. The stress lines in Figure III-49 concentrated on the upper part of the diagram represent response in the line shafting, and lines on the bottom part are stresses in the various segments of the crankshaft.

It is obvious that axial vibratory stresses, in all segments of the propulsion system are negligible (maximum stress calculated shown in Figure III-49, is below 1 [N/mm^2]) in comparison to those developed due to torsional vibration. Therefore, it can be concluded there is no contribution from the axial vibration in total vibrational response.

Figure III-51 shows axial dynamic forces in all segments of the propulsion system, and axial vibratory force in intermediate shaft, respectively. The force in intermediate shaft is presented in Figure III-52. This diagram is extracted from the aggregate display in order to show parameters which are specific to the intermediate shaft where maximal force occurs (i.e. ultimate tensile strength and diameters). The upper cluster of lines in III-51 represents forces in line shafting, and the lower group of lines are forces acting in the crankshaft. The analysis of the response shows that the amplitudes of axial forces in the shafting are not significantly changed in comparison to

the imposed excitation. The reason for this is rigid shafting, and lack of the axial resonance within operating range of speeds.

Axial vibration data (Table III-8), table of natural frequencies (Table III-9), stress and force diagrams (Figures III-49 to III-52) are attached below.

AXIAL VIBRATION CALCULATION

INPUT DATA FOR: Engine 5L60MC MAN_B&W Under-critical

Rated Power 7830.0 [kW]
Rated Speed 111.0 [1/min]

MASS-ELASTIC SYSTEM

Mass No.	Mass kg	A.Flex m/N	A.Dmp. %	Sh.Flex. m/N	R.Dmp. %	Shaft Dia [m] out	in	Name
1	3097	0.000E+00	0.00	6.000E-12	0.00	0.672	0.115	Flng
2	4582	0.000E+00	0.00	1.846E-09	0.00	0.672	0.322	cyl_1
3	9165	0.000E+00	0.00	1.293E-09	0.00	0.672	0.115	cyl_2
4	9165	0.000E+00	0.00	7.930E-10	0.00	0.672	0.322	cyl_3
5	9165	0.000E+00	0.00	1.231E-09	0.00	0.672	0.322	cyl_4
6	9165	0.000E+00	0.00	1.067E-09	0.00	0.672	0.115	cyl_5
7	4582	0.000E+00	0.00	5.000E-12	0.00	0.672	0.115	Cam
8	8322	4.760E-10	0.00	1.300E-11	0.00	0.672	0.115	Thrust
9	13914	0.000E+00	0.00	2.115E-10	0.00	0.670	0.000	Flywh
10	10941	0.000E+00	0.00	1.556E-11	0.00	0.670	0.000	flng
11	1620	0.000E+00	0.00	1.815E-11	0.00	0.710	0.000	Pr-Int
12	5897	0.000E+00	0.00	1.016E-10	0.00	0.710	0.000	Pr_Frt
13	6138	0.000E+00	0.00	2.370E-11	0.00	0.705	0.000	Pr-St
14	23067	0.000E+00	5.00					Propeller

ENGINE EXCITATION
Cylinder Diameter : 0.600 [m]
Piston Stroke : 1.944 [m]
Connecting Rod Length : 2.340 [m]
Reciprocating Mass/Cyl. : 5389 [kg]
Engine Speed Range from 30 [rpm] to 111 [rpm]

PROPELLER EXCITATION DATA

Propeller Type/Series: Wageningen_B4-40-80
Number of blades: 4
Diameter : 6.150 [m]
P/D ratio : 0.800
A/Ao ratio : 0.400
Mass : 21933 [kg]
Rot.Inertia : 28515 [kgm2]
Kt (Thrust coef.): 0.27
Media density : 1025.0 [kg/m3]
Excitation order: 4

Table III-8 Axial mass-elastic system for undercritical solution

AXIAL VIBRATION CALCULATION OF
NATURAL DAMPED FREQUENCIES AND MODAL VECTORS

	0 Node 797 [1/min]	1 Node 1489 [1/min]	2 Node 2370 [1/min]
[1]	1.0000000E+00	1.0000000E+00	1.0000000E+00
[2]	9.9987059E-01	9.9954821E-01	9.9885574E-01
[3]	9.0115433E-01	6.5499247E-01	1.2654511E-01
[4]	7.5763704E-01	2.2493865E-01	-5.7679417E-01
[5]	6.3126866E-01	-7.8561905E-02	-7.5001227E-01
[6]	3.8550184E-01	-5.2814603E-01	-4.9784134E-01
[7]	1.4622249E-01	-7.9226278E-01	2.0525586E-02
[8]	1.4507788E-01	-7.9305914E-01	2.2925715E-02
[9]	1.4595482E-01	-8.1470284E-01	2.9639443E-02
[10]	1.5722895E-01	-1.1084967E+00	1.3348104E-01
[11]	1.5787198E-01	-1.1255231E+00	1.3972137E-01
[12]	1.5859000E-01	-1.1445865E+00	1.4675019E-01
[13]	1.6194798E-01	-1.2346375E+00	1.8068630E-01
[14]	1.6256681E-01	-1.2512659E+00	1.8697983E-01

	3 Node 3684 [1/min]	4 Node 4447 [1/min]	5 Node 5180 [1/min]
[1]	1.0000000E+00	1.0000000E+00	1.0000000E+00
[2]	9.9723454E-01	9.9597001E-01	9.9453168E-01
[3]	-1.1089421E+00	-2.0709468E+00	-3.1634086E+00
[4]	-6.2841864E-01	1.1033270E+00	4.9560609E+00
[5]	3.4600807E-01	1.3110305E+00	-6.6419252E-01
[6]	1.2776745E+00	-1.5743981E+00	-7.1835082E+00
[7]	2.2573421E-01	-7.3636737E-01	7.8382949E+00
[8]	2.2003512E-01	-7.2878160E-01	7.8558421E+00
[9]	2.0768412E-01	-7.1186293E-01	7.8659086E+00
[10]	-8.4175861E-02	1.7623555E-02	1.2185566E+00
[11]	-1.0351502E-01	7.0639577E-02	6.6849054E-01
[12]	-1.2562886E-01	1.3205353E-01	2.0831484E-02
[13]	-2.3823231E-01	4.5872996E-01	-3.6089414E+00
[14]	-2.5932777E-01	5.2042083E-01	-4.3007120E+00

Table III-9 Axial eigenvalues for undercritical solution

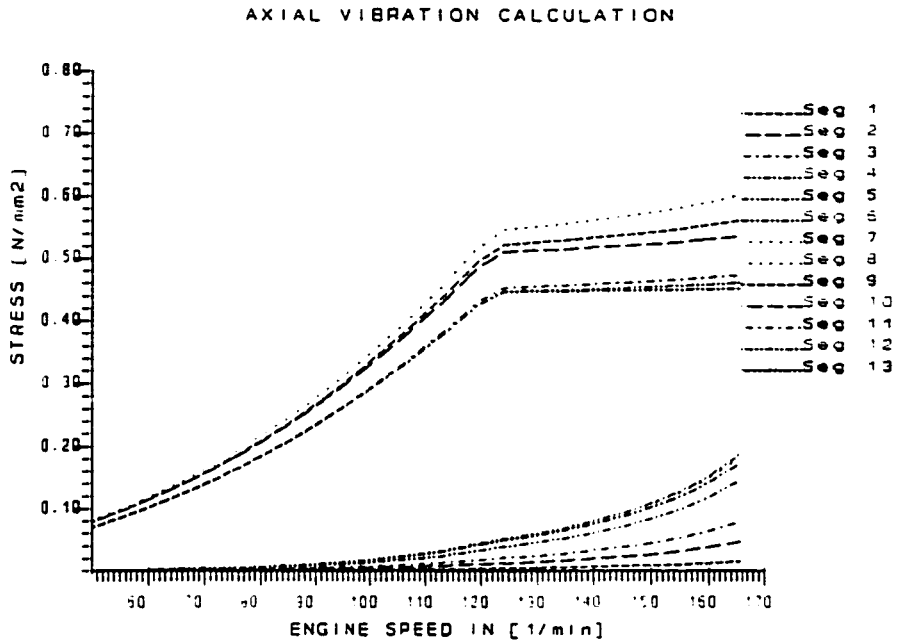

Figure III-49 Axial stresses [N/mm²] in the system - Undercritical solution

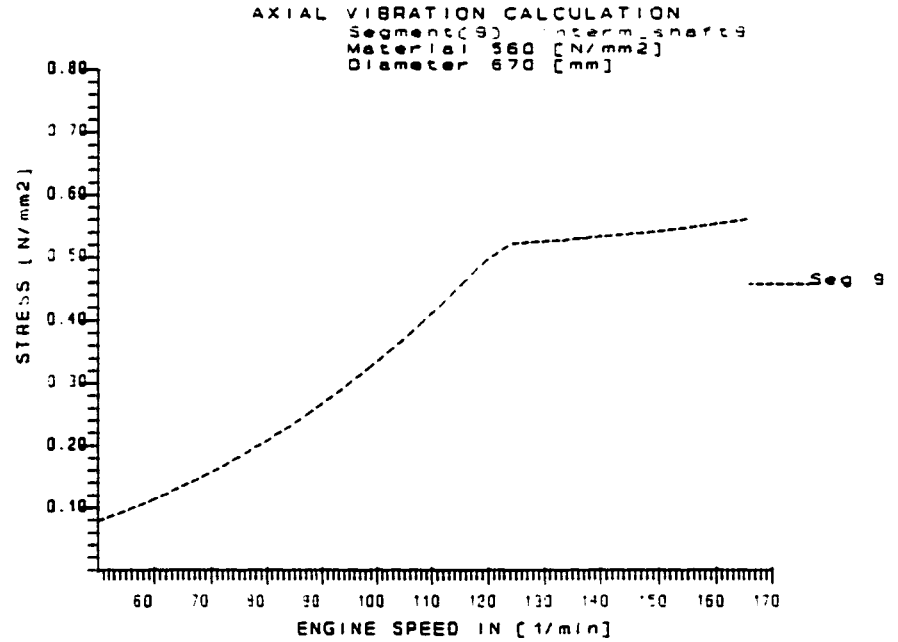

Figure III-50 Axial stress [N/mm2] in intermediate shaft - Undercritical solution

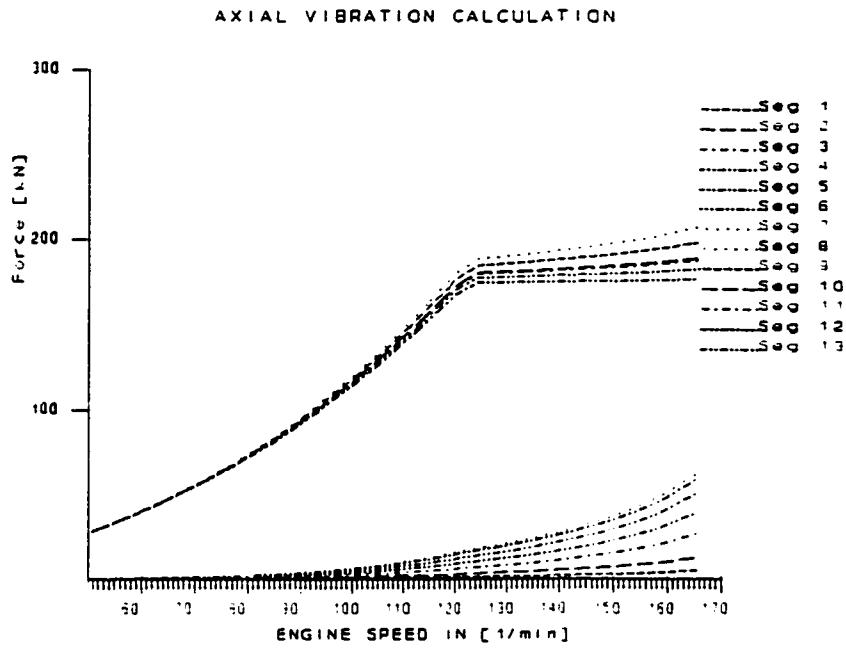

Figure III-51 Axial forces [kN] in the system - Undercritical case

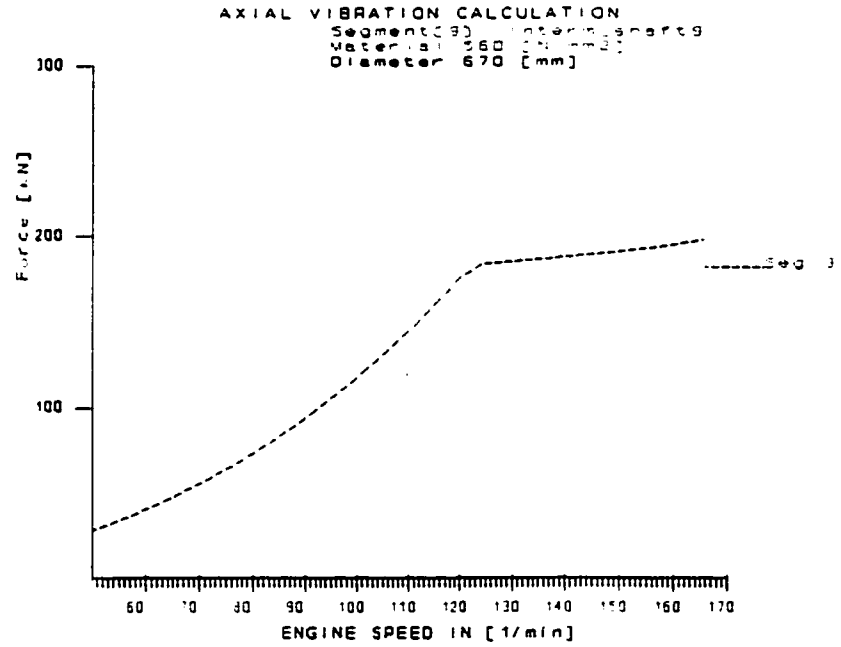

Figure III-52 Axial force [kN] in intermediate shaft - Undercritical solution

III.3.4.2. *Overcritical Solution*

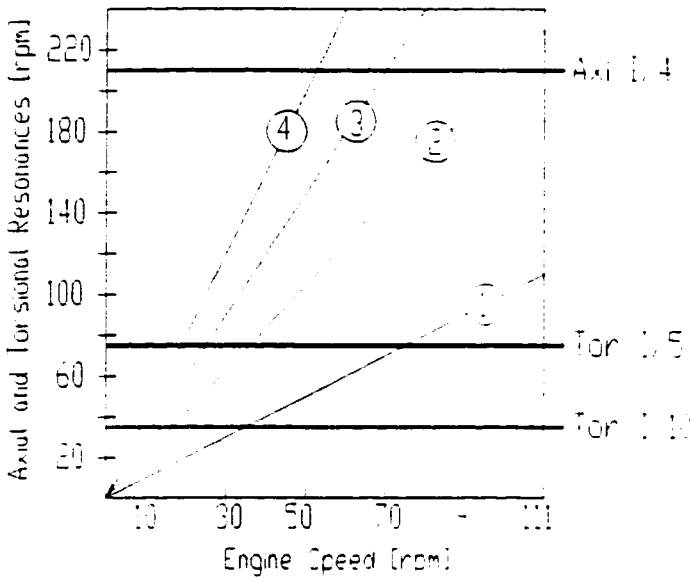

Figure III-53 Campbell diagram for overcritical case

In the overcritical torsional vibration solution the resonance of the 4th order propeller's axial vibration will maintain approximately the same value (i.e. 200 [1/min]) as in the undercritical solution, while the torsional resonances of the 5th and 10th order are much lower. Therefore, in this case considering Campbell diagram in Figure III-53, the same can be concluded as for undercritical solution; i.e. there is no interference between main torsional and axial resonances, and dominant axial resonance is far above operating speeds of the installation.

The response of the system to axial excitation is shown in Figures III-54 to III-57. Diagrams in Figures III-54 and III-55 show the stress distribution in the whole system, and the intermediate shaft, respectively. The stresses, although double in

intensity than for the undercritical solution, do not exceed 1[N/mm^2] at nominal propeller speed of 111[rpm]. Therefore stresses are negligible in comparison to those produced by torsional vibrations.

In diagrams on Figures III-55 and III-56 the force distribution in all elements of the propulsion system, and intermediate shaft are shown respectively. Due to the high stiffness of the shafting, and no presence of the axial resonances within analyzed speed range, the response (axial dynamic force) is not significantly different in the line shafting from the imposed excitation force.

Figures III-55 and III-57 show stress and force diagrams which are extracted from the aggregate display, in order to present parameters (i.e. ultimate tensile strength and diameters) which are specific to the intermediate shaft where maximal stress occurs .

The segments of the crankshaft (segment 1 to segment 7, in Mass-Elastic Table III-10) forward from the thrust bearing, are barely influenced by axial excitation from the propeller. The reason for this is that thrust bearing has absorbed almost total dynamic force, because it practically separates the axial system into two independent systems.

Data describing the propulsion installation (mass-elastic system) are shown in Table III-10, followed by natural frequencies Table III-11, and forced vibration analysis results Figures III-54 to III-57.

AXIAL VIBRATION CALCULATION

INPUT DATA FOR: Engine 5L60MC MAN_B&W Overcritical Solution

Rated Power 7830.0 [kW]
Rated Speed 111.0 [1/min]

MASS-ELASTIC SYSTEM

Mass No.	Mass kg	A.Flex m/N	A.Dmp. %	Sh.Flex. m/N	R.Dmp. %	Shaft Dia [m] out	in	Name
1	3097	0.000E+00	0.00	6.000E-12	0.00	0.672	0.115	Flng
2	4582	0.000E+00	0.00	1.846E-09	0.00	0.672	0.322	cyl_1
3	9165	0.000E+00	0.00	1.293E-09	0.00	0.672	0.115	cyl_2
4	9165	0.000E+00	0.00	7.930E-10	0.00	0.672	0.322	cyl_3
5	9165	0.000E+00	0.00	1.231E-09	0.00	0.672	0.322	cyl_4
6	9165	0.000E+00	0.00	1.067E-09	0.00	0.672	0.115	cyl_5
7	4582	0.000E+00	0.00	5.000E-12	0.00	0.672	0.115	Cam_drv
8	8322	4.760E-10	0.00	1.300E-11	0.00	0.672	0.115	Thr_cam
9	7810	0.000E+00	0.00	6.087E-10	0.00	0.425	0.000	Flywh.
10	5027	0.000E+00	0.00	6.038E-11	0.00	0.520	0.000	flng
11	1386	0.000E+00	0.00	3.164E-11	0.00	0.526	0.000	Pr_Frt
12	1715	0.000E+00	0.00	8.799E-11	0.00	0.520	0.000	Pr_Stn
13	2759	0.000E+00	0.00	1.065E-10	0.00	0.520	0.000	Pr_Aft
14	23446	0.000E+00	5.00					Propeller

ENGINE EXCITATION DATA

Cylinder Diameter : 0.600 [m]
Piston Stroke : 1.944 [m]
Connecting Rod Length : 2.340 [m]
Reciprocating Mass/Cyl. : 5389 [kg]
Engine Speed Range from 30 [rpm] to 111 [rpm]

PROPELLER EXCITATION DATA

Propeller Type/Series: Wageningen_B4-40-80
Number of blades: 4
Diameter : 6.150 [m]
P/D ratio : 0.800
A/Ao ratio : 0.400
Mass : 21933 [kg]
Rot.Inertia : 28515 [kgm2]
Kt (Thrust coef.): 0.27
Media density : 1025.0 [kg/m3]
Excitation order: 4

Table III-10 Axial mass-elastic system for overcritical solution

AXIAL VIBRATION CALCULATION
NATURAL DAMPED FREQUENCIES

MODAL VECTORS

	0 Node 802 [1/min]	1 Node 1431 [1/min]	2 Node 2306 [1/min]
[1]	1.0000000E+00	1.0000000E+00	1.0000000E+00
[2]	9.9986900E-01	9.9958274E-01	9.9891685E-01
[3]	8.9994207E-01	6.8135383E-01	1.7316251E-01
[4]	7.5476588E-01	2.7714845E-01	-5.2483687E-01
[5]	6.2705684E-01	-1.5981981E-02	-7.3057764E-01
[6]	3.7893552E-01	-4.6696914E-01	-5.6950140E-01
[7]	1.3774601E-01	-7.5533278E-01	-1.0525581E-01
[8]	1.3659354E-01	-7.5629549E-01	-1.0293977E-01
[9]	1.3722343E-01	-7.7761638E-01	-9.9080311E-02
[10]	1.6211970E-01	-1.6929774E+00	1.0910091E-01
[11]	1.6424215E-01	-1.7722297E+00	1.2781926E-01
[12]	1.6530355E-01	-1.8120129E+00	1.3730098E-01
[13]	1.6807968E-01	-1.9165195E+00	1.6246423E-01
[14]	1.7109024E-01	-2.0303122E+00	1.9012542E-01

	3 Node 3514 [1/min]	4 Node 4257 [1/min]	5 Node 4974 [1/min]
[1]	1.0000000E+00	1.0000000E+00	1.0000000E+00
[2]	9.9748412E-01	9.9630714E-01	9.9495799E-01
[3]	-9.1889197E-01	-1.8146129E+00	-2.8398128E+00
[4]	-7.8686394E-01	4.9003893E-01	3.6054795E+00
[5]	6.8396457E-02	1.1956942E+00	4.4821771E-01
[6]	1.2915683E+00	-3.8979500E-01	-5.8250206E+00
[7]	6.4172401E-01	-1.0065213E+00	4.1938083E+00
[8]	6.3668828E-01	-1.0048287E+00	4.2146867E+00
[9]	6.3165794E-01	-1.0062666E+00	4.2603550E+00
[10]	-1.0483013E-02	-1.2286142E-01	9.0298064E-01
[11]	-7.3743194E-02	-2.7829911E-02	4.9561445E-01
[12]	-1.0645376E-01	2.2209207E-02	2.7625718E-01
[13]	-1.9525528E-01	1.6071538E-01	-3.4514872E-01
[14]	-2.9492335E-01	3.1890020E-01	-1.0694241E+00

Table III-11 Axial eigenvalues for overcritical solution

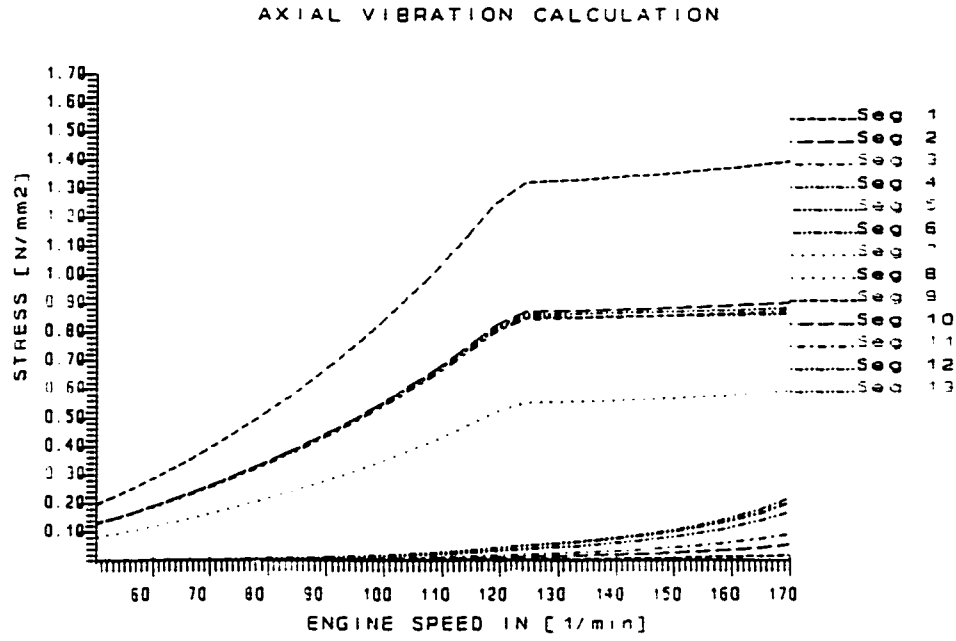

Figure III-54 Axial stresses [N/mm2] in the system - Overcritical solution

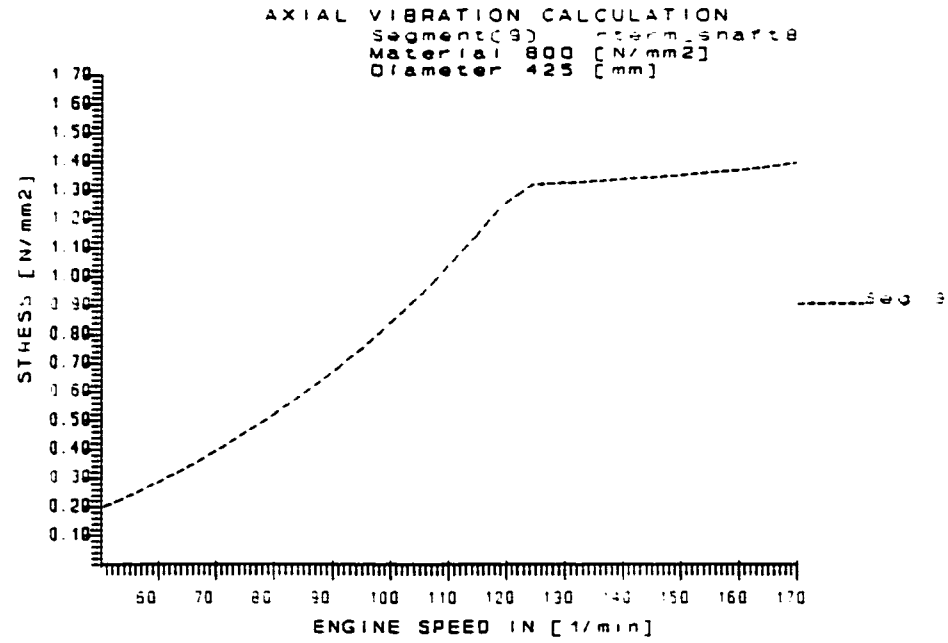

Figure III-55 Axial stress [N/mm2] in intermediate shaft - Overcritical solution

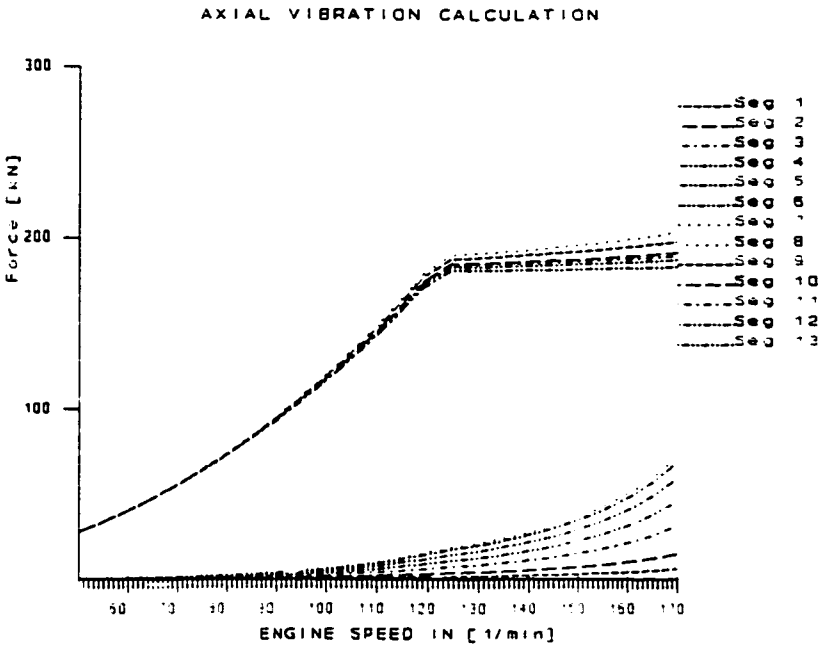

Figure III-56 Axial forces[kN] in the system - Overcritical solution

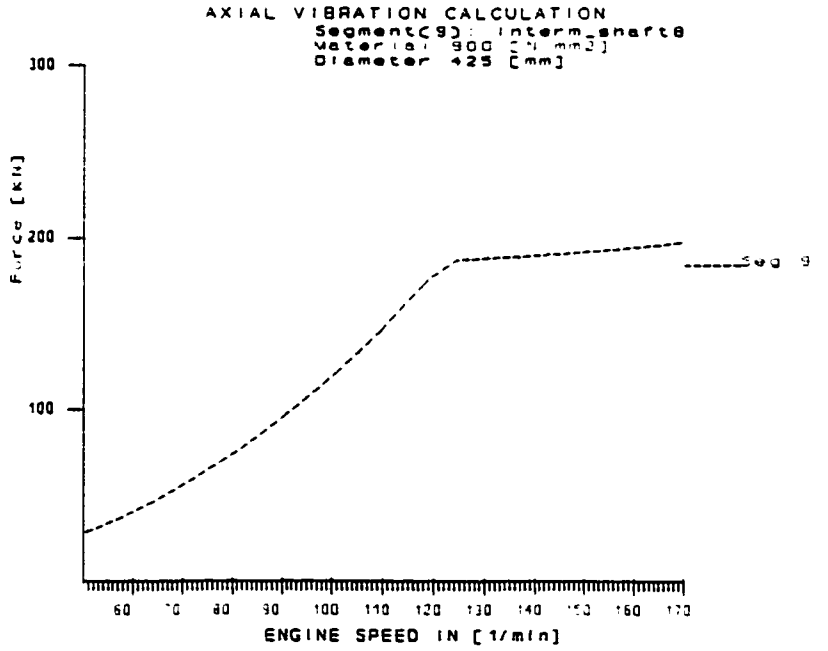

Figure III-57 Axial force [kN] in intermediate shaft - Overcritical solution

III.4. CONCLUSION

It is now obvious that for very rigid line shafting design the axial vibrations do not influence the line shafting strength, and plain axial vibration analysis provides no useful information for line shafting design. Therefore, torsional vibrations are the only necessary design criteria for the line shafting.

From the two boundary solutions to the shafting design, which correspond to:

- small diameter line shafting, and overcritical solution, and
- big diameter line shafting, and undercritical solution,

one can conclude that overcritical solution does not satisfy propulsion installation vibratory criteria without installing torsional vibration dampers or vibration tuners. Dampers would be highly efficient, big dimensions, and very expensive in order to decrease the resonant amplitudes. Partial intervention to the system which can lead to acceptable solution would be installation of the smaller (although still expensive) damper that will lower the stress level only enough to be acceptable as a transient solution. The transient solution can be achieved also with installation of the heavy rotating masses that will tune down extreme resonances. These detuners are restricted by allowable bearing loads, and not desired because the whole propulsion system is less responding.

Therefore, from the conventional line shafting design it can be concluded that the Undercritical Solution to the shafting design is an overall better choice than Overcritical Solution, for the following reasons:

- no restricted speed range is necessary

- no need for installation of additional equipment (dampers)

- cheaper solution than with installed damper.

Weak points of the solution are:

- big diameter and therefore heavier shafting

- more expensive shafting bearings for bigger diameter shafting.

In the conventional shafting design of the line shafting it is obvious that no propeller exciting axial vibration will significantly influence design. However, influence of the axial excitation generated by the main engine is not considered. The reason for that is in thrust bearing which separates system into two practically independent axial structures. In this case, and when there are no dominant resonances within operating speed range, it is fully acceptable to assume that for axial vibration analysis of the line shafting only propeller excitation may be important, and that there is no influence from the axial excitation generated by the main engine.

As stated above undercritical design would be preferred option in case design is performed considering only shafting strength requirements. This solution satisfies Classification Society rules without restrictions, and it is an overall cheaper design. However, this choice may be wrong if coupling effect between torsional and axial vibration analysis is not taken into account, and the structure of the ship is not designed to accommodate expected excitation.

It will be demonstrated in the following chapter, and confirmed by measurements (Appendix D and E) that torsionally induced propeller thrust variation produces much higher axial force than the estimated propeller thrust oscillation.

CHAPTER IV

TORSIONALLY INDUCED AXIAL VIBRATION

IV.1. GENERAL

In this chapter the effect and significance of torsionally induced axial vibration will be examined. The purpose of this study is to show that the intensity of dynamic axial force generated by torsional/axial coupling on the thrust bearing is so high that its impact on overall hull design must not be neglected. Results presented at the end of this chapter, confirmed by the measurements (Appendix D, and E), prove the necessity for such analysis.

Computation of dynamic thrust force is performed using the example from Chapter III. The force acting on the thrust bearing which has its origin in propeller's ability to couple torsional and axial vibrations is shown to be a major contributor to the total dynamic force on the thrust bearing.

Coupling between torsional and axial vibrations of the propeller shaft has its origin in the crankshaft of the engines and the propeller. The coupling produces additional axial force on engine's trust bearing and there is a high probability that force so generated can be a significant contributor to excessive vibrations of the ship's hull superstructure in particular.

The coupling that originates in the engine crankshaft is not considered. It is however, thoroughly analyzed by engine makers (as in Jacobsen (1991)- B&W, and Jenzer and Welte (1991)-Sulzer). Significance of crankshaft generated coupling in the total response is reduced somewhat with axial vibration dampers that have become an unavoidable part of modern diesel engines.

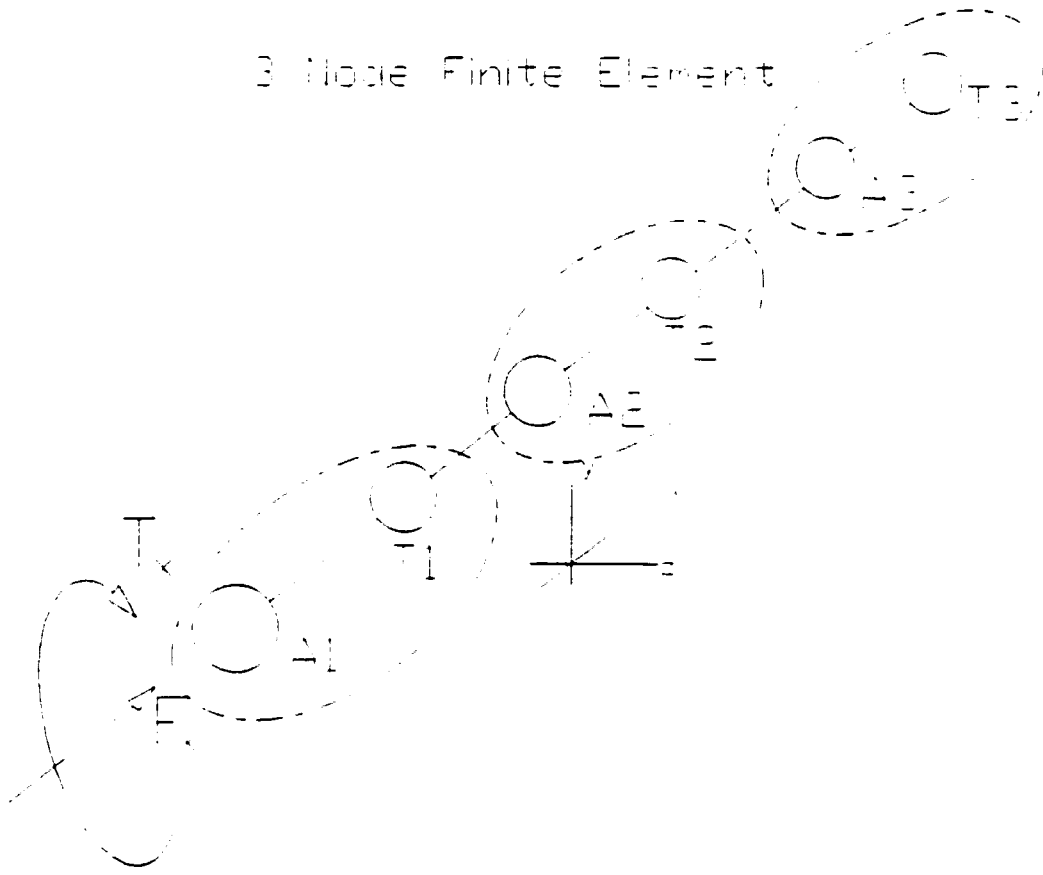

Figure IV-1 Three node - six DOF finite element

Finite element method (see Appendix B) is applied for the analysis of axial dynamic force on the engine's thrust bearing. The modelling is performed using one

dimensional, three node beam elements. For the presented model FEA is not deemed necessary, but it is used in this thesis as a basis that may be extended to adopt FE of higher dimension, as well as to include stress concentration analysis in the line shafting and reactions in bearings. Three node elements are also convenient for transverse vibration analysis when shear cannot be neglected, which would be the case here.

IV.2. THE MODEL

The three node elements, as shown in Figure IV-1, are used to model the line shafting. Each node has two degrees of freedom in order to accommodate longitudinal and torsional displacement. In Figure IV-1 nodes are divided into two subnodes (*A* and *T*), thus creating three nodal pairs. Each nodal pair serves to separate longitudinal and rotational degrees of freedom and to adapt physical system into the form suitable for matrix analysis.

The displacement {u} along the element can be expressed by the product of the chosen shape function [N] and a displacement vector {q}. The shape function [N] maps the original variables into the normal space and defines a distribution of the main variable within the element in a new coordinate system. For an isoparametric concept, where such a mapping is valid, the same functional relationship is used to define coordinate transformation as well.

$$\{u\} = \begin{bmatrix} x \\ \theta \end{bmatrix} \tag{IV-1}$$

$$\{q\} = [a_1, \theta_1, a_2, \theta_2, a_3, \theta_3] \tag{IV-2}$$

Element displacement vector {q} is chosen so to ensure the lowest bandwidth of the system matrices. The shape matrix [N] will therefore have the form as shown in Equation (IV-3).

$$[N] = \begin{bmatrix} [N_x] \\ [N_\theta] \end{bmatrix} = \begin{bmatrix} N_1 & 0 & N_2 & 0 & N_3 & 0 \\ 0 & N_1 & 0 & N_2 & 0 & N_3 \end{bmatrix} \tag{IV-3}$$

Finally, displacement {u} is:

$$\{u\} = [N(\xi)]\{q\} \tag{IV-4}$$

The coordinate of any point within the element can be similarly expressed in normal coordinates (Equation (IV-5)), where vector $\{x_i\}$ contains original nodal coordinates.

$$\{x(\xi)\} = [N(\xi)]\{x_i(x)\} \tag{IV-5}$$

The derivation of transformed coordinates (Jacobian) is:

$$x_{,\xi} = [N_{,\xi}]\{x_i\} = J \tag{IV-6}$$

IV.2.1. **Strain Energy**

The strain can be defined in normal coordinates by:

$$\{u_{,x}\} = J^{-1}\{u_{,\xi}\}$$

$$\begin{bmatrix}\varepsilon_x \\ \varepsilon_\theta\end{bmatrix} = J^{-1}\begin{bmatrix}x_{,\xi} \\ \theta_{,\xi}\end{bmatrix} \qquad \textbf{(IV-7)}$$

$$\{\varepsilon\} = J^{-1}[N_{,\xi}]\{q\}$$

$$\{\varepsilon\} = [B]\{q\}$$

From variational formulation for total potential energy (derived in the Appendix B), the strain energy for no initial strain and stress is:.

$$\delta U = \int_{(V)} \{\sigma\}^T \delta\{\varepsilon\}\, dV \qquad \textbf{(IV-8)}$$

The stress vector consists of normal and tangential components that respectively correspond to stresses developed by axial and torsional vibration.

$$\{\sigma\} = \begin{bmatrix} \sigma_x \\ \tau_{yz} \end{bmatrix} = \begin{bmatrix} E & 0 \\ 0 & G \end{bmatrix} \begin{bmatrix} [N_{x,\xi}] \\ [N_{\theta,\xi}] \end{bmatrix} \{q\} \qquad \textbf{(IV-9)}$$

Considering coordinate transformation (Equation (IV-10)), and incorporating (IV-9) and (VI-10) into Equation (IV-8) for strain energy, the following relationship is obtained:

$$dx = J\,d\xi \qquad \textbf{(IV-10)}$$

$$\delta U^e = \delta\{q\}^T \left(\int_{-1}^{1} J[B]^T \begin{bmatrix} AE & 0 \\ 0 & I_p G \end{bmatrix} [B]\, d\xi \right) \{q\} \qquad \textbf{(IV-11)}$$

$$\delta U^e = \delta\{q\}^T [k^e] \{q\}$$

From (IV-11) the stiffness matrix can be extracted as:

$$k^e = J \int_{-1}^{1} [B]^T \begin{bmatrix} AE & 0 \\ 0 & I_p G \end{bmatrix} [B]\, d\xi \qquad \textbf{(IV-12)}$$

IV.2.2. **Mass Matrix**

The mass matrix is derived from the kinetic energy equation:

$$\delta T^e = \rho \int_{(V)} \delta \{u_x\}^T \{u_x\} \, dV \qquad \text{(IV-13)}$$

where nodal velocities are:

$$\{u_x\} = [N(\xi)] \{q_x\} \qquad \text{(IV-14)}$$

After substitution of Equation (IV-14) into (IV-13), kinetic energy may be expressed as:

$$\delta T^e = \delta \{q_x\}^T \left(\int_{-1}^{1} \rho J [N]^T \begin{bmatrix} A & 0 \\ 0 & I_x \end{bmatrix} [N] \, d\xi \right) \{q_x\} \qquad \text{(IV-15)}$$

Element mass matrix is then defined as:

$$[m^e] = \rho J \int_{-1}^{1} \begin{bmatrix} [N_x] \\ [N_\theta] \end{bmatrix}^T \begin{bmatrix} A & 0 \\ 0 & I_x \end{bmatrix} \begin{bmatrix} [N_x] \\ [N_\theta] \end{bmatrix} d\xi \qquad \text{(IV-16)}$$

IV.2.3. **Assembly of the System Matrices**

The system stiffness and mass/inertia matrices are assembled following the nodal connectivity requirements defined as input parameter for each element of the structure. In case of linearly connected one dimensional elements without branching,

connection will be established on element's end-nodes only. For branching system, branch attachment to the main line may be at any node of an element.

The actual system is constructed in part from finite elements, and in part from conventional linear elements. The reason for such a solution is that usually designer of the propulsion system has no detailed data of, and no influence on, the main engine crankshaft construction. Therefore, one has to rely on data for crankshaft stiffness and mass/inertia that are provided by engine maker, and can be used as conventional elements.

Mass and inertia matrices (IV-17) will therefore consist of blocks representing the FE structure, and the diagonal mass/inertia block for conventional elements. However, in case where coupling exists among nodes of conventional elements, conventional part of the matrix will no longer be diagonal.

Propeller coupling will create additional connections between torsional and axial degree of freedom (IV-17) only on the node where the propeller is defined. The propeller is treated as a rigid body, and thus it possesses only mass and inertia (no elasticity) which is concentrated at a single node.

The stiffness matrix (IV-18) has similar form as the mass/inertia matrix, with the difference that conventional elements form a tri-diagonal matrix.

$$[M] = \begin{bmatrix} \left[\sum_{(e)} m_{FE}\right] & & & & & & & \\ & m_{ii}^{c} & & & & & & \\ & & I_{i+1,i+1}^{c} & & & & & \\ & & & \ddots & & & & \\ & & & & m_{jj}^{c} & -C_{jk}^{c} & & \\ & & & & -C_{kj}^{c} & I_{kk}^{c} & & \\ & & & & & & \ddots & \\ & & & & & & & m_{nn}^{c} \\ & & & & & & & I_{nn}^{c} \end{bmatrix} \qquad \text{(IV-17)}$$

$$[K] = \begin{bmatrix} \left[\sum_{(e)} k_{FE}\right] & & & & & & & \\ & \ddots & & -k_{i-1}^{t} & & & & \\ & & k_{i-2}^{a}+k_{i}^{a} & & -k_{i}^{a} & & & \\ & -k_{i-1}^{t} & & k_{i-1}^{t}+k_{i+1}^{t} & & -k_{i+1}^{t} & & \\ & & -k_{i}^{a} & & k_{i}^{a}+k_{i+2}^{a} & & -k_{i+2}^{a} & \\ & & & -k_{i+1}^{t} & & k_{i+1}^{t}+k_{i+3}^{t} & & -k_{i+3}^{t} \\ & & & & -k_{i+4}^{a} & & \ddots & \\ & & & & & & & \ddots \end{bmatrix} \qquad \text{(IV-18)}$$

The finite element part of the stiffness and mass/inertia matrices will be an assembly of n 6x6 matrices, and since one dimensional mesh is adopted, the assembly matrix bandwidth (BDW) will remain the same as for a single element; i.e. BDW=6[1].

IV.2.4. **Damping Matrix**

The damping matrix is not developed from individual element matrices, but is created directly for the whole system. Due to the character of propulsion, no structural damping within the line shafting or crankshaft has significant effect on the propulsion system's vibration. Main damping effect is generated on the propeller due to its hydrodynamic interaction with surrounding water. If propulsion system is equipped with torsional and/or axial vibration dampers, their effect on the global damping matrix will depend on the character of the damping (e.g. frequency dependent, constant damping, etc.).

In general for the conventional propulsion system, damping matrix will be a diagonal matrix with only few non-zero off-diagonal elements. This will be the case when only absolute damping, which is applied directly on the mass/inertia, is considered. However, off-diagonal nonzero elements occur due to the following reasons:

- branching of the system
- coupling effect between nodes

[1] This is true only if no internodal coupling or branching creates nonzero elements which are located further from the main diagonal than half-band-width spans.

- existence of the vibration dampers and elastic couplings.

IV.2.4.1. *Propeller Damping*

Propeller damping can be derived analysing the propeller operation in unsteady wake flow using lifting surface theory, or it can be adopted as a heuristic value obtained from experience that has been built for considered class of merchant ocean-going ships. Either of two approaches is equally valid, although heuristic values are more frequently in use primarily due to lack of exact propeller data in early project stages. In case propeller data is on hand, a good practice would be to compare calculated and heuristic data, and then decide which will be used.

Experience has shown (as per engine maker MAN B&W Diesel A/SI, Denmark) that for low speed, big diameter propellers which operate in the wake generated behind the ship, a reliable approximation for the propeller damping would be:

- 5 % of the critical damping for longitudinal vibration, and
- 5.5 % of torsional critical damping.

The computation of propeller damping for given hydrodynamic coefficients derived from the lifting surface method, will be shown below.

IV.2.4.2. *Damping Generated by the Main Engine*

Energy dissipated due to the friction in engine bearings and cylinders is usually adopted from the engine maker's experience. For low speed diesel engines damping is normally given at the crankpin as a compound value incorporating both the

absolute damping due to the friction in cylinders, and relative damping generated between cylinders. Values for damping (MAN B&W Diesel A/SI, Denmark) in the engine are as follows:

- cylinder damping factor: 0.85 % of the critical damping on the mass concentrated at the location of crankpin
- cam-shaft drive damping factor: 0.85% of the critical damping
- fly-wheel damping factor: 0.5 % of the critical damping

IV.2.5. **Excitation Matrix**

The excitation matrix is created on the global level; it is not assembled from the element's load matrices. The matrix is created in accordance with input data requirements:

- location (node number) where excitation is acting; excitation is applied only at nodes
- phase difference between reference excitation and actual one (reference excitation is usually taken at cylinder number one),
- combustion condition (normal firing, reduced combustion, no firing)
- firing order
- harmonic components (consist of sine and cosine components of the Fourier decomposition of the exciting forces for steady state conditions).

In order to ensure possibility of simultaneous application of excitation forces at all cylinders regardless of the existing phase shift among them (see the transfer matrix method), and in order to optimize computational memory, the excitation matrix contains only two excitation vectors. The first vector carries the information about cosine and the second about sine component of the applied force. Response is calculated for each harmonic and results are preserved in order to be added to the values calculated in the next iteration. This procedure is repeated for all harmonics required.

Developed software allows torsional and axial excitation to be applied to the system simultaneously. Response to each, torsional and axial vibrations, can be obtained separately, or their combined effect can be obtained. However, for analysis of the torsionally induced axial vibration, only the torsional excitation is applied and its results are presented.

Torsional excitation is applied in identical form as in Appendix A. Thus, it is necessary to consider cosine and sine component of the excitation forces simultaneously in order to enable parallel application of excitation on all cylinders, regardless of the phase shift among them.

Therefore, the cosine and sine components of the excitation forces, which will constitute the first and the second excitation vector respectively, are

$$f_c = \left[F_p^c \cos(p\,\alpha_i) + F_p^s \sin(p\,\alpha_i) \right] \cos(p\,\omega\,t)$$

$$f_s = \left[-F_p^c \sin(p\,\alpha_i) + F_p^s \cos(p\,\alpha_i) \right] \sin(p\,\omega\,t) \qquad \textbf{(IV-19)}$$

where F_p^c is torque obtained after premultiplying cosine harmonic component with cylinder area and crank radius, F_p^s is torque similarly obtained from sine harmonic component of excitation force, and α is excitation phase shift measured from the selected reference point.

IV.2.6. **Propeller Hydrodynamic Coefficients**

Adopted propeller hydrodynamic coefficients obtained for actual propeller are derived by Hylarides and Van Gent (1979) using Lifting Surface Theory. The propeller interaction with surrounding media is defined via hydrodynamic propeller coefficients, as explained in detail in Chapter II, section 6. Due to the character of the problem treated in this study, only coefficients involved in torsional and longitudinal vibration and their mutual interaction are considered.

Coefficients are nondimensional hydrodynamic reaction forces, which are independent of the propeller diameter and density of the surrounding media[2], reduced to the unit velocity and acceleration in rotational and longitudinal direction.

Presented axial and torsional equations of motion (IV-20) and (IV-21) consider propeller itself in interaction with surrounding media. Propeller connection to the shafting is included in force F_t and torque T_t, for axial and torsional case, respectively.

---

[2] Propeller hydrodynamic coefficient invariance of its diameter and density of surrounding media is valid only for the propellers of the same series where the principle of hydrodynamic similitude is satisfied.

$$(m_p - a_{xx})\ddot{x} - c_{xx}\dot{x} - a_{x\theta}\ddot{\theta} - c_{x\theta}\dot{\theta} = F_t \qquad \text{(IV-20)}$$

$$(I_p - a_{\theta_x\theta_x})\ddot{\theta} - c_{\theta\theta}\dot{\theta} - a_{\theta x}\ddot{x} - c_{\theta x}\dot{x} = T_t \qquad \text{(IV-21)}$$

As it was explained in Chapter II, *a* coefficients are related to the acceleration, and *c* coefficients to the velocity of the vibrating propeller. In the matrix in (IV-22), the diagonal coefficients related to acceleration represent virtual increase of the propeller mass and inertia. The off-diagonal coefficients related to acceleration, a_{12}^{at}, define virtual increment of the mass due to propeller rotary acceleration in the water, and a_{21}^{ta} is propeller's increment of rotary inertia due to its longitudinal acceleration.

$$\begin{bmatrix} a_{11}^{a} & a_{12}^{at} \\ a_{21}^{ta} & a_{22}^{t} \end{bmatrix} \qquad \text{(IV-22)}$$

The coefficient in the function of vibrational velocity of the propeller represents damping in two vibrating directions (longitudinal and torsional). Coupling effect related to the velocity of vibration is causing interaction between vibrations in one direction and damping effect in the other (similar to the mass/inertia coefficients).

IV.2.6.1. *Added Mass and Inertia*

Given the hydrodynamic coefficients, the propeller added mass and inertia (for known propeller data and sea water conditions) can be calculated as presented below.

Propeller data:

- Type: Wageningen B4-40-80
- Number of blades: 4
- Tip diameter D: 6150 [mm]
- Expanded area A/Ao: 0.4
- Pitch P: 4.92 [m]
- P/D: 0.8
- Mass in air: 15410 [kg]
- Rotary inertia in air: 28515 [kgm^2]
- Sea water density : 1025 [kg/m^3]

Diagonal elements of the added mass matrix can be calculated for the selected propeller as shown below:

$$a_{xx} = \frac{F_x}{\ddot{x}} \rho D^3 = -0.0274 * 1025 * 6.15^3 = -6532 \ [kg]$$

$$a_{\theta\theta} = \frac{M_x}{\ddot{\theta}} \rho D^5 = -0.000443 * 1025 * 6.15^5 = -3995 \ [kgm^2] \qquad \text{(IV-23)}$$

There is obvious disagreement between added inertia computed in (IV-23), and data obtained from the propeller model basin test, which is much larger (i.e. 6460 [kgm^2]). This discrepancy may be caused by the following reasons:

- propeller does not fully correspond to standard series type (e.g. real propeller blade area ratio *Ao* is greater than for B4-40-80)

- propeller model measurements in the basin may result in certain error (this is less likely).

Usually, in early project stage basin model data, which are more accurate than analytical ones, are not available. Also, during the basin tests, propeller can be altered to avoid cavitation and to fit better ship hull requirements. All these influence propeller coefficients and its vibration response; therefore in initial stage it is safer to select heavier propeller which will give higher response and increase safety margin.

IV.2.6.2. *Inertia Coupling*

Inertia coupling defines virtual inertia increment because of propeller acceleration due to longitudinal vibrations and vice versa.

From propeller coefficients, the value of inertia coupling is:

$$a_{x\theta} = \frac{F_x}{\ddot{\theta}} \rho D^4 = 0.00348 * 1025 * 6.15^4 = 5103[kgm] \qquad \text{(IV-24)}$$

IV.2.6.3. *Propeller Damping*

Propeller coefficients related to the vibration velocity are known as damping coefficients. Damping values related to each particular vibration form, are placed on main diagonal in the damping matrix, and their values are obtained as:

$$c_{xx} = \frac{F_x}{\dot{x}} \rho f D^3 = -0.595 * 1025 * 6.15^3 * f = -141862 * f[Ns/m] \quad \text{(IV-25)}$$

$$c_{\theta\theta} = -\frac{T_x}{\dot{\theta}} \rho f D^5 = -0.00965 * 1025 * 6.15^5 f = -87022 * f[Nms/rad]$$

Damping is given as a function of frequency of revolution of the propeller *f [1/s]*. Comparing damping values computed above with heuristic values, it is seen that there is a slight disagreement in intensity of the damping in different directions. The explanation for the differences is the same as for added mass and inertia coefficients.

Experience has demonstrated that in majority of cases for conventional line shafting, damping factor in the axial direction is lower than in torsional. Therefore, in this calculation, damping on the propeller is chosen as 5 % of critical damping for axial, and 5.5 % of critical damping for torsional vibration.

IV.2.6.4. *Damping Coupling*

Damping value defining interaction between torsional and axial vibration is defined by the following equation:

$$c_{x\theta} = -\frac{T_x}{\dot{x}} \rho f D^4 = -0.0758 * 1025 * 6.15^4 = -111146 * f[Ns/radm] \quad \text{(IV-26)}$$

IV.2.7. **Thrust Bearing - Support Condition**

Propulsion system needs to be supported in axial direction in order to restrain the propeller generated thrust within ship structure and enable propulsion. For the merchant ocean going ships this task is performed by thrust bearings, which are normally incorporated into the structure of the main engine.

Thrust bearings in modern engines have significant flexibility. Actual engine structure is assumed to be a support with zero displacement.

To simulate support conditions which will simultaneously provide support reaction the following procedure is adopted:

- average stiffness K_{ave} of all diagonal elements of the system stiffness matrix is calculated
- $H = 10^{(p/2)} * K_{ave}$ is added to the node where support is created, where p is the number of decimal digits used in computation.

Reaction in the support located at i-th degree of freedom is therefore achieved from the following equilibrium equation:

$$\begin{bmatrix} R_1 \\ \cdot \\ \cdot \\ R_i+H\delta \\ \cdot \\ \cdot \end{bmatrix} = \begin{bmatrix} k_{11} & & & & \\ & \cdot & & & \\ & & \cdot & & \\ & & & k_{ii}+H & \\ & & & & \cdot \\ & & & & & \cdot \end{bmatrix} \begin{bmatrix} q_1 \\ \cdot \\ \cdot \\ q_i \\ \cdot \\ \cdot \end{bmatrix} \qquad \text{(IV-27)}$$

It is evident from the Equation (IV-27) that with sufficiently large stiffness at the i-th node, displacement q_i will tend to zero, where δ represents prescribed displacement.

To introduce an elastic support to the system, which will restrain one degree of freedom, the total number of degrees of freedom must be increased by one. Stiffness matrix around the node will be changed as:

$$\begin{bmatrix} \cdot & & & \\ & \cdot & & \\ & & k_{33}+k_{44} & -k_{44} \\ & & -k_{44} & k_{44}+H \\ & & & \cdot \\ & & & & \cdot \end{bmatrix} \qquad \text{(IV-28)}$$

For the present installation with MAN B&W 5L60MC engine thrust bearing data are:

- thrust cam mass: 8322 [kg]
- stiffness of the thrust block: $2.10084*10^9$ [Nm/rad]

IV.2.8. **Damper and Elastic Coupling Condition**

When dampers and elastic couplings are installed in the system mass/inertia, stiffness and damping matrices must be adjusted accordingly. Axial vibration damper requires identical transformation of the system matrices as the thrust bearing.

Torsional vibration damper and couplings require similar transformation of the system matrices. The difference between them is only that the former, due to its relatively high damping characteristic and moderate stiffness, has the sole function of reducing dominant vibratory amplitudes, and the latter which has high flexibility practically separates the system into two independent systems.

For of over-critical solution to the line shafting geometry (i.e. small diameter shafting), damper is necessary in order to reduce the amplitude of the 5-th order torsional resonance below the limits for continuous operation. Damper has to be attached to the free end of the main engine.

Data for a tuned torsional damper which would satisfy the requirements on stress limit in the intermediate shaft, are as follows:

- Required inertia on damper secondary member I_s: 5000 [kgm^2]
- Nondimensional damping factor: 0.28
- Damper stiffness and linear viscous damping are a function of the engine frequency of rotation *f [1/s]*, and can be calculated from the following equations.

$$k_d \le f_e^2 I_s \quad [Nm/rad]$$

$$c_d = 0.28 \frac{k_d}{f} \quad [Nms/rad] \qquad \text{(IV-29)}$$

IV.2.9. **Displacement Matrix**

Response analysis is performed for the steady-state excitation condition. The steady-state condition assumes that the excitation pattern remains the same for every process periodically repeated within the same time period. Practically, the steady state condition is achieved when ship is running at a steady speed, in calm sea, and with even rudder. In that case engine combustion is also stable. Harmonic components used in the following calculations correspond to such conditions. To analyze transient response, excitation needs to be given in the form expressing excitation as a function of time.

Displacements are calculated for each excitation vector couple (consisting of cosine and sine components) and maximum displacement and maximum displacement differences between two consecutive nodes are preserved for each cycle. Thus, the time period required to close the full cycle is divided into a number of time steps. For each time step the response is calculated, compared with previously calculated values, and maximal displacement is preserved.

The same process is repeated for each harmonic of the excitation force and for each speed defined within the speed range.

IV.2.10. **Forces, Torques and Stresses**

Once displacements are calculated, stresses in finite elements on the element level can be calculated according to the following formulation:

$$\{\sigma\} = \begin{bmatrix} \sigma \\ \tau \end{bmatrix} = \begin{bmatrix} E & \\ & G \end{bmatrix} \begin{bmatrix} [N_{x,\xi}] \\ [N_{\vartheta,\xi}] \end{bmatrix} \{q\} \qquad \textbf{(IV-30)}$$

For conventional elements, stress is simply derived from the product of preserved maximal nodal displacement differences, and stiffness between them, all divided by the area or the polar moment of inertia of the elements cross section. Division by area is applied for axial stresses, and polar inertia of the cross section is used for torsional stresses.

$$\sigma = \frac{(a_i - a_j)\, k_{ij}^{a}}{A}$$

$$\tau = \frac{(\vartheta_i - \vartheta_j)\, k_{ij}^{t}}{W_p} \qquad \textbf{(IV-31)}$$

IV.3. **EXAMPLE**

The propulsion system design, as explained in Chapter III is primarily defined by torsional vibration analysis, and checked for resonance with axial vibrations. Transverse

vibrations are usually excluded from the analysis because of relatively high stiffness of the line shafting and low frequency of revolution, which diminishes its influence in the total response. This is also true for axial vibrations (see result below, and the response analysis in Chapter III, section 3). The axial vibration analysis is performed because of existing coupling effect between torsional and axial vibrations which significantly influences the ship hull. From the presented results it is obvious that axial vibration stresses made no contribution to the line shafting strength (stresses are negligible in comparison to torsional vibrations). The axial force generated due to propeller's coupling characteristic was the reason for one comprehensive axial vibration analysis, in order to show that none of axial stresses are significant.

Therefore, in the conventional approach to the propulsion system, the design geometry of the line shafting will entirely correspond to the torsional vibration strength criteria. By not taking a comprehensive approach in analysis of excitation that is transmitted and influenced by certain line shafting geometry, the designer can easily ill design the ship structure. Problems may be significant in the domain of excitation which was *not known* to cause notable response in the ship hull structure. This is true for the propeller coupling of the torsional and axial vibrations.

In conventional approach, Chapter III, the following four solutions to the line shafting design are discussed:

- Under-critical solution (UC)

  This is solution with relatively big diameters of the shafts, and therefore high stiffness. It causes main resonance of the fifth order to be moved beyond

nominal operating speeds of the installation. No restrictions are imposed on this solution according to criteria proposed by Classification Societies.

- Over-critical solution (OC) without damper

  This is solution with flexible line shafting and small diameters. Solution does not satisfy strength criteria because the main resonance, which is placed within the operational speed range of the installation, is exceeding stress limits. Solution is called over-critical because installation normally operates on the frequencies over main critical resonance.

- Over-critical solution with damper

  With installed torsional vibration damper overcritical design fully complies with requirements. No prohibited speed range is necessary.

- Over-critical solution with tuning wheel

  When tuning wheel is installed, the peak amplitude of the main resonance can be lowered below the limits for transient operation of the propulsion system. This will ensure that the installation can run above and below the critical area at steady condition, and only pass swiftly through the barred range.

Force on the main engine's thrust bearing is computed for the above four possible solutions to the propulsion system line shafting in order to examine the effect of propeller coupling of torsional and axial vibrations. Results are given in two diagrams:

- the first one (Figure IV-2) showing total response on all harmonics of excitation force, and

- the other (Figure IV-3) gives only response to the dominant 5-th order harmonic.

Next, the torsional and torsionally induced axial stresses are presented in Figures IV-6, IV-7, and IV-8 in order to show that axial stresses cannot influence line shafting strength.

In Appendices D and E, axial vibration measurements and ship hull vibration measurements for undercritical and overcritical installation are presented. Computed results agree well with measured values, as demonstrated in sections IV.3.1 and IV.3.2. The differences between measured and computed variational thrust forces may exist due to following reasons:

- error in calculation due to input data approximation (e.g. material properties, wake excitation, discretization, etc.)

- the strain-gauges (used in measurements) are installed on intermediate shaft, thus the measured force is lower than the one acting on the thrust bearing.

- the measured values contain the contribution from the axial forces generated due to crankshaft coupling effect, which are of the same order as propeller coupled torsional forces[3].

The ship hull vibration measurements performed at the ship's wheel-house (Appendix E, Figure E-1),show the difference in vibration levels in the superstructure

[3] In the analysis of crankshaft vibration coupling (Jacobsen (1991)- MAN B&W) it is shown that in 5 cylinder engines propeller coupling produces many times greater reaction force on thrust bearing than torsionally induced vibration coupling generated in the crankshaft (for 5L80MC engine this difference is 8 times).

for undercritical and overcritical line-shafting design[4]. Measured at the same location at wheel-house, the overcritical solution is obviously resulting in a significantly lower vibration level in longitudinal direction than the undercritical case.

Dashed line in Figure E-1 represents measured 5th order vibratory velocities in longitudinal direction for undercritical solution. Measured 5th order velocity amplitudes peak at approximately 100 [rpm] engine speed, with extremely high value of 17 [mm/s]. Figure E-2 represents ISO guidelines for mechanical vibration and shock, for the overall evaluation of vibration in merchant ships. Comparing measured values with ISO guidelines, we see that measured longitudinal amplitude is close to the area regarded by ISO as hazardous for ship operation. Thus, the undercritical line shafting design may not be an acceptable solution. One needs to point out that longitudinal velocities measured for undercritical case are obtained with diesel engine restrained with longitudinal top-bracings, which produced lower response at the wheel-house.

The full curves in Figure E-1 show longitudinal vibratory response at the wheelhouse for overcritical solution to the line shafting design. Results are given as a function of engine speed. Three different measurements were performed. and results are presented for the engine speeds closer to the rated revolutions. There is no big difference among the three measurements, and recorded vibratory velocities at wheelhouse are not found to exceed 6.5 [mm/s]. Comparing measured values with ISO guidelines, overcritical solution to the line shafting is found acceptable.

---

[4] Measurements have been taken on two sister-ships differing only in the design of the line shafting.

Another excitation in longitudinal direction corresponds to the 4th order of the propeller blade frequency. The response produced by excitation of fourth order as estimated by equation (III-6) in III.3.3.2., is presented by Figures III-51 to III-52 for undercritical case, and Figures III-55 to III-57 for overcritical case. However, the axial vibration measurement report for undercritical case in Appendix D shows that real 4th order response is much lower than the calculated one:

- computed axial vibratory force in intermediate shaft (Figure III-52), at nominal engine speed of 111 [rpm] is approximately 150 [kN]

- from Appendix D, Figure D-1, measured force in intermediate shaft at 111 [rpm] is found to be 45 [kN].

IV.3.1. **Undercritical Solution**

Among the solutions to the line shafting design, the undercritical solution produces the greater reaction force at the thrust bearing (Figure IV-2). Carrying signal is the 5-th order resonance (Figure IV-3) with visible significant contribution on its flank from the 10-th, the 8-th, and the 7-th order engine excitation harmonic components.

At the nominal engine revolution of 111 [rpm] the force is 574 [kN]. The 7-th order resonance has obvious impact on the reaction at nominal speed. Even higher reaction forces are obtained at revolutions corresponding to the 10-th, and the 8-th order (i.e. 79 [rpm] and 99 [rpm] respectively).

The 10-th order resonance of under-critical solution produces higher reaction force than the main resonance of the 5-th order in overcritical solution with damper. Moreover, 79 [rpm] which corresponds to excitation of the 10th order harmonic, is an important operational speed because it may correspond to the manoeuvering condition, or canal and river navigation speeds. At that revolution, the high longitudinal vibration on the superstructure and in the engine room can influence operation of the equipment, causing failure or malfunction, consequently resulting in their break-down.

Vibratory axial forces at propeller revolution 111 [rpm] are:

- torsionally induced total (16 harmonic synthesis) axial force is 570 [kN] @ 111 [rpm]
- torsionally induced 5th order axial force
  - calculated (Figure IV-3): 270 [kN] @ 111 [rpm]
  - measured (Appendix E, Figure E-1): 320[kN]
- propeller generated 4th order axial force
  - calculated (Chapter III, Figure III-52): 150 [kN] @ 111 [rpm]
  - measured (Appendix D, Figure D-1): 45 [kN]

Comparing measured and calculated values the following can be concluded:

1. Calculated torsionally induced axial forces generated on the propeller are in line with the measured ones. The reasons for existing differences are described in section IV.2.6.1.
2. Propeller generated axial force is much higher than measured. This is not

surprising considering very rough approximation in defining propeller thrust variation (see Chapter III, section 3.3.2.). However, margin of error can be corrected if exact wake data is available and response calculated for it.

Axial thrust forces due to non-coupled axial vibrations produced by propeller are not included in Figure IV-2. These axial forces have been calculated in Chapter III, Figure III-51 and III-52, and they are shown here again in Figures IV-4 and IV-5. Forces are below 150 [kN] at nominal engine speed of 111 [rpm]. If compared with torsionally induced axial thrust for undercritical line shafting design (Figure IV-2) these forces can make some contribution to the total response. For the present case, considering the fact that coupling calculation has already overestimated the real thrust force, the significance of the propeller-developed oscillatory thrust is not so high. Moreover, vibration measurement of the thrust force for undercritical line shafting (Appendix D, Figure D-1) shows that the 4-th order axial force, which corresponds to propeller oscillatory thrust is more than 3 times lower than the calculated one.

Computations of the torsional and axial stresses in the intermediate shaft are also performed. There is a good agreement between torsional vibration results performed by transfer matrix method and the finite element method (Figure IV-6). However, since finite element modeling results in stiffer structure, and thus yields lower stresses, summation of the responses to all harmonics of excitation force has been done linearly; i.e. neglecting the phase shift between them. This approximation increases the safety margin, resulting in higher response than that obtained with the transfer matrix method.

Axial stresses shown in Figure IV-6, are only those induced by propeller coupling of the torsional vibrations. The axial vibration stresses due to propeller excitation are the same as presented in analysis in Chapter III, Figures III-49 and III-50, and are not included because of their negligible intensity (lower than 1 [N/mm^2]).

IV.3.2. **Overcritical Solution**

Overcritical solution without damper, or tuning wheel, does not satisfy strength criteria for the line shafting; its reaction in thrust bearing is demonstrated only for comparison purposes. Torsional and induced axial stresses in intermediate shaft are presented in Figure IV-7. It is obvious (as in the analysis with the transfer matrix method - Chapter III, Figures III-6 to III-17) that the 5th order torsional stresses are too high, and that installation is not operational without additional vibration tuners or dampers.

When tuning wheel is installed in the system the amplitude of the 5th order main resonance can be lowered below limit for transient operation and allow running of the propulsion installation with barred speed range. If torsional vibration damper is attached to the system, vibrational amplitudes can be reduced further and ensure unrestricted operation of the system in the whole operational speed range (Figure IV-8).

It can be also seen from Figures IV-2 and IV-3, that for all three variations of the overcritical case, the 5-th order resonance dominates the response and there is no notable contribution from other orders. Moreover, Figure IV-7 shows no contribution

from the axial vibrations either.

Considering axial force transmitted to the ship hull structure, the overcritical solution with damper generates significantly lower force than undercritical design. As seen from Figures IV-2 and IV-3, calculated forces on thrust bearing are:

- from Figure IV-2 torsionally induced total (16 harmonic synthesis) axial force is 160 [kN] @ 111 [rpm]
- from Figure IV-3 torsionally induced 5-th order axial force is 100 [kN] @ 111 [rpm]
- propeller generated 4-th order axial force (Figure III-57) is 150 [kN]

Note: measurements for this solution were not available.

For the overcritical solution to the line shafting, the analysis in Chapter III, Figures III-56 to III-57, shows that the influence of the 4-th order axial oscillatory thrust in total response at nominal engine speed is much higher than for line shafting with big diameters. The reason is that propeller generated thrust force is not significantly different for either of the two design solutions to the line shafting. However, it is expected that this will not produce significant effect on the hull vibration, because real excitation level is much lower. Although measurements for this solution were not available, it can also be expected that non-coupled axial forces are overestimated in vibration analysis for overcritical case. In the discussion presented here the existing phase shift between harmonic orders of the responses are neglected.

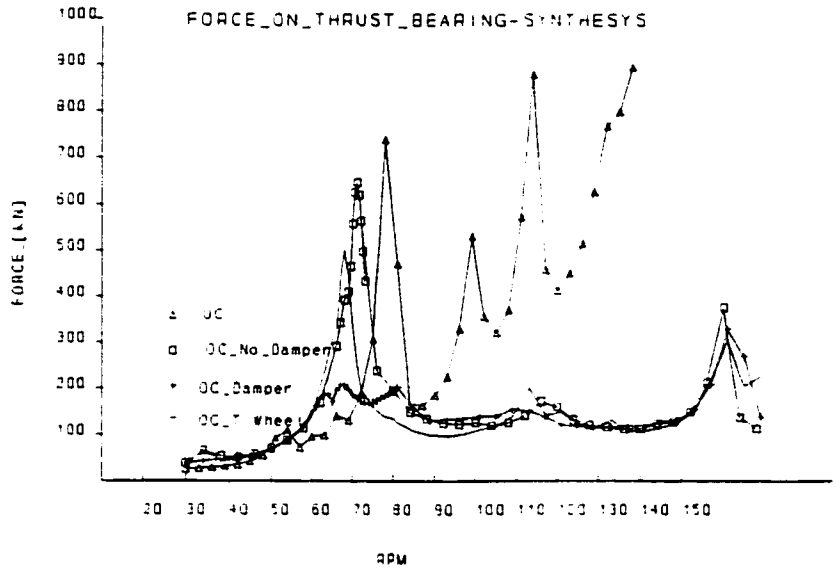

Figure IV-2 Total torsionally induced axial force on thrust bearing [kN]

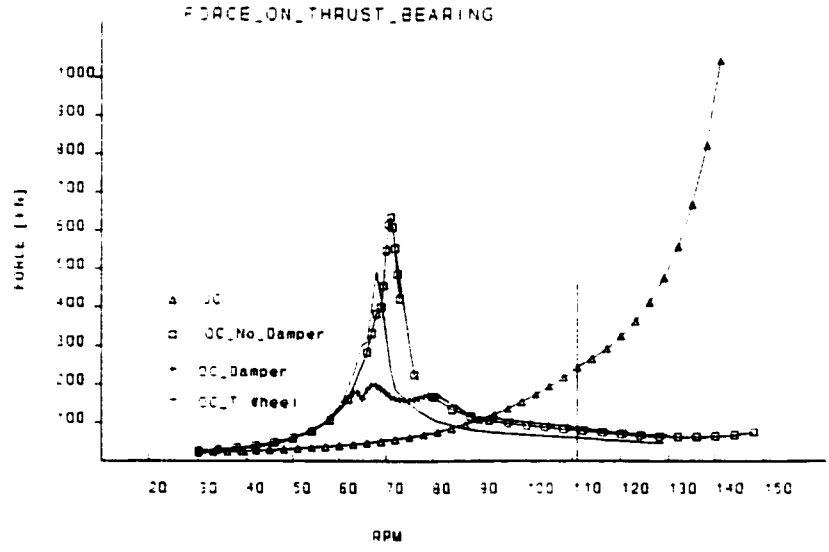

Figure IV-3 Axial response on thrust bearing [kN] , induced by 5th order torsional excitation

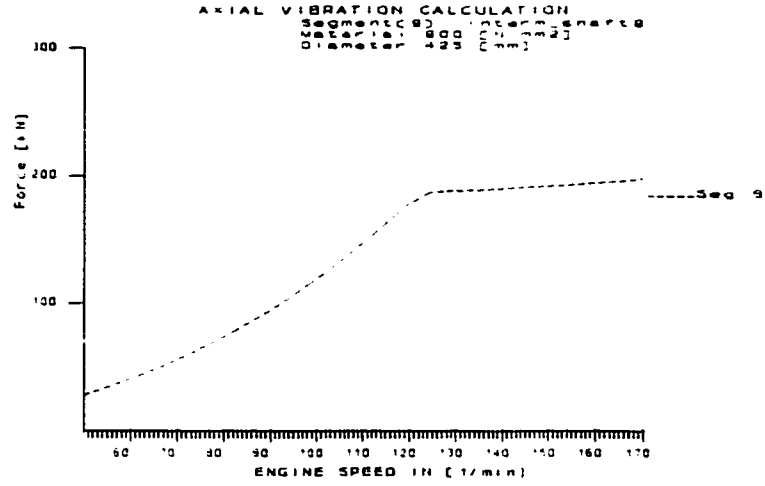

Figure IV-4 Axial force [kN] in intermediate shaft - Overcritical solution

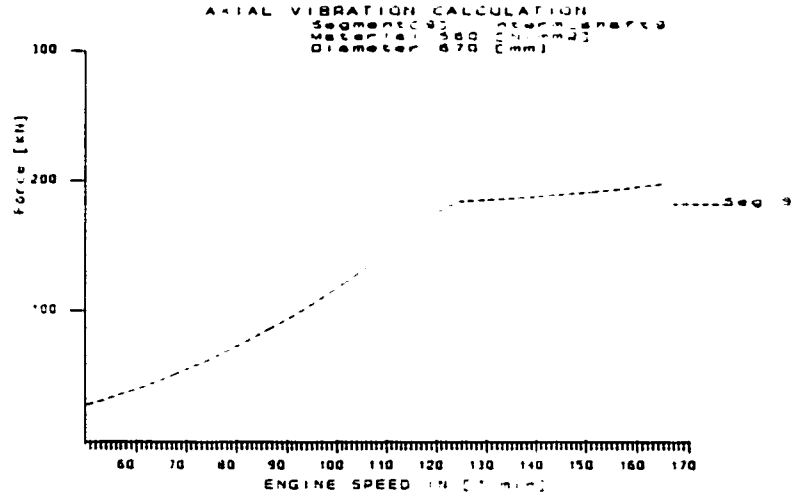

Figure IV-5 Axial force [kN] in intermediate shaft - Undercritical solution

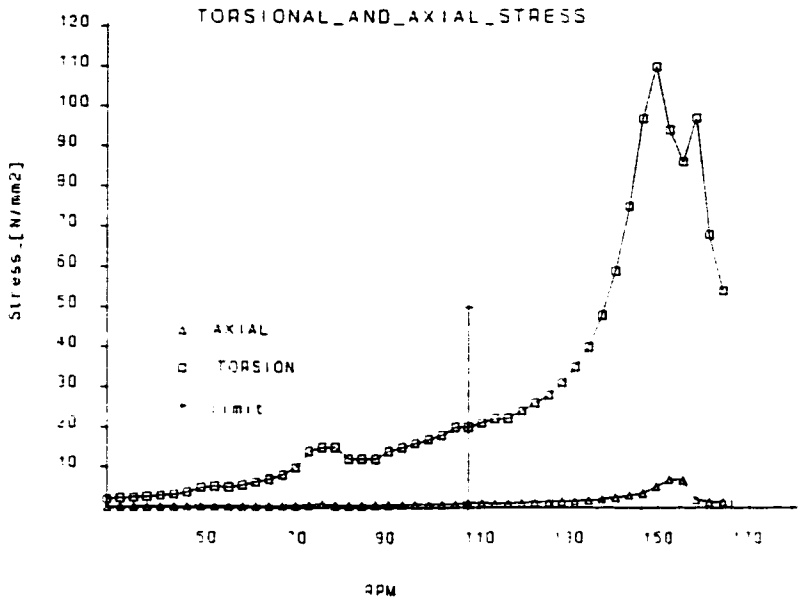

Figure IV-6 Torsional and torsionally induced axial stresses [N/mm²], intermediate shaft - Undercritical solution

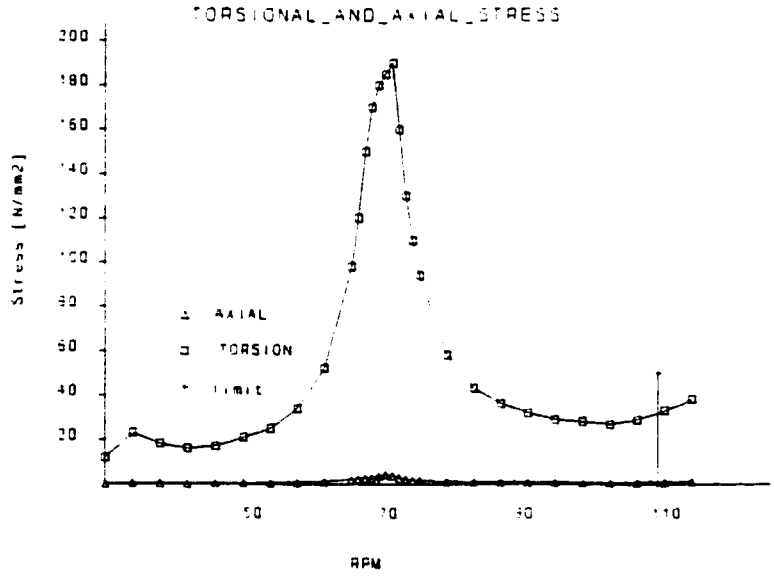

Figure IV-7 Torsional and induced axial stresses [N/mm2], in intermediate shaft -Overcritical solution

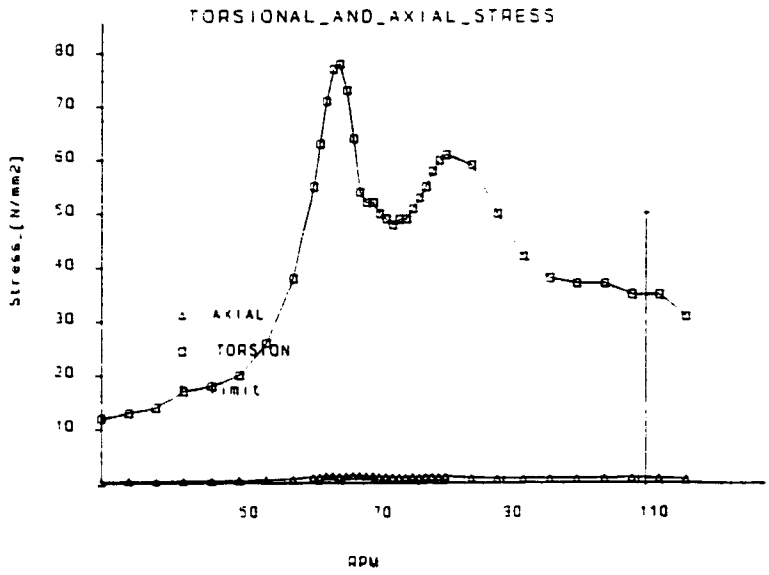

Figure IV-8 Torsional and induced axial vibration [N/mm2] in intermediate shaft - Overcritical solution with damper

CHAPTER V

CONCLUSIONS

In this thesis the line shafting design in merchant ocean going ships is carried out by taking into consideration the torsional-axial coupling in the line shafting due to propeller action. Initially, the design is carried out following the conventional approach by considering the torsional and axial vibration independently, in order to show the importance of the coupling action.

From a comparison of the presented analysis results (Chapters III and IV), and vibration measurements (Appendices D and E), it is clear that not taking into account propeller coupling of torsional and axial vibrations in propulsion installation analysis may result in an improper line shafting design and, cause severe vibration problems on the ship structure. The conventional approach in designing line shafting, which considers separate analysis of the two major vibration modes (i.e. torsional and axial) and does not take into account vibration coupling, will not provide enough information to the ship hull designers for a proper hull structure design.

In conventional approach the line shafting is optimized only considering its strength and overall design cost, while no information is given about the propulsion system interaction with its surroundings. It is confirmed in this thesis that relying only on the information obtained by conventional approach can produce a crucial error in

selection of the line shafting geometry. The example of a conventional design is presented in Chapter III. It is demonstrated that the conventional approach in line shafting design finds the undercritical solution to suit best a set of criteria normally required by Classification Societies, such as:

- stresses in line shafting are within the limits for nonrestricted operation
- no dampers or vibration tuners are required
- solution is cheaper than small diameter shafting with installed damper.

Unfortunately, excessive longitudinal vibration of the hull is related to the undercritical solution. The frequency of structural vibration is found to correspond to the 5-th order excitation of the engine. The analysis presented here examined the relationship between longitudinal vibration of the hull structure and the propeller coupling of the torsional and axial oscillation. It is clearly seen from the vibration measurement at the superstructure (Appendix E), and from Figures IV-2 and IV-3 in Chapter IV, that the vibratory thrust force induced on the propeller is responsible for the high response at the ship's superstructure.

Overcritical design of the propulsion installation will require additional equipment in order to secure its proper operation. This will either be a torsional vibration damper, which will ensure nonrestricted operation of the installation throughout the entire engine speed range, or control equipment to avoid the possibility of engine operation in the area of main resonance. This design, although more expensive than the undercritical solution, will result in lower excitation level in the superstructure, ensuring better living conditions aboard the ship and more secure operation of the installed equipment.

Measurement of the thrust variation presented in Figure D-1 in Appendix D, confirms calculation in Chapter IV. In Appendix E the vibration measurements at the wheel-house (Figure E-1) are presented for undercritical and overcritical line shafting design. Measurements were taken on two sister ships, one with big-shafting propulsion system, and the other with small diameter shafting. Results confirm that big diameter shafting causes approximately 2.5 times higher longitudinal vibratory velocities[5] than the shafting with small diameter. Recorded values at nominal engine speed of 111 [rpm] fall beyond vibratory limits proposed by ISO (see Appendix E, Figure E-2), suggesting that the vibration level of the ship exceeds the margin set for normal equipment operation, and that vibrations can be harmful for the crew aboard the ship.

Presented results point clearly to the torsionally induced axial vibration which originates on the propeller and the crankshaft of the main engine. The propeller coupling of the torsional and axial vibrations is considered in this thesis in order to show its significance in total axial thrust variation and consequences which can result if vibration coupling is neglected.

For proper design of the ship in the early project stage, designers thus need information about the torsionally induced axial force on the thrust bearing, besides the conventional data. A more comprehensive picture of excitation forces which act on the system will enable designers to choose whether to intervene in the design of the hull, or to choose overcritical line shafting geometry. Moreover, it is important to have reliable, relatively accurate, and at the same time simple and fast computational tool available,

---

[5] Vibratory velocities were measured in order to achieve maximum accuracy of the recorded data.

which will also provide the ship hull designers with information about longitudinal force generated on the thrust bearing.

V.1. SUGGESTIONS FOR FUTURE WORK

The study carried out in this thesis is by no means exhaustive. Several assumptions have been made to simplify the analysis. Many improvements in the analysis can follow by releasing some of these assumptions. Accordingly some suggestions for future work are:

1. Inclusion of transverse vibration analysis to study its influence on the force transmitted to the hull structure.
2. Models of bearings which include the flexibility and damping effect in hydrodynamic bearings.
3. Considerations of the variation in the gas pressure loads in the analysis of the vibration of the shafting.
4. Influence of the turbulent wake on the line shafting dynamics.
5. Inclusion of the drag force into analysis.

LIST OF REFERENCES

American Bureau of Shipping (1994): *Rules*

Bathe, K.J. (1982): *Finite Element Procedures in Engineering Analysis*, Prentice Hall, N.J.

Breslin, J.P. (1975): "Techniques for estimating Vibratory Forces Generated by Propeller", *SNAME Technical Research Bulletin*

Breslin, J.P. and Andersen, P. (1994): *Hydrodynamic of the Ship Propellers*, Cambridge Ocean Technology Series 3

Bureau Veritas (1981): *Machinery Hull Interaction, Vibrations II*

Hadler, J.B. and Cheng, H.M. (1965): "Analysis of Experimental Wake Data in Way of Propeller Plane of Single and Twin-Screw Ship Models", *SNAME Transactions*, V 73;pp. 287-414

Hinton, E. and Owen, R.J. (1979): *An Introduction to Finite Element Computation*,

Printeridge Press Ltd. Swansea, U.K.

Homori, S., Kamata, M. and Sasaki, Y. (1989): "Study on the Vibration and Strength of Long Stroke Diesel Engine Crankshafting", *NK Technical Bulletin*; pp. 36-53

Hylarides, S. and Van Gent, W. (1974): "Propeller Hydrodynamic and Shaft Dynamic", *Symposium on High Powered Propulsion of Large Ships - Wageningen*, The Netherlands; pp. xiv,1-xiv,54

Hylarides, S. and van Gent, W. (1979): "Hydrodynamic Reactions to Propeller Vibrations", *Proceedings, Conference on Operational Aspects of Propulsion Shafting System*, London; pp. 383-393

Jakobsen, S.B. (1991): "Coupled Axial and Torsional Vibration Calculation on Long-Stroke Diesel engines", *SNAME Transactions*, V 99; pp. 405-419

Jeras, Dušan (1975): *Motori s Unutrašnjim Izgaranjem*, Tehnički Školski Centar KoV JNA, Zagreb

Jenzer, J. and Welte, Y. (1991): "Coupling Effect Between Torsional and Axial Vibration in Installations with Two stroke Diesel Engines ", *New Sulzer Diesel*

Jeon, H. and Tsuda, K. (1974): "Theoretical Analysis of the Coupled Torsional-Axial Forced Vibration of the Marine Diesel Engine Shafting", *Journal of Faculty of Engineering*, The University of Tokyo; pp. 535-561

Johnson, A.J. and McClimont, W. (1963): "Machinery Induced Vibrations", *BSRA;* pp. 121-168

Lewis, F.M. and Auslander, J. : "Virtual Inertia of Propellers", *Journal of Ship Research*, 9,1; pp. 37-46

Lewis, F.M. (1969): "Propeller Vibration Forces in Single-Screw Ships", *SNAME Annual Meeting*; pp. 318-343

Lewis, E.V., ed., (1988): *Principles of Naval Architecture, Volume II: Resistance, Propulsion and Vibration* , SNAME (1988)

MAN B&W MC Programme (1993), *Engine Selection Guide*, Diesel A/S Two-stroke Engines

MAN B&W (1994) *List of Reference* , March 25

Mikuličić, Miroslav (1976): *Motori 1*, Školska Knjiga Zagreb

O'Brien, T.P. (1962): *The Design of Marine Screw Propellers*

Panagopulos, E. (1950): " Design-Stage Calculations of Torsional, Axial, and Lateral Vibrations of Marine Shafting", Presented at annual SNAME meating in New York 1950; pp. 329-384

Parsons, M.G., Vorus, W.S. and Richard, E. (1980): *Added Mass and Damping of Vibrating Propellers*, Research paper, University of Michigan, The Department of Naval Architecture and Marine Engineering

Parsons, M.G. and Vorus, W.S. (1981): "Added Mass and Damping Estimates for Vibrating Propellers", *SNAME Propellers '81, A Symposium*; pp. 273-302

Parsons, M.G. (1983): "Mode Coupling in Torsional and Longitudinal Shafting Vibration ", *Marine Technology*, 20, 3; pp. 257-271

Pastel, E.C. and Leckie, A. (1963): *Matrix Methods in Elastomechanics*, Mc Graw Hill

Reddy, J.N. (1986): *Applied Functional Analysis and Variational Methods in Engineering*, McGraw Hill

Senjanović, I. (1980): *Vibracije Broda (Ship Vibrations)* Vol. I, II, III, University of

Zagreb

Sparenberg, J. A. (1960): "Application of Lifting Surface Theory to Ship Screw", *International Shipbuilding Progress*, 7, 67; pp. 99-106

Timoshenko, S.P. and Goodier, J.N. (1972): *Theory of Elasticity*, Third edition, McGraw Hill

Tsakonas, S., Jacobs, W.R. and Ali, M.R. (1973): "An "Exact" linear Lifting Surface Theory for a Marine Propeller in Nonuniform Flow Field", *Journal of Ship Research*, V 17; pp 169-207

Van Gent, W. (1975): "Unsteady Lifting Surface Theory for Ship Screws: Derivation and Numerical Treatment of Integral Equation", *Journal of Ship Research*, V 19; pp. 269-317

Van Lammeren, W.P.A., Van Manen, J.D. and Oosterveld, W.W.C. (1969): "The Wageningen B-Screw Series", *SNAME Annual Meeting*

Van Manen, J.D. and Lap,A.J. (1956): *Fundamentals of Ship Resistance and Propulsion*, Netherlands Ship Model Basin

Van Manen , J.D. and Wereldsma, R. (1960): "Propeller Excited Vibratory Forces in the Shaft of a Single Screw Tanker", *International Shipbuilding Progress*, 7,73; pp. 371-389

Vassilopoulos,L. and Triantafyllou, M. (1981): "Prediction of Propeller Hydrodynamic Coefficients Using Unsteady Lifting Surface Theory", *SNAME Symposium on Propellers*; pp. 253-272

Zienkiewicz, O.C. and Cheung, Y.K. (1967): *The Finite Element Method, in Structural and Continuum Mechanics*

Zienkiewicz, O.C. and Cheung, Y.K. (1971): *The Finite Element Method in Engineering Science*

APPENDIX A

TRANSFER MATRIX METHOD

A.1. POINT MATRIX

A.1.1. Compatibility and Equilibrium Conditions

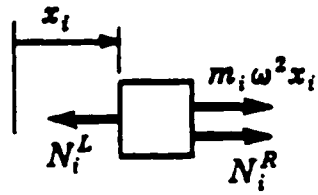

Figure A-2 Forces acting on the single mass - axial model

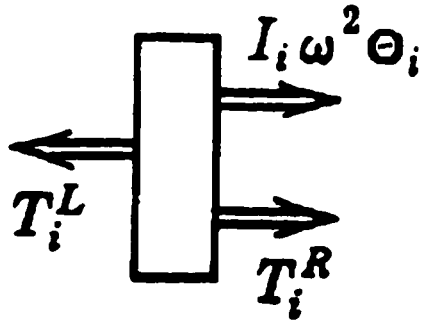

Figure A-1 Forces acting on the single mass - torsional model

Compatibility. Masses in the discrete model are assumed absolutely rigid and

undeformable. Thus, complex displacements on both, left and right, sides of the mass (Figure A-1) are equal:

$$\begin{aligned} \bar{x}_i^R &= \bar{x}_i^L \\ \bar{X}_i^R &= \bar{X}_i^L \end{aligned} \qquad \text{(A-1)}$$

In Figure A-2, torsional model is shown with forces acting on the left and right side of the rotary inertia. Derivation of the point matrices for axial and torsional are similar. Compatibility and equilibrium matrices, as well as equations for torsional system differ from the axial system only in notation.

Equilibrium. Forces, however, depend on physical characteristics of the mass (i.e. its inertia, damping and absolute stiffness forces) and on applied external forces (Figure A-1 and A-3). Equilibrium equation for the rigid-mass element can thus be expressed as:

$$\begin{aligned} N_i^R &= N_i^L + m_i\ddot{x}_i + r_i\dot{x} + k_i^a x_i - F_i \\ \bar{N}_i^R &= \bar{N}_i^L - m_i p^2 \omega^2 \bar{X}_i + jpr_i\omega \bar{X}_i + k_i^a \bar{X}_i - \bar{F}_i \end{aligned} \qquad \text{(A-2)}$$

This equation considers complex amplitudes of the forces acting on the mass. The complex amplitude of the resultant force on the right and left side of the mass depends on:

- complex amplitude of the acceleration forces,
- complex amplitude of the damping forces,
- complex amplitude of the absolute stiffness forces,
- complex amplitude of the external forces.

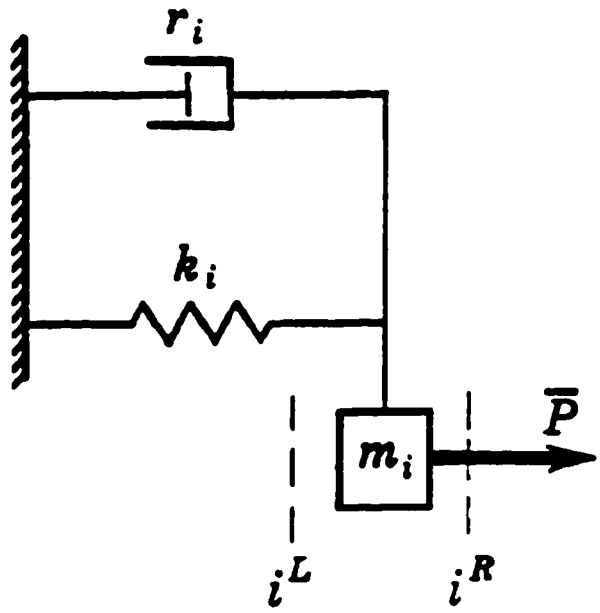

Figure A-3 Absolute stiffness and damping - axial model

A.1.2. **Matrix Representation**

Complex equations are expressed in matrix form. Two vectors are state

vectors defining conditions on the right and left side of the mass, and 3x4 matrix is the point transfer matrix.

$$\begin{bmatrix} \bar{X} \\ \bar{N} \\ 1 \end{bmatrix}_i^R = \begin{bmatrix} 1 & 0 & 0 \\ jpr\omega - mp^2\omega^2 + k^a & 1 & -\bar{F} \\ 0 & 0 & 1 \end{bmatrix}_i \begin{bmatrix} \bar{X} \\ \bar{N} \\ 1 \end{bmatrix}_i^L \tag{A-3}$$

This matrix equation can be symbolically represented as:

$$\{z\}_i^R = [P]_i \{z\}_i^L \tag{A-4}$$

In order to separate real part of the matrix from its imaginary part, the following is applied:

$$\begin{bmatrix} \bar{X} \\ \bar{N} \\ 1 \end{bmatrix}_i^R = \left(\begin{bmatrix} 1 & 0 & 0 \\ -mp^2\omega^2 + k^a & 1 & -F^{Re} \\ 0 & 0 & 1 \end{bmatrix}_i + j \begin{bmatrix} 0 & 0 & 0 \\ rp\omega & 0 & -F^{Im} \\ 0 & 0 & 0 \end{bmatrix} \right) \begin{bmatrix} \bar{X} \\ \bar{N} \\ 1 \end{bmatrix}_i^L \tag{A-5}$$

For further expansion of the above equation, the following derivation is introduced:

$$\begin{aligned} [\bar{P}] &= [P^{Re}] + [P^{Im}] \\ \{\bar{z}\}_i^R &= [\bar{P}]_i \{\bar{z}\}_i^L \end{aligned} \tag{A-6}$$

$$(z^{Re}+jz^{Im})_i^R = (P^{Re}+jP^{Im})_i(z^{Re}+jz^{Im})_i^L$$
$$(z^{Re}+jz^{Im})_i^R = P^{Re}z^{Re}-P^{Im}z^{Im}+j(P^{Im}z^{Re}+P^{Re}z^{Im}) \quad \text{(A-7)}$$

$$\begin{bmatrix} z^{Re} \\ z^{Im} \end{bmatrix}_i^R = \begin{bmatrix} P^{Re} & -P^{Im} \\ P^{Im} & P^{Re} \end{bmatrix}_i \begin{bmatrix} z^{Re} \\ z^{Im} \end{bmatrix}_i^L \quad \text{(A-8)}$$

or in complex notation:

$$\begin{bmatrix} \bar{z} \\ 1 \end{bmatrix}_{i+1}^L = \begin{bmatrix} \bar{P} & 0 \\ 0 & 1 \end{bmatrix}_i \begin{bmatrix} \bar{z} \\ 1 \end{bmatrix}_i^R \quad \text{(A-9)}$$

Axial System. The equation (A-2) can now be rewritten:

$$\begin{bmatrix} X^{Re} \\ N^{Re} \\ X^{Im} \\ N^{Im} \\ 1 \end{bmatrix}_i^R = \begin{bmatrix} 1 & 0 & 0 & 0 & 0 \\ -mp^2\omega^2+k^a & 1 & -rp\omega & 0 & -F^{Re} \\ 0 & 0 & 1 & 0 & 0 \\ rp\omega & 0 & -mp^2\omega^2+k^a & 1 & -F^{Im} \\ 0 & 0 & 0 & 0 & 1 \end{bmatrix}_i \begin{bmatrix} X^{Re} \\ N^{Re} \\ X^{Im} \\ N^{Im} \\ 1 \end{bmatrix}_i^L \quad \text{(A-10)}$$

Torsional System. For the torsional system, the matrix would be described as:

$$\begin{bmatrix} \theta^{Re} \\ T^{Re} \\ \theta^{Im} \\ T^{Im} \\ 1 \end{bmatrix}_i^R = \begin{bmatrix} 1 & 0 & 0 & 0 & 0 \\ -Ip^2\omega^2+k^a & 1 & -rp\omega & 0 & -M^{Re} \\ 0 & 0 & 1 & 0 & 0 \\ rp\omega & 0 & -Ip^2\omega^2+k^a & 1 & -M^{Im} \\ 0 & 0 & 0 & 0 & 1 \end{bmatrix}_i \begin{bmatrix} \theta^{Re} \\ T^{Re} \\ \theta^{Im} \\ T^{Im} \\ 1 \end{bmatrix}_i^L \quad \text{(A-11)}$$

A.1.3. **Excitation Forces**

As demonstrated in calculation of the engine excitation, periodic force is expanded into series of sine and cosine harmonic components by Fourier series analysis (A-12).

The response will be computed for any harmonic component whose order is designated as p, on each cylinder i with phase angle α_i from the reference cylinder.

$$f = \sum_{p=1}^{k} \left(F^c \cos(p\,\omega\,t + p\,\alpha_i) + F^s \sin(p\,\omega\,t + p\,\alpha_i) \right) \tag{A-12}$$

$$\begin{aligned}
f_p^{Re} &= F_p^s \sin[p(\omega t + \alpha_i)] + F_p^c \cos[p(\omega t + \alpha_i)] \\
f_p^{Re} &= Re\,[\bar{F}_p\, e^{jp(\omega t + \alpha_i)}] \\
\bar{F}_p &= F_p^{Re} + j F_p^{Im} \\
f_p^{Re} &= Re\,\{ F_p^{Re} \cos[p(\omega t + \alpha_i)] - F_p^{Im} \sin[p(\omega t + \alpha_i)] \\
&\quad + j(F_p^{Im} \cos[p(\omega t + \alpha_i)] + F_p^{Re} \sin[p(\omega t + \alpha_i)] \} \\
f_p^{Re} &= F_p^{Re} \cos[p(\omega t + \alpha_i)] - F_p^{Im} \sin[p(\omega t + \alpha_i)]
\end{aligned} \tag{A-13}$$

Since excitation is a real value, its application to the system expressed by complex notation needs adjustment; i.e. real force must be related to the real part of the

complex force. This procedure is formulated below for single harmonic p on cylinder i. The real part of the force is separated and then extracted from the total force. Comparing (A-12) and (A-13) the following relation is obtained:

$$F^c = F^{Re}$$
$$F^s = -F^{Im} \qquad \text{(A-14)}$$

The purpose of these equation rearrangements is to deal with the possibility of simultaneous application of excitation forces on all cylinders regardless of phase shift among them.

The notation in (A-13) is simplified by introducing two new variables, a and b, which represent sine and cosine values of the phase angles, respectively.

$$a = \cos(p\,\alpha_i)$$
$$b = \sin(p\,\alpha_i) \qquad \text{(A-15)}$$

Now, equation (A-13) becomes:

$$f_p^{Re} = (F_p^{Re} b + F_p^{Im} a)\cos(p\,\omega\,t) + (F_p^{Re} a + F_p^{Im} b)\sin(p\,\omega\,t) \qquad \text{(A-16)}$$

Components of the forces to add to the point matrix are:

$$f_p^{Re} = F_p^c \cos(p\,\alpha_i) + F_p^s \sin(p\,\alpha_i)$$
$$f_p^{Im} = -F_p^c \sin(p\,\alpha_i) + F_p^s \cos(p\,\alpha_i) \qquad \text{(A-17)}$$

A.2. THE FIELD MATRIX

A.2.1. General Concept

Figure A-4 Spring model

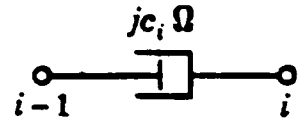

Figure A-5 Damper model

The field matrix is developed for different 'types' of massless elastic elements:

- simple spring element, and
- dissipating element (damper).

These two elements are shown in Figure (A-4) and Figure (A-5) and they can be arranged in spring-damper parallel or spring-damper series connection.

A.3. SPRING-DAMPER PARALLEL CONNECTION

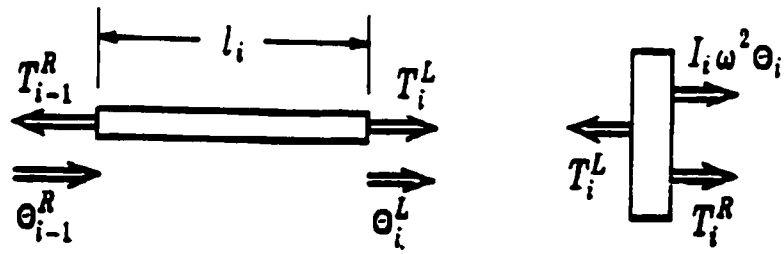

Figure A-6 Torques and displacements - torsional system

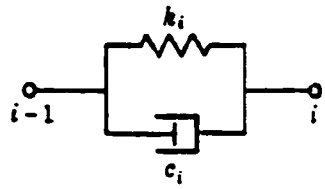

Figure A-7 Spring-damper parallel connection

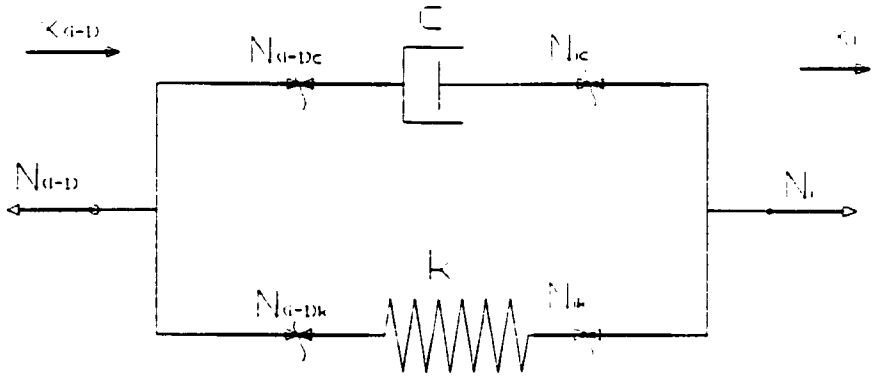

Figure A-8 Forces and displacements - axial system

A.3.1. **Compatibility and Equilibrium Conditions**

Boundary conditions at both ends of the spring-damper aggregate are described in Figure A-8, and defined by (A-18) and (A-19).

$$N_{i+1}^{L} = N_i^{R}$$
$$\bar{N}_{i+1}^{L} = \bar{N}_i^{R} \qquad \text{(A-18)}$$

Torsional Vibration System. Figure A-6 shows for field transfer matrix torsional vibration model. *R* and *L* are, respectively, abbreviations for the right masses to which the field element is connected. Positive direction of the torques and angular amplitudes is shown in Figure A-6, and it corresponds to adopted sign convention. Development of the matrices is similar for torsional and axial systems.

Axial Vibration System. Figures A-7 and A-8 show the axial field element, for which the derivation of the field matrix is presented.

Equilibrium. Forces relation between two end points of the spring-damper is given by (A-18).

Compatibility. Relationship between displacements at both boundaries is:

$$N_{i+1}^{L} = k_i(x_{i+1}^{L} - x_i^{R}) + c_i(\dot{x}_{i+1}^{L} - \dot{x}_i^{R})$$
$$\bar{N}_{i+1}^{L} = k_i(\bar{X}_{i+1}^{L} - \bar{X}_i^{R}) + j\omega c_i(\bar{X}_{i+1}^{L} - \bar{X}_i^{R}) \qquad \text{(A-19)}$$
$$\bar{X}_{i+1}^{L} = \bar{X}_i^{R} + \frac{\bar{N}_i^{R}}{k_i + j\omega c_i}$$

A.3.2. **Matrix Representation**

Arranging equations (A-18) and (A-19) in the matrix form, end state vector on the left side of the mass $i+1$ will be:

$$\begin{bmatrix} \bar{X} \\ \bar{N} \\ 1 \end{bmatrix}_{i+1}^{L} = \begin{bmatrix} 1 & \frac{1}{k+jp\omega c} & 0 \\ 0 & 1 & 0 \\ 0 & 0 & 1 \end{bmatrix}_i \begin{bmatrix} \bar{X} \\ \bar{N} \\ 1 \end{bmatrix}_i^{R} \qquad \textbf{(A-20)}$$

This matrix equation can be symbolically expressed as:

$$\{z\}_{i+1}^{L} = [F]_i \{z\}_i^{R} \qquad \textbf{(A-21)}$$

Considering similar principle as applied for point matrix in (A-6) to (A-9), the field matrix can be expanded into real and imaginary parts (A-22). Final forms of matrices for axial and torsional systems are given by (A-23) and (A-24), respectively.

$$\begin{bmatrix} \bar{X} \\ \bar{N} \\ 1 \end{bmatrix}_{i+1}^{L} = \left(\begin{bmatrix} 1 & \frac{k}{k^2+p^2\omega^2c^2} & 0 \\ 0 & 1 & 0 \\ 0 & 0 & 1 \end{bmatrix} + j \begin{bmatrix} 0 & -\frac{p\omega c}{k^2+p^2\omega^2c^2} & 0 \\ 0 & 0 & 0 \\ 0 & 0 & 0 \end{bmatrix} \right)_i \begin{bmatrix} \bar{X} \\ \bar{N} \\ 1 \end{bmatrix}_i^{R} \qquad \textbf{(A-22)}$$

Axial System

$$\begin{bmatrix} X^{re} \\ N^{Re} \\ X^{Im} \\ N^{Im} \\ 1 \end{bmatrix}_{i+1}^{L} = \begin{bmatrix} 1 & \frac{k}{k^2+p^2\omega^2c^2} & 0 & \frac{p\omega c}{k^2+p^2\omega^2c^2} & 0 \\ 0 & 1 & 0 & 0 & 0 \\ 0 & -\frac{p\omega c}{k^2+p^2\omega^2c^2} & 1 & \frac{k}{k^2+p^2\omega^2c^2} & 0 \\ 0 & 0 & 0 & 1 & 0 \\ 0 & 0 & 0 & 0 & 1 \end{bmatrix}_{i} \begin{bmatrix} X^{re} \\ N^{Re} \\ X^{Im} \\ N^{Im} \\ 1 \end{bmatrix}_{i}^{R} \qquad \text{(A-23)}$$

Torsional System

$$\begin{bmatrix} \theta^{re} \\ T^{Re} \\ \theta^{Im} \\ T^{Im} \\ 1 \end{bmatrix}_{i+1}^{L} = \begin{bmatrix} 1 & \frac{k}{k^2+p^2\omega^2c^2} & 0 & \frac{p\omega c}{k^2+p^2\omega^2c^2} & 0 \\ 0 & 1 & 0 & 0 & 0 \\ 0 & -\frac{p\omega c}{k^2+p^2\omega^2c^2} & 1 & \frac{k}{k^2+p^2\omega^2c^2} & 0 \\ 0 & 0 & 0 & 1 & 0 \\ 0 & 0 & 0 & 0 & 1 \end{bmatrix}_{i} \begin{bmatrix} \theta^{re} \\ T^{Re} \\ \theta^{Im} \\ T^{Im} \\ 1 \end{bmatrix}_{i}^{R} \qquad \text{(A-24)}$$

A.4. SPRING-DAMPER SERIAL CONNECTION

A.4.1. General

An intermediate stage *m* is introduced, and the transfer matrix is developed in two stages:

- for the spring, and

- for the damper element.

A.4.2. **Spring Transfer Matrix**

A.4.2.1. *Compatibility and Equilibrium Condition*

Figure A-9 Spring element

Equilibrium of the forces gives:

$$N_i^m = N_i^R$$
$$\bar{N}_i^m = \bar{N}_i^R \qquad \textbf{(A-25)}$$

Compatibility is expressed by:

$$\bar{N}_i^m = k_i(\bar{X}_i^m - \bar{X}_i^R)$$
$$\bar{X}_i^m = \bar{X}_i^R + \frac{\bar{N}_i^m}{k_i} \qquad \textbf{(A-26)}$$

A.4.2.2. *Matrix Representation*

$$\begin{bmatrix} \bar{X} \\ \bar{N} \end{bmatrix}_i^m = \begin{bmatrix} 1 & \frac{1}{k} \\ 0 & 1 \end{bmatrix}_i \begin{bmatrix} \bar{X} \\ \bar{N} \end{bmatrix}_i^R \qquad \textbf{(A-27)}$$

A.4.3. **Damper Transfer Matrix**

A.4.3.1. *Compatibility and Equilibrium Conditions*

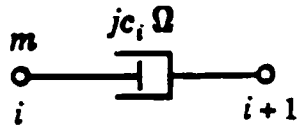

Figure A-10 Damper element

To develop transfer matrix for an element with damping only, (Figure A-10), similar procedure is followed as for the spring element.

Equilibrium:

$$\begin{aligned} N_{i+1}^L &= N_i^m \\ \bar{N}_{i+1}^L &= \bar{N}_i^m \end{aligned} \qquad \textbf{(A-28)}$$

Compatibility:

$$\begin{aligned} N_{i+1}^L &= c_i(\dot{x}_{i+1}^L - \dot{x}_i^m) \\ \bar{X}_{i+1}^L &= \bar{X}_i^m + \frac{\bar{N}_{i+1}^L}{jp\omega c_i} \end{aligned} \qquad \textbf{(A-29)}$$

A.4.3.2. *Matrix Representation*

$$\begin{bmatrix} \bar{X} \\ \bar{N} \end{bmatrix}_{i+1}^{L} = \begin{bmatrix} 1 & \frac{1}{jp\omega c} \\ 0 & 1 \end{bmatrix}_i \begin{bmatrix} \bar{X} \\ \bar{N} \end{bmatrix}_i^{m} \tag{A-30}$$

A.4.4. **Field Matrix Assembly**

$$\begin{bmatrix} \bar{X} \\ \bar{N} \\ 1 \end{bmatrix}_{i+1}^{L} = \begin{bmatrix} 1 & \frac{1}{k} + \frac{1}{jp\omega c} & 0 \\ 0 & 1 & 0 \\ 0 & 0 & 1 \end{bmatrix}_i \begin{bmatrix} \bar{X} \\ \bar{N} \\ 1 \end{bmatrix}_i^{R} \tag{A-31}$$

These two elements can be linked together by simple substitution; i.e. in the equation for the spring element the intermediate state vector $\{z\}^m$ can be substituted with $\{z\}^m$ that is derived for damper element. The result of this substitution is shown in (A-31) and (A-32).

$$\begin{bmatrix} \bar{X} \\ \bar{N} \\ 1 \end{bmatrix}_{i+1}^{L} = \begin{bmatrix} 1 & \frac{1}{jp\omega c} & 0 \\ 0 & 1 & 0 \\ 0 & 0 & 1 \end{bmatrix}_i \begin{bmatrix} 1 & \frac{1}{k} & 0 \\ 0 & 1 & 0 \\ 0 & 0 & 1 \end{bmatrix}_i \begin{bmatrix} \bar{X} \\ \bar{N} \\ 1 \end{bmatrix}_i^{R} \tag{A-32}$$

The matrix is further rearranged, according to expansion shown in equations (A-6) to (A-9), into the form:

$$\begin{bmatrix} X^{Re} \\ N^{Re} \\ X^{Im} \\ N^{Im} \\ 1 \end{bmatrix}_{i+1}^{L} = \begin{bmatrix} 1 & \frac{1}{k} & 0 & \frac{1}{p\omega c} & 0 \\ 0 & 1 & 0 & 0 & 0 \\ 0 & -\frac{1}{p\omega c} & 1 & \frac{1}{k} & 0 \\ 0 & 0 & 0 & 1 & 0 \\ 0 & 0 & 0 & 0 & 1 \end{bmatrix}_{i} \begin{bmatrix} X^{Re} \\ N^{Re} \\ X^{Im} \\ N^{Im} \\ 1 \end{bmatrix}_{i}^{R} \qquad \text{(A-33)}$$

A.5. DAMPING CHARACTERISTICS

The biggest unknown in vibration analysis is damping, which is present in all oscillatory systems as an entropy appreciable as a dissipated heat.

There is still no simple and effective method for inclusion of damping calculation. Most of the presently used damping factors are strictly limited to certain type of dynamic systems and error can be significant if appropriate damping is not used. This damping is usually estimated by measurements and measured values are statistically processed.

In the developed program for vibration calculation following damping types are considered here:

- constant damping (where damping is not a function of frequency) and
- frequency dependent damping.

The above mentioned damping can be further classified as:

- absolute damping, which usually refers to Coulomb damping or friction between mass and surrounding structure. It is usually related to the system inertias (point matrix).

- relative damping, which occurs due to inter-structural friction or energy dissipation within the elastic elements of the system.

The constant damping can be expressed as dimensional value (in [Nms/rad] for torsional damping or in [Ns/m] for longitudinal vibrations), or as dimensionless factor.

Damping factor is preferably used, especially due to lack of an accurate damping calculation method. Moreover, damping coefficient does not depend on geometry, or physical characteristics of the respective dissipative element, and it is therefore applicable for the classes of elements which have higher damping characteristics.

A.5.1. Constant Damping

Constant damping means that the damping force (torque) will be a function of the exciting frequency. This follows from the solution of the second order differential equation of motion, and it is shown in (A-34)

$$\bar{F}_d = j\,\omega\, c\, \bar{X} e^{j\omega t} \qquad \text{(A-34)}$$

where c is a constant ($c \neq c(\omega)$).

A.5.2. **Frequency dependent damping**

If damping c is a function of the frequency of vibration, as presented below, then damping force becomes free of exciting frequency. This particular damping can be referred to as structural damping, and it also represents the damping behavior of some commercial dampers.

$$c = k\frac{\zeta}{\omega} \tag{A-35}$$

In this formulation k is damper's stiffness (or spring constant if the structural damping is considered), ζ is non-dimensional damping coefficient, and ω is forced frequency of the system.

Damping force is not a function of the exciting frequency any more; it depends only on the spring constant and on the constant damping coefficient ζ.

$$\bar{F}_d = j k \zeta \bar{X} e^{j\omega t} \tag{A-36}$$

A.5.3. **Complex Impedance**

By analogy with complex impedance in electric theory, the complex impedance or complex stiffness in mechanical systems is defined as:

for spring and damper in parallel, and

$$\bar{z} = k + jp\omega c \tag{A-37}$$

$$\bar{z} = \frac{1}{\frac{1}{k} + \frac{1}{jp\omega c}} \tag{A-38}$$

for spring-damper combination in series.

A.5.4. **Admittance**

Reciprocal value of impedance is called admittance and in analogy with that, complex admittance or complex flexibility is defined as:

$$\bar{a} = \frac{1}{k + jp\omega c} \tag{A-39}$$

for spring and damper in parallel, and

$$\bar{a} = \frac{1}{k} - j\frac{1}{p\omega c} \tag{A-40}$$

for spring-damper in series.

When structural damping is applied in the form expressed in equation (A-34), then (A-37) and (A-38) will become for spring-damper in parallel:

$$\bar{z} = k(1 + jg) \tag{A-41}$$

and for spring-damper in series:

$$\bar{z} = \frac{k}{1 - j\frac{1}{g}} \tag{A-42}$$

After applying structural damping formulation, field matrices become independent of the excitation frequency, provided that excitation phase-shift is constant over entire frequency range[1].

A.6. FORCED VIBRATION SOLUTION

A.6.1. Open System

Once point and field matrices are defined, the system can be solved by simple chain multiplication of the point and field transfer matrices.

$$\{\bar{z}\}_n^R = [\bar{P}]_n \prod_{i=1}^{n-1} [\bar{F}]_i [\bar{P}]_i \{\bar{z}\}_1^L \tag{A-43}$$

[1] Similar relation can be established for the inertia matrix when damping can be treated as a function of forced frequency.

A.6.1.1. *Torsional Vibration*

Propulsion system is an open system (semi-definite system) from the torsional point of view. For an open system the first natural frequency is zero, i.e. the system is behaving as a rigid body.

Formulation of the problem as presented in equation (A-43) is valid for systems that have unrestrained inertias on their free ends. Therefore state vectors are defined for the free-end side of the end inertias.

A.6.1.2. *Axial Vibration*

Using the same system for torsional and axial vibration was made possible by adding absolute stiffness and absolute damping to the inertia matrix. Therefore, as presented in Figure A-11, system can be restrained for axial vibration calculation at any point within the system. At the same time constraints applied on the free-ends of the end masses can be preserved as if they were for torsional vibration.

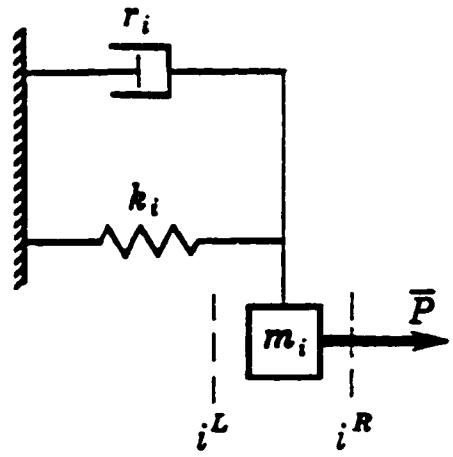

Figure A-11 Axial system

A.6.1.3. *Boundary Conditions, Constraints*

It is easy to conclude that unrestrained free ends of the system will bear no resistance to the forces acting on the system, and therefore the first and the last state vector will look as presented below (only appropriate indices need to be applied):

$$\{z\} = \{ X^{Re}, 0, X^{Im}, 0, 1 \}$$

The second and the fourth element of the end-state vector, which represents the forces, are zero, and only displacements are left to be found. There are four unknown displacements, two at each end of the system, and four equations necessary to calculate them are known after the transfer matrix multiplication for the whole system is done.

A.6.1.4. *System Transfer Matrix*

The solution to the transfer matrix multiplication in the Equation (A-43) is a square 5x5 matrix which is called the system transfer matrix. This matrix contains in it complete information about the dynamic system between two free ends.

For particular excitation frequency, and with known boundary conditions solution to the dynamic system can be found by calculating end displacements first. End displacements can be obtained as shown below:

$$\begin{bmatrix} X^{Re} \\ 0 \\ X^{Im} \\ 0 \\ 1 \end{bmatrix}_n^L = \begin{bmatrix} a11 & a12 & a13 & a14 & 0 \\ a21 & a22 & a23 & a24 & 0 \\ a31 & a32 & a33 & a34 & 0 \\ a41 & a42 & a43 & a44 & 0 \\ 0 & 0 & 0 & 0 & 1 \end{bmatrix}_i \begin{bmatrix} X^{Re} \\ 0 \\ X^{Im} \\ 0 \\ 1 \end{bmatrix}_1^R \tag{A-45}$$

Four equations necessary for solution are:

$$\begin{aligned} X_n^{Re} &= a11 * X_1^{Re} + a13 * X_1^{Im} \\ 0 &= a21 * X_1^{Re} + a23 * X_1^{Im} \\ X_n^{Im} &= a31 * X_1^{Re} + a33 * X_1^{Im} \\ 0 &= a41 * X_1^{Re} + a43 * X_1^{Im} \end{aligned} \tag{A-46}$$

Finally, knowing end-state-vectors displacement and forces, state vector can be found at any station k within the system by simple multiplication:

$$\{\bar{z}\}_k^R = [\bar{P}]_k \prod_{i=1}^{k-1} [\bar{F}]_i [\bar{P}]_i \{\bar{z}\}_1^L \tag{A-47}$$

The following Appendix B presents the theoretical basis for finite element method which is applied for calculation of torsionally induced axial vibration.

APPENDIX B

FINITE ELEMENT METHOD

B.1. FORMULATION FOR SINGLE FINITE ELEMENT

The definition of equation of motion for one finite element will contain all expressions in tensor and matrix formulation. Kinetic energy for a finite element of volume V is defined by relations (B-1) and (B-2) in tensor and matrix notation respectively as:

$$T = \frac{1}{2}\int_{(V)} \rho \; u_{i,t} \; u_{k,t} \; dV \qquad \textbf{(B-1)}$$

$$T = \frac{1}{2}\int_{(V)} \rho \; \{u_{,t}\}^T \; \{u_{,t}\} \; dV \qquad \textbf{(B-2)}$$

Non-conservative damping forces are given by:

$$D_i = -c\, u_{i,t} \qquad \{D\} = -[c]\,\{u_{,t}\} \tag{B-3}$$

Total potential energy is the sum of strain energy, and potential energy due to external forces:

$$\Pi = U + V \tag{B-4}$$

which are expressed as:

$$U = \frac{1}{2}\int_{(V)} \varepsilon_{ij}\,\sigma_{ij}\,dV \qquad U = \frac{1}{2}\int_{(V)} \{\sigma\}^T\{\varepsilon\}\,dV \tag{B-5}$$

$$V = -\int_{(V)} f_i\,u_i\,dV - \int_{(S_t)} t_i\,u_i\,dS \qquad V = -\int_{(V)} \{f\}^T\{u\}\,dV - \int_{(S_t)} \{t\}^T\{u\}\,dS \tag{B-6}$$

where strain and potential energy developed due to body forces is defined over the volume V of an element, and the potential energy developed due to traction forces is

defined over portion of the surface[2] S_t where traction is prescribed.

Transforming these equations into variational notation the following equilibrium equation, presented in tensor notation, is obtained:

$$\int_{t_1}^{t_2}\left(\int_{(V)}(\rho\, u_{i,s}\,\delta u_{k,s} + f_i\,\delta u_i - \sigma_{nm}\,\delta\varepsilon_{nm})\,dV - \int_{(S_t)} t_s\,\delta u_s\,dS\right)dt - \int_{t_1}^{t_2}\left(\int_{(V)} c\,u_{p,s}\,\delta u_{r,s}\,dV\right)dt = 0 \qquad \textbf{(B-7)}$$

B.1.1. **Equation of Motion in FEM Notation**

From the theory of linear elasticity (see Timoshenko and Goodier (1972)), the variation of the strain vector developed in elastic body can be defined as the product of a transposed matrix of linear operators and variation of the displacement vector as given by:

$$\delta\{\varepsilon\} = [d]^T\,\delta\{u\} \qquad \textbf{(B-8)}$$

A linear operator [d] is a matrix of partial derivatives that yields from element's equilibrium equation (B-9), shown in tensor notation. Transpose of the same

---

[2] Surface S of an element is defined as a sum of the surfaces where displacements are prescribed, S_u, and the portion of the surface where tension is prescribed, S_t.

matrix of linear operators satisfies compatibility equation (B-10). The shape of the matrix [d] depends on the nature of the problem to be solved:

$$\sigma_{ij,i} + f_i = 0 \tag{B-9}$$

$$\varepsilon_{ij} = \frac{1}{2}\left(u_{i,j} + u_{j,i}\right) \tag{B-10}$$

Following the finite element method and Hamilton's variational principle, displacement field variation {u} is represented here as the product of the shape function [N] and element's nodal displacements vector variation {q}:

$$\delta\{u\} = [N]\,\delta\{q\} \tag{B-11}$$

Matrix [B] is introduced to define shape function derivatives. The matrix formulates the strain as a function of generalized displacements as:

$$\begin{aligned} [B] &= [d][N] \\ \delta\{\varepsilon\} &= [B]\,\delta\{q\} \end{aligned} \tag{B-12}$$

Applying Hook's law the relationship between stress and strain fields is defined by the elasticity matrix [E] as shown by:

$$\{\sigma\} = [E]\{\varepsilon\} \tag{B-13}$$

Substitution of (B-13) back into equations for total potential energy, kinetic energy, and work done by non-conservative forces, yields the following equations.

Total potential energy:

$$\begin{aligned}\delta\Pi = \delta\{q\}^T\left(\int_{(V)}[B]^T[E][B]\,dV\right)\{q\} \\ - \delta\{q\}^T\int_{(V)}\left([B]^T[E]\{\varepsilon_o\} - [B]^T\{\sigma_o\}\right)dV \\ - \delta\{q\}^T\int_{(V)}[N]^T\{f\}\,dV - \delta\{q\}^T\int_{(S_t)}[N]^T\{t\}\,dS\end{aligned} \tag{B-14}$$

Kinetic energy:

$$\delta T = \delta\{q_{,t}\}^T\left(\int_{(V)}\rho[N]^T[N]dV\right)\{q_{,t}\} \tag{B-15}$$

Damping energy:

$$\delta W_d = \delta\{u_{,t}\}^T\{D\} \tag{B-16}$$

Damping force is:

$$\{D\} = -\int_{(V)} [c]\ \{u_{,t}\}\, dV \tag{B-17}$$

$$\{D\} = -\int_{(V)} [N]^T [c]\ [N]\, dV\, \{q_{,t}\} \tag{B-18}$$

Potential, kinetic and dissipation energy can be derived as in (B-19), (B-20) and (B-21), with equilibrium condition satisfied, and velocity derivative of total potential energy and the displacement derivative of kinetic energy (B-19), are zero.

$$\frac{\partial \Pi}{\partial q_{i,t}} = 0 \qquad \frac{\partial T}{\partial q_i} = 0 \tag{B-19}$$

$$\frac{\partial T}{\partial q_{i,t}} = \left(\int_{(V)} \rho\, [N]^T [N]\, dV \right) \{q_{,t}\} \tag{B-20}$$

$$\frac{d}{dt}\left(\frac{\partial T}{\partial q_{i,t}} \right) = \left(\int_{(V)} \rho\, [N]^T\, [N]\, dV \right) \{q_{,tt}\} \tag{B-21}$$

$$\frac{\partial W_d}{\partial q_{i,t}} = -\int_{(V)} [N]^T [c]\ [N]\, dV\, \{q_{,t}\} \tag{B-22}$$

$$\frac{\partial \Pi}{\partial q_i} = \left(\int_{(V)} [B]^T [E][B] dV \right) \{q\} - \int_{(V)} \left([B]^T [E] \{\varepsilon_o\} - [B]^T \{\sigma_o\} \right) dV - \int_{(V)} [N]^T \{f\} dV - \int_{(S)} [N]^T \{t\} dS \tag{B-23}$$

From the above formulation, expressions (B-24), (B-25) and (B-26) can be extracted, respectively representing mass (inertia), damping, stiffness and force matrices for a single finite element.

Mass matrix:

$$[m] = \int_{(V)} \rho [N]^T [N] dV \tag{B-24}$$

Damping matrix[3]:

$$[c] = \int_{(V)} [N]^T [C] [N] dV \tag{B-25}$$

Stiffness matrix:

$$[k] = \int_{(V)} [B]^T [E] [B] dV \tag{B-26}$$

[3] Damping matrix is usually not created on the element basis, but generated directly for the whole system.

Forces acting on the element can be further expanded into:

Initial strain-stress forces

$$\{Q_i\} = \int_{(V)} [B]^T [E] \{\varepsilon_0\} dV - \int_{(V)} [B]^T \{\sigma_0\} dV \qquad \textbf{(B-27)}$$

Body-forces

$$\{Q_b\} = \int_{(V)} [N]^T \{f\} dV \qquad \textbf{(B-28)}$$

Surface-forces (traction)

$$\{Q_s\} = \int_{(S)} [N]^T \{t\} dS \qquad \textbf{(B-29)}$$

Finally, the Lagrange equation of motion for one finite element becomes:

$$\begin{gathered} [m^{(e)}]\{q_{,tt}\} + [c^{(e)}]\{q_{,t}\} + [k^{(e)}]\{q\} = \sum_{k=1}^{p} \{Q_k^{(e)}\} \\ [Q^{(e)}] = \sum_{k=1}^{p} \{Q_k^{(e)}\} \end{gathered} \qquad \textbf{(B-30)}$$

Force matrix is here presented as a sum of p force vectors. Response {q} can be calculated directly on all p vectors, or as $\{q_k\}$ on each particular excitation vector separately where total response {q} is a sum of all p individual responses.

Generalized displacement, {q}, and its time derivatives, have dimension that corresponds to the number of degrees of freedom of an element. Indices corresponding to nodal degree of freedom are unique for each node.

Having developed equations of motion for each particular element of the structure the next step is to assemble them to represent the complete structure.

B.1.2. **Assembly of System's Equation of Motion**

Assembly procedure for the equation of motion of the whole structure is based on construction of the system's mass, damping and stiffness matrices. The procedure is actually an algebraic addition of the matrix components, ensuring nodal connectivity conditions. Therefore, in the following equation the summation symbol represents addition over identical nodal indices (degrees of freedom) of each finite element.

$$[M] = \sum_{e=1}^{n} [m^{(e)}]$$
$$[K] = \sum_{e=1}^{n} [k^{(e)}] \qquad \textbf{(B-31)}$$

Force vector matrices can be created on the element level or global level, depending on the specific problem. Forces and moment acting in the direction of the particular degrees of freedom will carry their indices and be placed on appropriate

location in the load matrix.

Finally the system equation of motion will be:

$$[M]\{q_{,tt}\} + [C]\{q_{,t}\} + [K]\{q\} = [Q] \qquad \textbf{(B-32)}$$

B.2. **FORCED RESPONSE ANALYSIS**

Forced vibration analysis of the structure discretized as finite elements is carried out by solving the following equation of motion:

$$[M]\{q_{,tt}\} + [C]\{q_{,t}\} + [K]\{q\} = [Q] \qquad \textbf{(B-33)}$$

The equation of motion is assumed to be linear, and elements of the mass matrix [M], damping matrix [C], and stiffness matrix [K] are constant.

The forced response calculation can be performed either by the direct method or by the mode superposition method. The choice between the two will depend on the form of matrices [M] and [K], on damping characteristics of the system, on the number of degrees of freedom or other practical reasons related to the physical character of the system.

Direct method is not sensitive to characteristics of the system matrices [M], [C] and [K], and for calculation of the response no previous transformation of the equations of motion is necessary. The advantage is that calculation of natural frequencies and

modal vectors need not be completed prior to solving the equations for forced response. However, since this is a step by step method, stability and accuracy of the method and computational time will be directly proportional to the applied time step. This method will be particularly effective when response is calculated for a relatively small number of time steps.

Mode superposition method requires original equation of motion to be expressed in terms of the normal coordinates. This results in the uncoupling of equations of motion into a set of independent equations. This method requires modal vectors to be calculated first, so that transformation could be performed. Major disadvantage of this method is in the requirements on the damping matrix, in order to be able to diagonalize the damping matrix.

B.2.1. **Direct Steady State Analysis**

When the excitation is a harmonic function, and only the steady state response is sought, direct method would be the best option since computational time is much shorter than for direct integration method and there is no concern about stability and convergence. In comparison to the mode superposition method, direct analysis does not require previous transformation of the equation of motion.

In general case, harmonic excitation will be a complex one so the response of the system can be written as:

$$[q] = \left[[K] - \omega^2 [M] + i\omega [C] \right]^{-1} [Q]$$

$$[Q] = \sum_{j=1}^{hk} \{ F_j e^{i\omega t} \} \qquad \textbf{(B-34)}$$

Matrix [q] is the collection of all response vectors on each particular harmonic component, and [Q] is a force matrix containing excitation vectors for each harmonic component of the excitation force.

In order to invert the system matrix the following procedure is adopted:

$$[A_R] = [K] - \omega^2 [M] \quad ; \qquad \omega [C] = [A_I]$$

$$\left([A_R] + i[A_I] \right) = [B_R] + [B_I] \qquad \textbf{(B-35)}$$

$$[A_R][B_R] - [A_I][B_I] = [I]$$

$$[A_I][B_R] + [A_R][B_I] = 0 \qquad \textbf{(B-36)}$$

$$[B_R] = -[A_I]^{-1}[A_R][B_I] \qquad \textbf{(B-37)}$$

Manipulating the above equations, imaginary and real components of the inverse systems matrix can be found as follows:

$$[B_I] = -\left([A_I] + [A_R][A_I]^{-1}[A_R]\right)^{-1}$$

$$[B_R] = [A_I]^{-1}[A_R]\left([A_I] + [A_R][A_I]^{-1}[A_R]\right)^{-1} \quad \textbf{(B-38)}$$

The advantage of presented procedure is that there is no need to invert the matrix $[A_R]$, which may be singular when exciting frequency ω, and one of the systems natural frequencies coincide.

The following Appendix C describes the computer software which is designed based on the theory behind the transfer matrix method and the finite element method.

APPENDIX C

SOFTWARE DESIGN

C.1. GENERAL

All calculations in this study are performed with computer software which is specifically designed, entirely by the author, for this thesis.

Two separate programs are created. The first one, based on transfer matrix method (TMM), is used for conventional shafting design; i.e. for analysis of individual (non-coupled) torsional and axial vibrations in the propulsion system. The second program designed for calculation of the torsionally induced axial vibrations, is based on finite element method (FEM) and stiffness matrix method.

Both programs are created using C language, and structured programming, under the DOS and WINDOWS 3.1 operating system platform. TMM and FEM software are respectively compiled with Borland C++, and Turbo C++ compilers on IBM compatible personal computer.

Transfer matrix software requires less memory, but it is more computationally demanding than FEM. For that reason software is created to run under DOS platform.

Finite element software is designed in Turbo C++ under Windows 3.1 operating system which can easily handle memory demanding larger matrices and bigger codes.

Programming is performed using dynamic memory allocation, and therefore the only restriction in the size of the code and data is the capacity of the computer used for calculation.

For the purpose of matrix calculation separate matrix "header" routine is created. The routine performs following matrix operations:

- multiplication
- transposition
- summation
- inversion (Cholesky; Gauss)
- creating zero matrix
- creating unit matrix, and
- matrices printing.

C.2. TRANSFER MATRIX METHOD ALGORITHM

For the calculation of the natural frequencies and forced response of the system four routines are created:

- data preprocessing code
- eigenvalue and forced response calculation
- results post-processing, and
- graphics output code.

All routines function separately, interconnected with input and output data.

Graphics is designed as stand alone software to ensure presentation of results.

C.2.1. **Data Preprocessing**

Data defining the propulsion system are created and stored with minimum possible restrictions. To ensure this, data are preprocessed.

The advantage of data preprocessing:

- reducing the errors in data preparation

- time saving.

Data is organized so as to follow real physical-system. The elastic massless shaft segment is chosen as basic element, instead of mass/inertia that is usually the case. The benefit is that each segment is always bounded with two end masses, which resembles the real physical system, and requires less memory in creating data structure.

Each real shaft segment (building-block, or module) is approximated with discrete lumped model. As the system is lumped, each shaft element is divided into three subelements:

- two node elements (points),

- and one spring element (field).

This is the basic building-block, and system is simply defined by linking as many building-blocks, as desired or necessary. Linkage is performed following a predefined connectivity condition.

C.2.1.1. *The Building-Block*

The basic system, which is developed around the massless elastic shaft segment, will have left and right node where mass/inertia is concentrated.

Left and right node are defined with following data:

- description of the node [string]
- node number [integer]
- inertia [kgm2] , mass [kg]
- absolute damping [Nms/rad] , [Ns]
- absolute flexibility [rad/Nm] , [1/Nm]
- speed ratio [real]
- connectivity number [integer]
- control number [integer]
- description of the load applied [string]
- load type number [integer]
- load phase shift with respect to the first cylinder [deg]

Mass and torsional inertia of the shaft elements are calculated, halved, and added to each of the end nodes of the shaft.

If the building block consists of more than one subsegment, their inertia and mass are summarized for all subsegments within building block and then equally distributed to the end nodes.

Nodal inertia may be entered as zero or any positive number. This inertia

will be increased for:

- additional shaft inertia, and/or
- inertia of the node in contact.

The shaft nodes may be joined in different ways, which are defined by connectivity number. The connectivity number controls whether shaft node is common to more than one shaft, or defined only for this particular building-block.

The Elastic Spring Element

- description [string]
- number of different geometries within an element
- flexibility [rad/Nm] , [1/Nm]
- left diameter [m]
- right diameter [m]
- inner diameter [m]
- length [m]
- relative damping [Nms/rad] , [Ns/m]
- shear modules [N/m2] , elasticity modules [N/m2]
- material density [kg/m3]
- control number [integer]

If flexibility data is entered as zero it will be derived from data describing shaft geometry and physical properties.

There are two possible shaft designs available for flexibility calculations:

- plain shaft

- tapered shaft.

The flexibility of the particular building-block can be calculated from as many subsegments of the shaft as desirable.

Data need not be numerated in any particular order or sorted one after another (as in real,physical system). The preprocessor will sort and renumber the system in ascending order, and preserve data in two output files:

- Binary file (xxx.bin) - used for further processing.

- Output data (xxx.rep) - data prepared for report.

C.2.1.2. *Excitation Data*

C.2.1.2.1.*Engine Excitation*

Engine excitation (harmonic components) are presented in tabular form as a function of indicated pressure and particular harmonic order number.

Harmonic component matrix is developed after real engine's indicated diagram is expanded into sine and cosine series using Fourier transformation. Indicated diagrams are taken at the engine's test bench for a number of different engine loadings (indicated pressures). Using Fourier transformation desired number of harmonics are calculated for each of the load.

Engine excitation is defined below:

- number of engines

- type of engine (defining harmonic components data)

- engine number

- number of cylinders

- 'V' angle

- firing order

- type of load

    .normal firing

    .increased combustion pressure

    .decreased combustion pressure

    .no firing

    .no cylinder head

- load intensity

    .initial load in %

    .end load in %

    .load increment in %

- load definition range

    .initial harmonic-component number

    .end harmonic-component number

    .harmonic increment

- speed definition range

    .initial speed [rpm]

    .end speed [rpm]

    .speed increment [rpm]

- engine structural data

.cylinder bore [m]

.piston stroke (two times crankshaft radius) [m]

.connecting-rod length [m]

.reciprocating masses per cylinder [kg]

.rotating masses [kg]

C.2.1.2.2. *Propeller Excitation*

The propeller excitation is given as variation of the thrust force for axial vibration, and as torque variation for torsional vibration calculation.

The following data describes propeller excitation:

- thrust fluctuation [N], or torque fluctuation [Nm], for axial and torsional analysis respectively

- phase angle [deg]

C.2.2. **Eigenvector and Forced Response Analysis**

The program can calculate both eigenvector and forced response, either separately or together.

Software requires the input data in binary form (created by data preprocessor (xxx.BIN)).

The output results are stored in two files:

- natural frequencies and mode shapes (xxx.OUT)

- forced vibration results (xxx.BAR)

C.2.2.1. *Eigenvector and Eigenvalue Calculation*

Natural frequencies are calculated for selected number of frequencies. If zero is chosen calculation is entirely avoided. Maximum number of frequencies to be calculated equals the number of degrees of freedom of the system.

Algorithm for eigenvalues and eigenvector calculation is iterative procedure based on bi-section method, and is designed as demonstrated in sequence a to i:

a - start a calculation for selected range of frequencies

b - select initial frequency f_{in}

c - $f = f_{in}$

d - calculate eigenvector

e - check eigenvector's number of sign changes to define to which mode eigenvector frequency belongs

f - check if 'f' is within selected range of frequencies, if not repeat with new f_{in}

g - apply bi-section iteration until required precession is achieved. Precession is defined by end torque which need to be smaller than

$$500*N_{mod}^{3}$$

N_{mod} is mode number.

h - preserve eigenvector and eigenvalue

i - if any of lower modes is missed lower 'f' and repeat from d.

C.2.2.2. *Forced Response Calculation*

Forced response is calculated for all required harmonics, and for all speeds selected. Moreover, all resonant speeds (for all harmonics of excitation forces) defined from the calculated eigenvalues, are selected and response is calculated for them, so that maximal response is not omitted.

Response (displacement, forces/torques, and stresses) is calculated for all harmonic orders separately, and all orders summation is performed at the end. Results are preserved in binary file for further processing and graphics output.

The algorithm for forced response calculation is organized as follows:

a - select initial speed and harmonic

b - start speed loop

c - start harmonic loop

d - fill up point and field matrices

e - calculate displacement, force/torque, and stresses

f - preserve results for each harmonic order

g - repeat c until end harmonic is reached

h - synthesize all harmonic orders for current speed

i - save synthesis results

j - repeat speed loop b until end speed is reach

C.2.3. **Results Postprocessing Software**

Postprocessing software is designed to rearrange results of the forced vibration calculation into the form suitable for graphic presentation of the results.

Two files are imported into the program:

- binary output file created by forced response program (xxx.BAR), and
- structural data generated by preprocessing code (xxx.BIN).
- Output files are two groups of three binary files.The first group contains order_by-order calculation data

  xxx.OBS - for stresses file

  xxx.OBT - for torques file

  xxx.OBA - for amplitudes file

the second group of files contains synthesis data

  xxx.SBS - for stress file

  xxx.SBT - for torques file

  xxx.SBA - for amplitudes file

C.2.4. **Graphic Output**

Graphics output program is designed to present results to the screen, and to

create HPGL file which can also be imported by most of word processors.

Program consists of two parts. The first part creates screen and plotter output, and the second one generates ABS, and IACS torsional vibration limits that can be included on screen output or plotter file.

Input data are:

- structural data file data (xxx.BIN)

- two groups of response-files, first set is response on order by order excitation

    xxx.OBS - for stress file

    xxx.OBT - for torques file

    xxx.OBA - for amplitudes file

the second group of files is response on the synthesis calculation

    xxx.SBS - for stress file

    xxx.SBT - for torques file

    xxx.SBA - for amplitudes file

Input data is presented on the screen and/or saved into the plot files for repeated graphics display. Each screen output may be saved as plot file. Program is capable on incorporating stress limits for selected number of Classification Societies (e.g. ABS, IACS).

C.3. FINITE ELEMENT SOFTWARE DESIGN

The finite element software simultaneously calculates axial and torsional system. Displacements, forces/torques, and stresses can be calculated at the same time for both vibration forms. Moreover, if the coupling effect is included, the interaction between torsional and axial vibrations can be obtained as an output too.

For calculation of the torsionally induced vibration coupling input data is organized similar to transfer matrix calculation.

Data can be separated into two parts. The first one defines structural data of the system, and the second part presents excitation. The excitation data input is entirely identical to the TMM data.

The difference in data organization between TMM and FEM is that FEM modelling is arranged so to simultaneously create axial and torsional systems, while the TMM model is only capable to deal with one system at the time.

As finite and conventional elements may be combined, it is necessary to define both sets of data.

Common data are:

- number of FE
- number of conventional elements
- number of loaded nodes
- number of axial supports
- propeller coupling data

.element and node number

.hydrodynamic mass/inertia coupling coefficient

.hydrodynamic damping

.water density

.propeller diameter

C.3.1. **Finite Element Data Structure**

Finite elements data are entered in relation to the number of nodes (i.e. number of element's degrees of freedom). Data is saved into element structure, whose memory is dynamically allocated as a function of the number of elements. Element structure contains nodal substructure whose dimension depends on element's number of degrees of freedom. Distribution of the main parameters throughout the element is defined by interpolation matrix following the FEM principle.

Data for finite elements are organized as follows:

- FE number
- description
- absolute nodal coordinates
- segment diameters [m]
- concentrated nodal mass [kg]
- support conditions

- concentrated nodal mass moments of inertia [kgm2]

- axial nodal damping [Ns/m]

- torsional nodal damping [Nmrad/s]

- connectivity data

- material density [kg/m3]

- modules of elasticity [N/m2]

- shear modules [N/m2]

- nodal load data

C.3.2. **Conventional Element Data Structure**

For convention elements with only two nodes, data structure will resemble the transfer matrix method data organization. Thus, input is arranged around building-blocks which have the element (flexibility) as a basis.

Each building-block is approximated by a discrete - lumped model. As the system is lumped each shaft element structure contains two nodal structures:

- one spring element, and

- two node elements.

This is the basic building-block, and system is simply expanded by following the connectivity requirements and linking as many building-blocks as necessary

The basic system which is developed around the massless elastic shaft segment

will have left and right node where mass/inertia is concentrated, which are defined with following data:

- element number
- description of the node
- node number
- axial stiffness [N/m]
- torsional stiffness [Nm/rad]
- diameter [m]
- concentrated nodal mass [kg]
- support conditions
- concentrated nodal mass moments of inertia [kgm2]
- axial nodal damping [Nm/s]
- torsional nodal damping [Nmrad/s]
- connectivity data
- material density [kg/m3]
- modules of elasticity [N/m2]
- shear modules [N/m2]
- nodal load data

C.3.3. **Eigenvector and Eigenvalue Calculation**

Natural frequencies and modal vectors are calculated (if desired) using Gauss Generalized procedure (as explained in the Appendix B). Damping effect is not included, thus in cases when high frequency dependent damping is present in the system, the real location of the resonances will not match the values obtained by eigenvalues calculation.

C.3.4. **Forced Response Calculation**

In case excitation data are given for steady-state condition, the fastest approach to response calculation will be direct steady-state method (the method is explained in details in Appendix B).

Regardless of the method used, the algorithm for response calculation is as shown:

a - read system data

b - create FE and/or conventional element matrices

c - assembly system stiffness matrix

d - assembly system mass matrix

c - define support condition (if exist) and rearrange system stiffness and mass matrix

d - define propeller coupling condition (if exist) and rearrange system stiffness

and mass matrix

e - calculate eigenvalues and eigenvectors

f - select initial speed

g - start speed loop

h - select initial harmonic

i - start harmonic loop

j - create damping matrix

k - rearrange damping matrix for propeller coupling

l - define excitation matrix

m - rearrange excitation matrix for support condition

n - select time step for one complete excitation cycle

o - calculate reaction in thrust bearing, displacement, force/torque, and stresses

p - preserve results for each harmonic order

r - repeat h loop until end harmonic is reached

s - synthesize all harmonic orders for current speed

t - save synthesis results

u - repeat speed loop g until end speed is reach

C.3.5. **Results Postprocessing Software**

To present results into ready-for-graphics form, the output is saved into three

separate files:

xxx.OBO - force on the thrust bearing for each harmonic order

xxx.SYN - synthesized force on the thrust bearing

xxx.BIN - displacement and stress binary output adopted for further graphic processing.

APPENDIX D

AXIAL VIBRATION MEASUREMENT

Axial vibration measurements[1] presented below have been conducted on the ship with undercritical line shafting design (Chapter III). Measurements were performed on intermediate shaft. This needs to be taken into account while comparing results of measurements with computed solutions, because thrust force is calculated on the thrust bearing.

The recording is performed using strain gauges, with dual channel analyzer at the stationary engine speeds within whole engine speed range. Ship was kept on steady course, and the sea was calm.

From the measurements report only diagram showing propeller thrust variation on the intermediate shaft (Figure D-1), is extracted. Figure D-1 illustrates five dominant harmonic responses, and high dominance of the flank of the 5-th order main resonance. Main resonance for big diameter shafting is located far beyond engine operational speed; i.e. at frequency of 151 [cpm].

It is noticeable that the intensity of the recorded thrust force increases as the engine speed progresses towards nominal engine speed of 111 [rpm]. Resonance of the 10-th order has also a significant peak at 76 [rpm]. The 4-th order forces, which

[1] Presented measurement report is obtained curtesy of Uljanik Shipyard.

correspond to propeller blade frequency, are not high enough to significantly influence the response. However, 7-th and 8-th order torsional resonances are of considerable intensity.

The calculation of the torsionally induced axial vibration in Chapter IV agrees well with presented measurements. Calculation in Chapter IV represents the synthesis where phase shift between particular harmonic responses is not taken into account - responses are linearly summed up. This approximation is normally done in order to preserve higher safety margins.

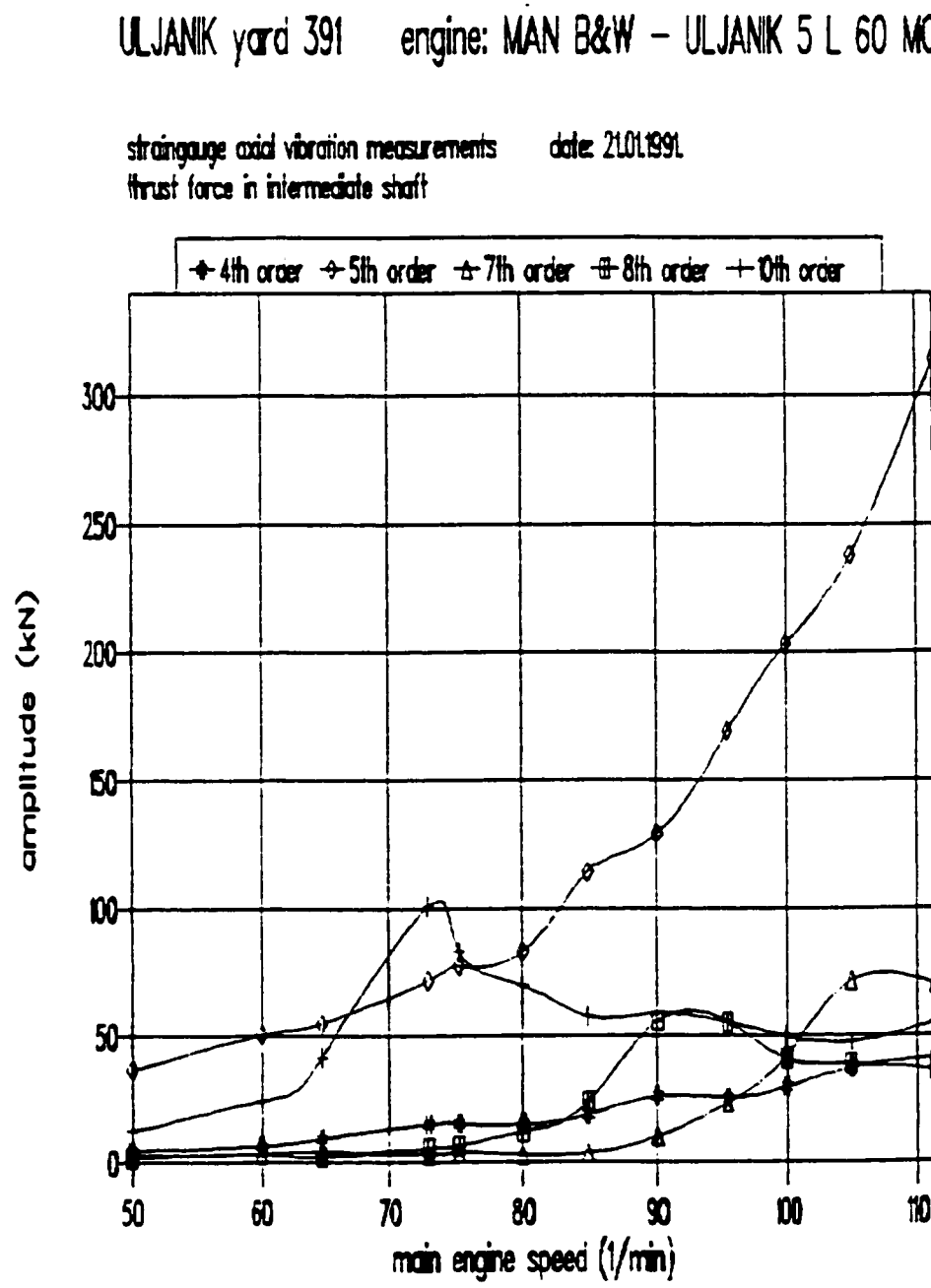

Figure D-1 Thrust force variation measurement in the intermediate shaft

APPENDIX E

SHIP HULL VIBRATION MEASUREMENT[2]

Vibration measurements shown in the following diagram were taken on two sister ships: one with big diameter line shafting (undercritical design), and the other with small diameter shafting (overcritical design). Vibration measurements were performed for both ships, and readings were taken at the wheel-house in the longitudinal direction at the approximately same location. Maximum recorded longitudinal vibratory velocities are found to coincide with 5-th order engine torsional excitation, which has its origin in capability of the propeller to couple vibration and in the main engine crankshaft coupling (i.e. torsionally induced axial vibrations).

The undercritical solution in Figure E-1 shows the existence of extreme 5-th order vibratory peak at a speed very close to nominal operational speed of the installation. Vibrations are overcoming ISO 6954 proposed level (see Figure E-2), and cannot be acceptable for safe operation of the ship. Readings presented below are taken for installation with 5 cylinder main engine equipped with longitudinal stays.

The remaining three curves in Figure E-1 present overcritical ship design. Engine is the same as for the undercritical case. Two readings were taken for transient

[2] Presented vibratory diagrams were obtained curtesy of Uljanik Shipyard

operational condition of the propulsion system, with and without longitudinal stays. The third reading is recorded for stationary operational condition with disengaged longitudinal stays. For these three cases the vibration level is much lower than for the undercritical design of the line shafting. Recorded vibratory velocities, although 2.5 times lower than for the undercritical case, are still very high, but within acceptable ISO limits.

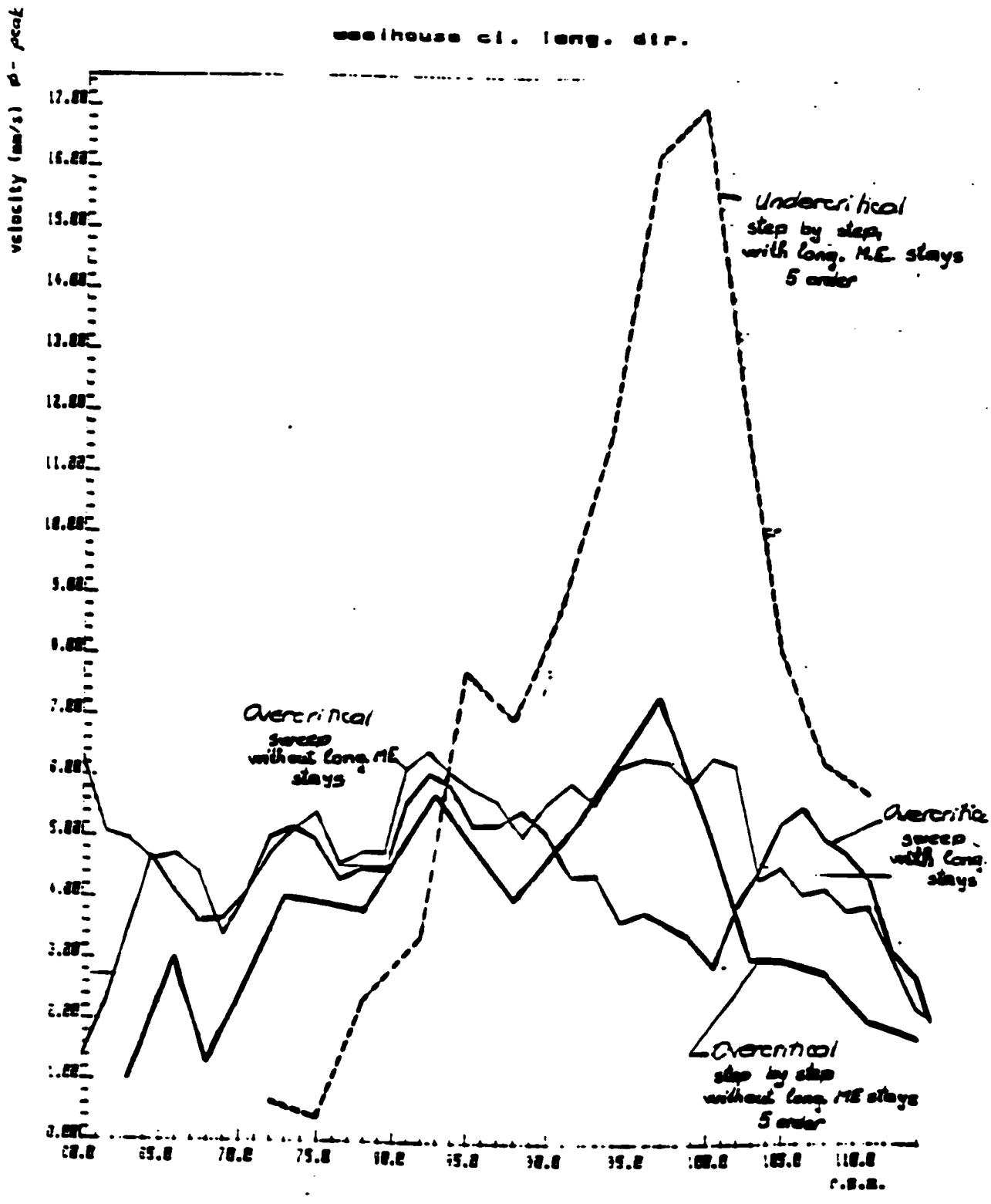

Figure E-1 Vibratory velocities [mm/s] measured at the wheel-house in longitudinal direction

I.S.O. 6954 : 1984 Mechanical vibration and shock – Guidelines for the overall evaluation of vibration in merchant ships

B.S. 6634 : 1985 British Standard Guide for Overall evaluation of vibration in merchant ships

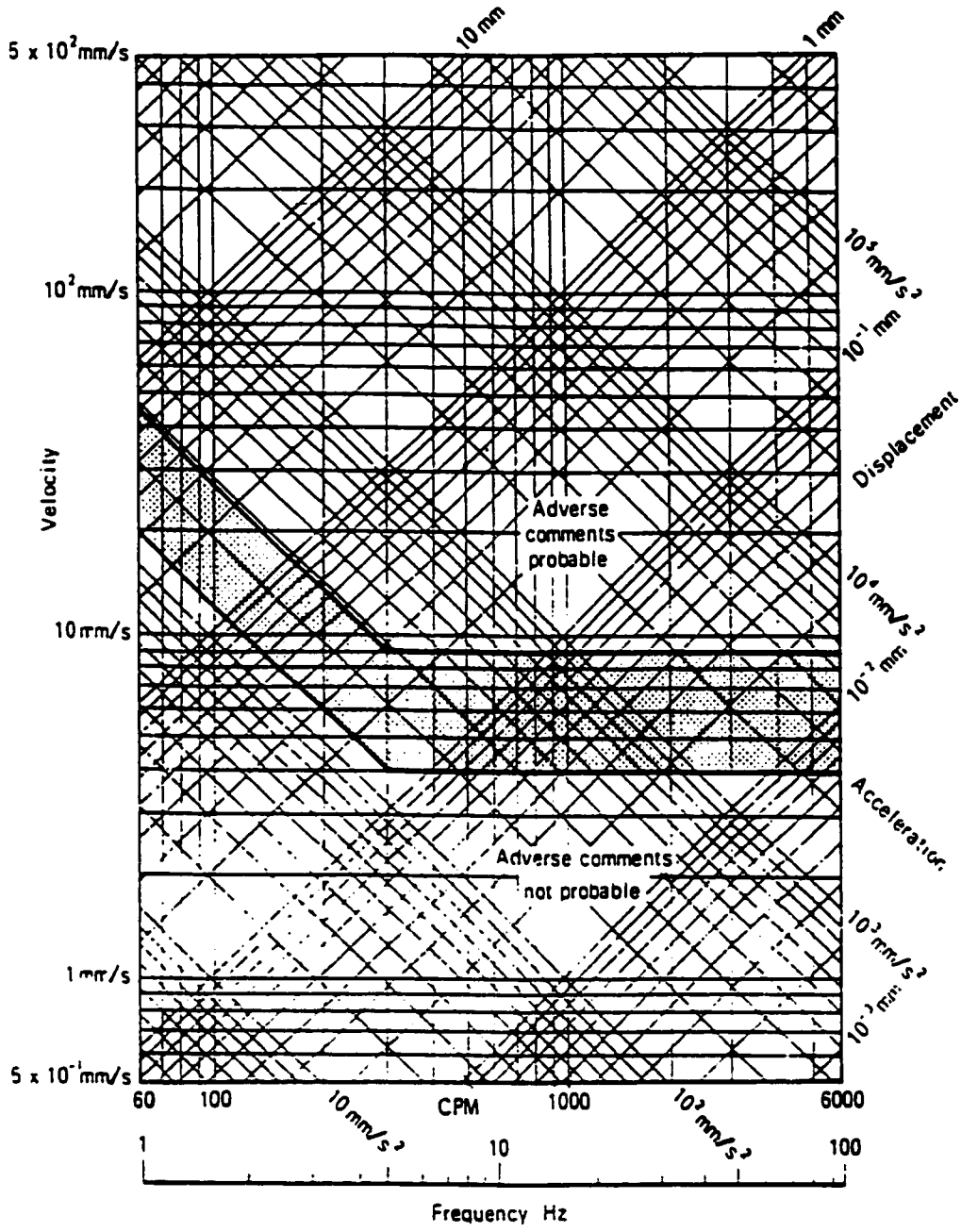

Curve	Frequency range	
	1 to 5 Hz	5 to 100 Hz
Upper	Peak acceleration = 285 mm/s²	Peak velocity = 9 mm/s
Lower	Peak acceleration = 126 mm/s²	Peak velocity = 4 mm/s

Figure E-2 Mechanical vibration and shock guidelines

GLOSSARY

ABS American Bureau of Shipping

IACS International Association of Classification Societies

BDC Bottom Dead Center

Piston position in the cylinder farthest from the cylinder head.

Effective pressure

Indicated pressure reduced by mechanical efficiency.

Indicated pressure

Force developed in combustion chamber during combustion process, reduced to piston area

Indicated diagram

Graph that relates developed pressure within cylinder and engine stroke. Recorded directly from the cylinder.

Mean (indicated/effective) pressure

Constant pressure that closes rectangular area above atmospheric line, and between TDC and BDC.

Propeller low

Cubic curve which relates engine power and revolution, related to the load of the propeller operated in water.

TDC Top Dead Center

Piston position in the cylinder closest to the cylinder head

Top bracing

Transverse stays (beams) supporting engine top structure to the ship's hull.

DTMB: David Taylor Model Basin

NSMB: Netherlands Ship Model Basin

SNAME: Society of Naval Architect and Marine Engineers

Advanced ratio

$J=nD/U$ n is propeller speed

D - propeller diameter

U - inflow velocity

Advanced velocity:

Propeller speed of advance relative to the wake inflow generated behind the ship.

Angle of incidence:

The angle between pitch-face and incident inflow

Aspect ratio:

$Ar=b/a$ - b is blade span

- a is chord

low aspect ratio -appr. <1 to 1, high $Ar > 4$

Low aspect ratio approximation when applied to the unsteady thrust, only projected area of the blade is concerned.

Basic Propeller Parameters

- Number of blades, z
- Diameter, D [m]
- Expanded area, A/Ao
- Pitch, P [m]
- Advance ratio (coefficient), J

"Conventional design" of the ship

Assumes category of Normal Form merchant ships which have Froude number below 0.3.

Coefficient

Block; Is measure of the fineness of the ship's form, expressed as ratio between underwater volume, and volume of the block L*B*D.

$$C_b = \frac{underwater\ volume}{L * B * D}$$

L is length,

B is breadth (width) and

D is draft of the ship.

Efficiency

$$\eta = \frac{P_{out}}{P_{in}} = \frac{T\,v}{Q\,\omega} = \frac{J}{2\,\pi}\,\frac{K_T}{K_Q}$$

$$J = \frac{v}{n D}, \quad K_T = \frac{T}{\rho n^2 D^4}, \quad K_Q = \frac{Q}{\rho n^2 D^5}$$

P_{out} - power on propeller [W]

P_{in} - power delivered to propeller [W]

v - inflow velocity (ship speed) [m/s]

J - advance ratio

Q - torque [Nm]

T - thrust [N]

ω - angular velocity [rad/sec]

K_T - thrust coefficient

K_Q - torque coefficient

n - rpm [1/min]

Expanded area ratio

A/Ao - A is total area of the blades

Ao is area of the circle of Do diameter.

Froude Number

$$F_n = \frac{v}{\sqrt{g L}}$$

v - ship speed [m/s]

L - length of the ship [m]

g - gravity acceleration [m/s2]

Midchord line (skew line)

Line connecting all midpoints on helicoidal surface at each radius (from hub to R)

Pitch

The distance that point on the propeller face advanced during one revolution is called pitch.

Pitch Ratio

$$P_r = \frac{propeller\ pitch}{propeller\ diameter}$$

Rake

Inclination of the midchord line from the y-z plane in x direction (one end of the midchord line is fixed in the coordinate system origin). Positive rake is in the direction of the ship astern movement.

Skew

Midchord line inclination from the x-y plane in z direction (one end of the midchord line is fixed in the coordinate system origin). Positive skew is in direction opposite to ahead rotation.